MODELLING STRUCTURAL DYNAMICS FOR CONTROL

by

Etienne Balmès

D.E.A. UPMC, Paris VI (1990)
Ingénieur de l'Ecole Polytechnique (1989)

Submitted to the Department of
Aeronautics and Astronautics
in partial fulfillment of the
requirements for the degree of

Master of Science
in
Aeronautics and Astronautics
at the
Massachusetts Institute of Technology

September, 1991

Signature of Author_____
Department of Aeronautics and Astronautics
July 30, 1991

Certified by_____
Professor Edward F. Crawley
Thesis Supervisor, Professor of Aeronautics and Astronautics

Certified by_____
Professor Andreas H. von Flotow
Co-thesis Supervisor, Professor of Aeronautics and Astronautics

Accepted by_____
Professor Harold Y. Wachman
Chairman, Department Graduate Committee

Modelling Structural Dynamics for Control

by

Etienne Balmès

Submitted to the Department of Aeronautics and Astronautics
on July 30, 1991 in partial fulfillment of the requirements for the
Degree of Master of Science in Aeronautics and Astronautics

Abstract

A critical study of the process necessary to create structural control models is made. Exact closed-form solutions of beams and truss-beams continuous models open and closed loop dynamics are given, and used to evaluate the low frequency accuracy of h- and p-refined finite element models. For trusses condensed models and refined joint behavior are considered, using the equivalent continuum approach and a refined "midbay plane" approach. Updates of the continuous idealized model and the corresponding finite element model are considered, in cases where component and global dynamic properties are known. An analysis of modelling assumptions leads to sensitivity analyses, giving a better understanding of the origins and form of uncertainties in modal models. High modal density is considered as a major limiting factor for modal model accuracy, and is linked to structural symmetries and uncoupled local vibrations. The stability of input-output characteristics is studied for a damped truss subject to modal localization, and the desensitizing influence of damping is shown. To obtain small input-output state-space models of the structural dynamic response, a systematic treatment of modal truncation is introduced. Open and closed loop static corrections are considered for structures with and without rigid-body modes. Finally correction modes are introduced to completely represent the asymptotic low frequency behavior of truncated modes in both open and closed loop cases.

Thesis Supervisor : Dr. Edward F. Crawley
Title : Professor of Aeronautics and Astronautics
Co-Thesis Supervisor : Dr. Andreas H. von Flotow
Title : Professor of Aeronautics and Astronautics

Acknowledgments

I would like to thank the DGA, Direction Générale de l'Armement, and Mr. Alain Quenzer, Directeur de l'Option Recherche, for supporting my research over the past two years.

I am deeply grateful to Professor Edward F. Crawley, for giving me the support of the SERC lab, and for his willingness to become my thesis advisor, thereby giving me so much of his time. He was always of interesting advice, and taught me a lot about engineering practice.

I am also grateful to Professor Andreas H. von Flotow, for all the interesting ideas we discussed together, and all the references he gave me. Thanks also to everyone in the Space Engineering Research Center who helped me have a good time, particularly those having desks in 462: Mark Campbell, Mathieu Mercadal, Marco Quadrelli, Daniel Rey, and Mark Webster. Special thanks go to Larry Leier and Kate Jacobs for correcting the English in important parts of my thesis, Daniel Rey for discussing many of my ideas, and the interferometer team, Gary Blackwood, David Miller, Sam Crawford, Brett Masters, Leonard Lublin, Joel Douglas, Andy Nisbet, Ron Spangler, Doug MacMartin, Kirk Gilpin, Joseph Bacla, for making the testbed what it is.

Finally, I am very grateful to my wife, Gwénaëlle, to whom I dedicate this thesis.

Table of contents

CHAPTER I

INTRODUCTION

1.1. Motivation and methodology

The growing development of Controls Structures Technology (ref. [1]) has made the need of accurate models of structural dynamics more important and more demanding. Because of stringent constraints on weight and stiffness, large spacecraft components (such as booms, solar arrays, or antennas) tend to flexible deflections which exceed requirements on allowable deflections. One solution to this problem is to accept the passive flexibility and use active control procedures to reduce either the flexibility itself or the observed flexibility seen by science instruments. Different laboratory testbeds have proved the feasibility of the method, but its use on a large scale still requires many improvements of the available methodology.

One of the essential problems of the method is the construction of accurate state-space input-output models (that will be called *structural control models*) of the low frequency structural dynamics, which contain a small number of dynamic states, and that give good models of the response in both open and closed-loop cases. Most often such models still cannot be created with sufficient confidence to assure high gain robust control. Therefore, improvements of the methods used to deal with the difficulties in structural modelling are needed.

This report will study the construction of structural control models and address some of the issues specific to the modelling of distributed-mass system dynamics. Much work has already been done and the report, referencing some of it, will evaluate the effect

of usual modelling errors on the response estimates, show some of the limitations of modal models for structures with a high modal density, and introduce a systematic way of constructing accurate control models from finite element results.

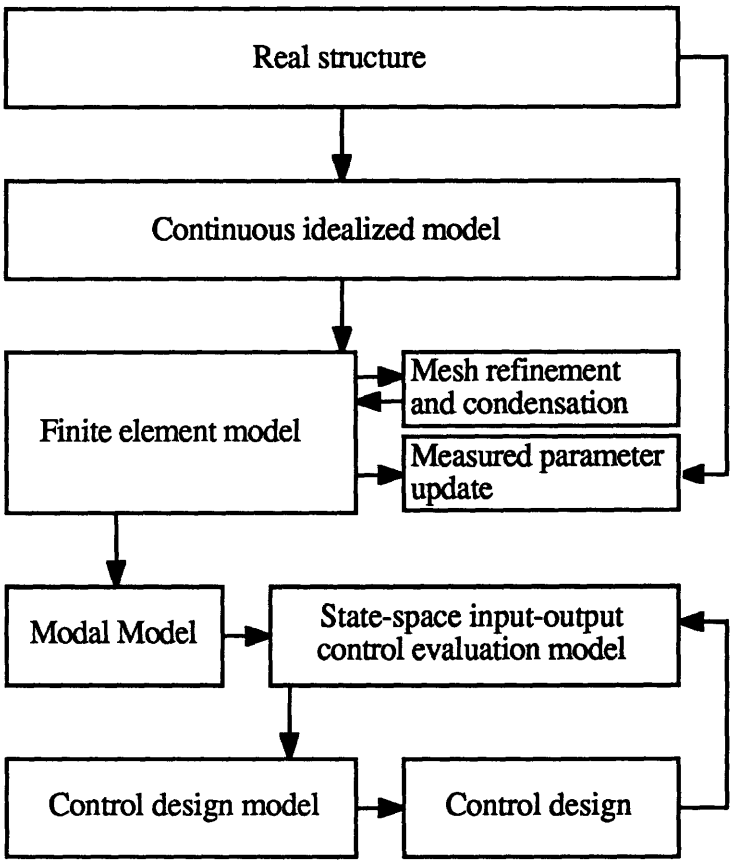

Figure 1.1. Structural control modelling methodology.

Figure 1.1. shows the standard methodology used to create structural control models. The first step is to create a conceptual continuous idealized model of the structure as an assembly of beams, rods, plates, joints, etc. A dynamic solution of this model can be computed exactly in some simple cases, but in general an approximate numerical solution is required. In this report finite element approximations will be considered.

Refinements of two types are done on the initial finite element model: first a better repartition of dynamic degrees of freedom can be made by refining the mesh where

important flexibilities are seen, while condensing other degrees of freedom if possible. Then an update of the finite element model can be made to correlate the model properties with actual measurements.

From the finite element solution only a part of the information is useful and, usually, accurate. Therefore, a finite number of modes and low frequency characteristics are retained in a modal model, which is transformed to a control evaluation model (state-space input-output of moderate order), which serves as a reference for future evaluation of designed high authority compensators on this best estimate of the "real structure." Low authority control is usually included in the evaluation model, as its effects are well known and its performance is robust.

The evaluation model is usually too detailed for use in a control design so that one further reduces it to get a control design model, used as a basis to design high authority controllers. The effect of the controller on the real structure is never exactly its effect on the design model. A check of the control design validity is made by impacting the controller on the evaluation model. This would eventually lead to changes in the control design, and potentially the structural model itself. The process could be pursued iteratively until satisfactory results are achieved.

1.2. Error and accuracy

1.1.2. Modal model errors

The objective in modelling the structural response is to obtain high fidelity representations of the transfer functions, over a finite frequency range. The frequency range of interest corresponds to the bandwidth affected by the controller including the band

in which the controller "rolls-off", which usually is at low frequencies. As pointed out in reference [2], the important characteristics of transfer functions cannot be completely defined without more precision on the use of the model: for example a poor open-loop model might give accurate closed-loop results. In this report, the attention will be focused on the open-loop response, except in the last chapter where the influence of modal truncation on the ability of a control model to give accurate closed-loop responses will be studied.

The only general purpose approach available to describe low frequency structural dynamics is the modal description. It will be used throughout this report, even though it will be shown to be unnecessarily sensitive to perturbations in the case of high modal density (the effects of sensitivity disappear if the damping is high enough for modal overlap). The frequency response of all continuous structures can be decomposed in an infinite sum of modal contributions of the form:

$$y(\omega) = \sum_i \frac{c\ \phi_i\ \phi_i^T\ b}{m_i(\omega_i^2+2j\omega\zeta_i\omega_i-\omega^2)} u(\omega) \qquad (1.1)$$

where ω_i is the modal frequency, ζ_i is the modal damping ratio, m_i the modal mass, ϕ_i the modeshape, c the observation matrix ($c\phi_i$ is the measured output for a unit modal amplitude), and b is the control matrix ($\phi_i^T b$ gives the influence of a unit generalized force on the mode).

All the terms of the modal contribution are subject to errors. Errors in frequency are usually treated first as the pole location is an important factor for control. Errors in damping ratios are difficult to deal with, as both estimates and measurements of damping tend to be very inaccurate, but by using minimum estimates stability and performance are often maintained. Errors in the modal masses correspond to global modeshape errors integrated over the whole structure. Only the weighted modeshape ($\phi_i/\sqrt{m_i}$) is a uniquely defined quantity of the problem, so that errors in the modal mass must be treated as scaling factors

of the observability ($c\phi_i$) and the controllability ($\phi_i^T b$). The observability and controllability correspond to measurements of the modal response at points or integrated over small regions. Corresponding amplitude errors can be important, especially near nodes (points where the quantity of interest is zero); and phase errors, due to sign flips, exist and will never be avoidable near nodes. Scaling errors due to the modal mass tend to be of lesser amplitude and are not as important for control purposes, as they do not induce phase errors.

Errors in the input-output modal contributions do not correspond exactly to the accuracy measurements generally used in structural dynamics. The accuracy of modal frequencies is the same, but for modeshapes structural dynamicist tend to define the errors in terms of quantities integrated over the whole structure; which is the case of the modal mass, but certainly not of the observability and controllability. It is therefore necessary, when using approximate modes, to clearly distinguish the accuracy in the sense of general structural modelling metrics and the metrics necessary for controlled structure applications.

All the modes of a continuous structure cannot be known, so that the objective of structural modelling for control can only be to create a finite state-space model that represents accurately the structure input-output open-loop response over a fixed frequency range (the low frequencies here). The closed-loop accuracy can only be checked *a posteriori*, as it will not be obtained if the truncated modes have a low frequency dynamic influence (spill-under), or the controller has unexpected interaction with poorly or unmodelled higher frequency modes (spill-over). However, for limited classes of controllers it may be possible to assess the closed-loop accuracy.

Control models are created by including some of the modes within the anticipated bandwidth, and by introducing correcting terms to get a reduced order realization of the dynamics of the truncated modes. The closed-loop accuracy is in most cases checked using a model with a much larger bandwidth than that of the controller, so that a natural distinction appears between the control design model and the control evaluation model.

No general theory enables the determination of important model characteristics for control design, but one can use the following heuristic arguments: most control techniques involving dynamic compensation consist in an approximate inversion of the open-loop dynamics and their replacement by the desired response. The most important dynamic characteristics for the dynamic inversion are pole and zero locations. The ability of different models to represent the pole/zero structure is therefore one of the most important factors in the model value. For lightly damped structures, the error in modal contribution (Eq. 1.1) is dominated by the error in modal frequency near the resonance and by the error in the modal residue ($\frac{c\phi_i \phi_i^T b}{m_i}$) elsewhere. So errors in zero placement are influenced by errors in the location of nearby poles and in the residues of all poles.

This confirms the assumption, which will be used throughout this report, that a good knowledge of the modal characteristics in the bandwidth of interest, and of the asymptotic behavior of other modes will result in models accurate for most uses. Further discussion of control model error definitions pertinent for different applications can be found in the literature (e.g., ref. [2] or [3]) and are of interest in the evaluation of the general performance of different control design methodologies.

1.2.2. Perturbation methods

Variations of the response when different model parameters are changed are studied for different reasons. For updates of an initial model, the influence of different possible errors can be computed to establish which are the most likely, so that a change in the model can be performed. For control design, the effects of some possible errors cannot be accepted, so that one designs controllers with a satisfactory response for all the possible plant dynamics. Such controllers are not the best possible, but guarantee *robust* performances.

The response could be recomputed for all possible values of an uncertain parameter, but this approach becomes impossible, if the parameter variation is continuous, or too expensive, if iterations have to be considered (as in optimal updating methods). The difficulty is circumvented by computing eigenvalue and eigenvector derivatives (also called sensitivities) with respect to different parameters. This multi-purpose approach is called the *perturbation method* and is described in many textbooks. The basic assumption is that variations from a nominal response of all the quantities involved in the problem can be accurately described as a series of terms, functions of a single parameter λ, and of increasing order in that parameter. In the case of an undamped structure described by a finite element model this assumption will translate into:

$$M = M^{(0)} + \lambda M^{(1)} + \lambda^2 M^{(2)} + o(\lambda^2)$$

$$K = K^{(0)} + \lambda K^{(1)} + \lambda^2 K^{(2)} + o(\lambda^2)$$

$$\omega_i^2 = \omega_i^{(0)2} + \lambda \omega_i^{(1)2} + \lambda^2 \omega_i^{(2)2} + o(\lambda^2)$$

$$\phi_i = \phi_i^{(0)} + \lambda \phi_i^{(1)} + \lambda^2 \phi_i^{(2)} + o(\lambda^2) \qquad (1.2)$$

where $M^{(i)}$, $K^{(i)}$, $\omega_j^{(i)2}$, $\phi_j^{(i)}$ are terms of the same order and λ is assumed small. Most of the time only the first perturbation (terms in λ) will be used, but, if the phenomena involves quadratic variations, the use of the second variation is definitely needed. As the series expansions involve terms of different orders, the general equation $(-\omega_i^2 M + K)\phi_i = 0$ gives rise to different equations for each order in the parameter λ. The first two orders give:

$$- \omega_i^{(0)2} M^{(0)} \phi_i^{(0)} + K^{(0)} \phi_i^{(0)} = 0 \qquad (1.3)$$

$$- \omega_i^{(0)2} M^{(0)} \phi_i^{(1)} + K^{(0)} \phi_i^{(1)} - \omega_i^{(0)2} M^{(1)} \phi_i^{(0)} + K^{(1)} \phi_i^{(0)} - \omega_i^{(1)2} M^{(0)} \phi_i^{(0)} = 0 \qquad (1.4)$$

The o^{th} order corresponds to the nominal response. From the first order one gets the sensitivities (or derivatives). Multiplying the 1^{st} order by $\phi_i^{(0)T}$ gives the perturbation on frequency:

$$\omega_i^{(1)2} = \frac{-\omega_i^{(0)2}\,\phi_i^{(0)T}\,M^{(1)}\,\phi_i^{(0)} + \phi_i^{(0)T}\,K^{(1)}\,\phi_i^{(0)}}{m_i^{(0)}} \tag{1.5}$$

One usually chooses to express $\phi_i^{(1)}$ as a linear combination of the $\phi_j^{(0)}$ with no first order component in the direction $\phi_i^{(0)}$ (this choice is arbitrary but affects the error on the modal mass, so that the estimate of $\phi_i/\sqrt{m_i}$ is correct):

$$\phi_i^{(1)} = \sum_{j \neq i} C_{ij}\,\phi_j^{(0)} \tag{1.6}$$

Multiplying the 1^{st} order equation (1.6) by $\phi_j^{(0)T}$ gives the different C_{ij} coefficients:

$$C_{ij} = \frac{\phi_j^{(0)T}\,\{-\omega_i^{(0)2}M^{(1)}+K^{(1)}\}\,\phi_i^{(0)}}{m_j\,(\omega_i^{(0)2} - \omega_j^{(0)2})} \tag{1.7}$$

The first order perturbation on the modal mass can be computed by solving the 1^{st} order equation linked to the evaluation of $\phi_j^T M \phi_j$:

$$m_i^{(1)} = \phi_i^{(0)T}\,M^{(1)}\,\phi_i^{(0)} \tag{1.8}$$

Eventually, one is interested in the variation of the modal residue $\frac{c\phi_i\,\phi_i^T b}{m_i}$, whose first order perturbation can be found by using the first order perturbations on the modeshapes and modal mass :

$$\left\{\frac{c\phi_i \phi_i^T b}{m_i}\right\}^{(1)} = -\frac{m_i^{(1)}}{m_i^{(0)}}\left\{\frac{c\phi_i^{(0)}\phi_i^{(0)T} b}{m_i^{(0)}}\right\} + \sum_{j\neq i} C_{ij}\left\{\frac{c\phi_i^{(0)}\phi_j^{(0)T} b}{m_i^{(0)}} + \frac{c\phi_j^{(0)}\phi_i^{(0)T} b}{m_i^{(0)}}\right\} \quad (1.9)$$

If the variations of K and M are regular enough this first perturbation corresponds to a derivative, but in some cases the perturbation gives good results even if the derivative does not exist. When eigenvalues are multiple, one has to use higher order derivatives to solve for the actual modes and first order sensitivities.

Equation (1.9) shows how different errors influence the modal residue. The first term is the error on the modal mass (or equivalently on the normalization of the modeshape). If the variation in the mass distribution (M) is not due to initial omission of important masses, this error is usually small. The following terms, which correspond to the errors in modeshapes, can be important if either the controllability or the observability ($\phi_i^T b$ or $c\phi_i$), and the error components (C_{ij}) are important. The error components are inversely proportional to the modal frequency separation , so that the magnitude of errors increases with modal density. For usual cases, errors on the observability and controllability completely dominate the error on residues. Throughout this report it will be assumed that the only significant errors in the modal residue come from inaccurate approximations of the modeshapes. Equations (1.5) and (1.7) also give a useful insight on how different modelling errors affect the estimate. The numerator is the energy estimation error and, for modeshapes, the denominator includes the frequency separation which corresponds to the energy level separation between different modes. So, errors in frequency are as important as errors in energy estimation, and errors on modeshapes depend on the relative importance of energy estimation errors and on the energy level separation between different modes.

1.3. Major examples

To be of any use, considerations on the construction of structural control models must be related to realistic examples. Many practical problems are linked to structures with local resonances and high modal density. A truss-beam, presenting these two properties, will be used to assess the levels of finite element refinement, needed to get accurate modal characteristics, and to analyze different properties linked to high modal density. To address some of the difficulties encountered in practice, the MIT/SERC interferometer testbed and the Sandia National Laboratory Γ-truss testbed will be used. Different modelling errors found during the development of their models will be analyzed, and the interferometer will be studied as a structure presenting symmetry induced modal degeneration.

The truss-beam sample problem

Truss structures are envisioned for use in many large space structure applications, and have therefore been the focus of great deal of research. Their modes include low frequency local resonances, which is one of the main difficulties associated with the use of large structures with distributed mass. And they have the advantage that known closed-form solutions of their dynamics exist for standard cases, so that a good evaluation of model accuracy is possible.

A truss-beam will be used in this report as a supporting example in the description of the modelling process. The sample problem considered was first designed (ref. [42]) by E. Wehrli and R. Ohayon at ONERA/OR (BP 72, 92322 Chatillon Cedex, France), and corresponds to very similar trusses studied by different authors (see refs. [14], [18], [41], or [43]).

The truss is formed of 20 square bays with a diagonal stiffener of constant orientation along the truss. All the struts, formed of duralium tubes, have the following properties: $\rho = 2800$ kg/m^3, $E = 75\ 10^9$ Pa, section area $S = 1.1309\ 10^{-4}$ m^2, section inertia $I = .458\ 10^{-8}$ m^4. The joints, considered as massless, constrain the strut tips in position and can be (for rotation) pinned, rigid, or rotationally stiff.

As was shown in the initial study by E. Wehrli, modelling problems are important for this truss, so that standard approaches such as equivalent continuum models are inaccurate. In chapter II, the influence of bending motions will be considered and the level of finite element refinement, needed to represent them, analyzed. In chapter IV a characterization of the modal response in terms of local resonances will be done. These resonances will then be shown: to induce a high modal density, be subject to localization, and present filtering properties, for damped motions, that are insensitive to perturbations.

The interferometer testbed

In the modelling process the analysis of actual properties of a structure is essential, and many points made in this report were motivated by research on the modelling of the MIT/SERC interferometer testbed (ref. [4]).

This testbed is meant to focus research on a real structure that captures most of the difficulties encountered to meet mission requirements of a 35 meter baseline orbiting optical interferometer. Large baseline interferometers pose stringent pathlength and pointing problems so that active control solutions seem necessary. Although many requirements motivate the research program (see ref. [4]), only the construction of analytical models of the structural dynamics will be considered here, for their necessity in the design of sensor/actuator architecture and high authority controllers.

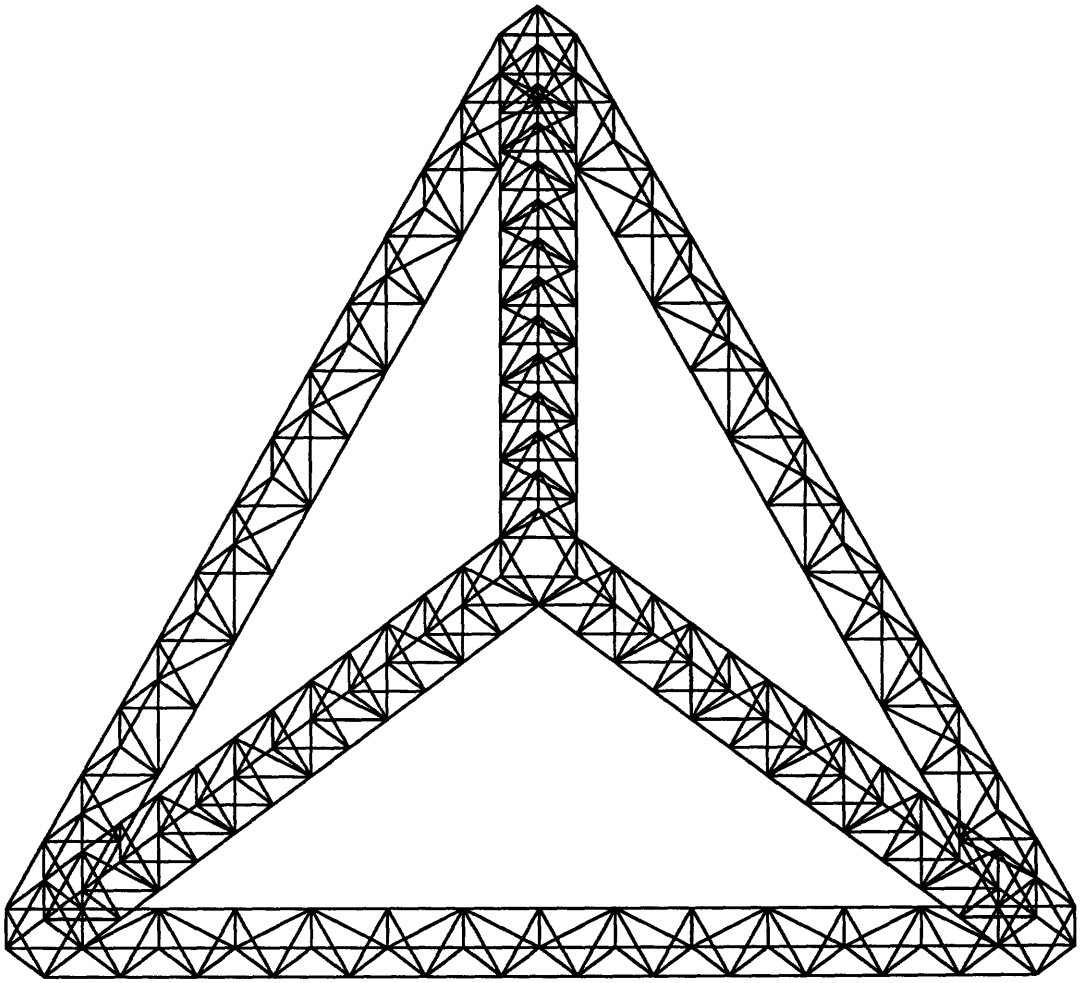

Figure 1.2. The naked interferometer testbed.

No full identification of the complete structure being available to date, the naked interferometer (without science instruments) will be considered here. The testbed is a 36 kg tetrahedral truss lattice (shown in figure 1.2.), constructed from 696 aluminum tubes of 3/8" outer diameter and .058" wall thickness, bolted tightly to 228 aluminum nodes. The struts have local bending resonances above 200 Hz, well above the fundamental frequency at 35 Hz.

In chapter III, an analysis of the truss structural response and of the sensitivity of its modal properties to modelling errors will be done. In chapter IV, a characterization of the observed modal degeneration will be done using symmetry properties of the structure.

The Gamma-Truss

This section is a summary of relevant information about the Γ-truss found in reference [22].

The Γ-truss is a research project of the Sandia National Laboratories initiated to gain experience in practical distributed parameter system control theory by focusing attention on a realistic control experiment. During the testbed development a careful attention was paid to the dynamic model, so many interesting points can be found in reference [22] on this issue.

The Γ-truss is constructed of polycarbonate tubes rigidly bonded into universal polycarbonate joining blocks. Each bay of the truss is a foot cube. A five-bay truss segment is cantilevered vertically from a large isolation mass supported by four air-bags. A horizontal three bay segment of the truss is cantilevered from the top of the vertical segment, forming a shape like the Greek letter Γ.

The vibration is sensed by four axial strain sensors (PVDF gauges) and the structure has four actuators formed of piezoelectric ceramic bonded to the outside of diagonal struts in the bottom bay of the truss.

Table 1.1. Modal frequencies of the Γ-truss and errors of initial estimate, estimate with updated axial stiffness, and estimate with air-bags modelled.

$\omega_{measured}$ (Hz)	$\Delta\omega_{initial}$ (%)	$\Delta\omega_{update\ 1}$ (%)	$\Delta\omega_{update\ 2}$ (%)
10.28	8.04	2.38	0.00
10.84	5.24	4.91	0.28
19.86	7.56	2.80	2.72
21.28	12.50	1.64	0.28
45.70	12.00	1.23	0.37
60.45	8.46	1.98	1.87
62.46	13.50	2.58	0.93
78.30	12.18	1.10	1.19
88.70	9.52	1.14	2.04
115.47	16.19	4.52	3.30

Table 1.1. reproducing data from reference [22], shows the close spacing of the modes of the Γ-truss and the accuracy obtained for different steps of the modelling. The initial error is important, but the updates give very good results for the frequency agreement, shown here, and also for modeshapes. The two updates were made using global dynamic measurements, and correspond respectively to an update of the strut axial stiffness, and a simultaneous update of the strut axial stiffness and of the isolation system stiffness. Finally, many more details on the Γ-truss can be found in references [22] and [26]. In chapter III, the Γ-truss will be used as a supporting example for the analysis of updating methodologies of initial continuous idealized models.

1.4. Report outline

Chapter II will consider the creation of a finite element model from an initial continuous idealized model. Exact closed-form solutions of the open and closed loop dynamic responses will be introduced for beam and truss beams. Then different refinement levels of finite element beam models will be considered, and their accuracy evaluated by comparison to exact solutions. For truss-beams, different descriptions will be introduced, degree of freedom condensations will be considered, and effects influencing the model accuracy will be analyzed.

Chapter III will consider the update of the initial model, by reviewing the possible modifications to the continuous idealized model in order to match measured properties better. A general methodology will be exposed and a list of usual modelling errors given. Throughout the development the interferometer testbed (see section 1.3.) and the Γ-truss (see section 3.2.) will be used to highlight different points.

One of the essential limitations to the possible modelling accuracy is high modal density, which implies descriptions highly sensitive to modelling errors. Chapter IV will expose some of the reasons that lead to high modal densities, to get a better understanding of dynamic characteristics important for the design of identification experiments and eventually of controllers. A general algebraic treatment of close modal spacing due to symmetry will be introduced and applied to the case of the naked interferometer testbed. Using the truss-beam sample problem, closely spaced modes linked to local resonances will then be considered . Near degeneration and localization will be shown. In the case of damped motions, filtering properties linked to the resonance of diagonal struts will be studied, and the input/output response will be shown to be insensitive to perturbations.

As it is impossible (and unnecessary) to represent all the modes, the objective of modelling is to give an accurate representation of the structure within a finite bandwidth. Chapter V will consider the corrections that should be introduced to represent the low frequency influence of truncated modes. First the usual approach of a static correction for the truncated modes will be introduced. Structures with and without rigid-body modes, in both the open and closed loop cases, will be considered. Then a much more efficient approach, considering correction modes, will be exposed and its accuracy will be compared with the static correction. This approach will be shown to provide a simple, general, and effective method to account for the open and closed-loop asymptotic effects of truncated modes.

Finally chapter VI will give some conclusions on the work examined in this report and give recommendations for future work.

CHAPTER II

CONTINUOUS MODELS AND SOLUTION PROCEDURES

2.1. Introduction

The standard methodology for creating a structural model for control has been described in chapter I. In the modelling process, two essential steps are to develop a continuous idealized model defined as an "exact" representation of the structure, and then a finite element model, which will actually be evaluated. This chapter will discuss the differences that may exist between the exact solution of the continuous idealized model and finite element estimates, using the definitions of error developed in chapter I.

The continuous model is, at least conceptually, formed of partial derivative equations characterizing the motions in volumes (areas for plates, and segments for beams). At boundaries, conditions characterize interface behavior on surfaces (lines for plates, and points for beams). In the case of beams, general closed-form solutions of the continuous model exist even though they are not always numerically computable. For plates and volumetric solids the exact solutions are rarely known, so approximate solutions must be used and accuracy estimation becomes a much more difficult problem.

Therefore in this chapter the approach will be to compare the results of "conceptual" models, in those cases where they can be exactly solved, and finite element models, to determine the nature and magnitude of errors introduced at this step in the structural modelling process.

In section 2.2., as a basis for the analysis of the accuracy of finite element methods, the computation of exact closed-form solutions of the dynamic response of beams and truss-beams is considered. Since the final objective is to compute closed-loop models of the structure, the effect on beams of actuation and of homogeneous feedback is also considered, briefly for actuators with a large spatial extension (called distributed) and in full detail for point actuators. Some of the effects falling in the category of distributed actuators are often included as open-loop effects so that they are considered in some detail.

In section 2.3., the quality of the representation of beam behavior by the finite element method is analyzed and a comparison of different model refinements is made. A study is made of different beam elements and the frequency range over which they can be expected to be an accurate representation of the continuous model.

In section 2.4., the approximate modelling of truss structures is discussed and detailed in the case of the truss-beam sample problem (described in chapter I). The validity ranges of equivalent continuum models and refined models are analyzed. The effect of rotational rigidities at joints is discussed in order to highlight the importance of carefully modelling bending effects in truss structures, as they are the usual limit of accuracy of the finite element models.

2.2. Exact solutions of beam and truss-beam continuous models

This section, describing beams and truss beams, discusses the type of structure for which closed form solutions of the continuous model are known. The objective is to introduce a methodology that enables the computation of closed form solutions of the structural response both in open- and closed-loop cases so that a good assessment of the

accuracy of approximate solutions found by the finite element method is possible. This comparison will then be the object of sections 2.3. and 2.4. below.

2.2.1. Exact solutions of beam models

The simplest structural form to analyze is a one dimensional rod/beam, both because it is important as a structural element and because it is the constituant element of trusses. It is unnecessary in a first step to use refined beam theories. Some structural modifications that necessitate the introduction of elaborated beam models will be discussed later in the section. More refined beam theories are described in reference [5].

In this report, the Bernoulli-Euler beam model will be used in general. Three types of displacements are considered: compression, bending, and torsion. They are assumed uncoupled. Given this assumption, motions can be described by a set of partial derivative equations for each beam segment, between discontinuities due to point actuators or joints:

$$EA\, u'' - \rho A\, \ddot{u} = F_u(x,t) \tag{2.1}$$

$$EI\, v'''' + \rho A\, \ddot{v} = F_v(x,t) \tag{2.2}$$

$$GJ\, \theta'' - \rho J\, \ddot{\theta} = M_u(x,t) \tag{2.3}$$

where u describes axial motions, so that (2.1) is the partial derivative equation describing compression; v describes transverse motions, so that (2.2) is the partial derivative equation describing bending; θ describes axial rotation, so that (2.3) is the partial derivative equation describing torsion. E is Young's modulus, A is the section area, I is the section moment of inertia about the horizontal axis, G is the shear modulus, J is the section polar moment of inertia.

Free segments

For segments with no external force actuators ($F_u = 0$ ...), harmonic motions can be expressed simply as a superposition of basic harmonic motions corresponding to wave modes of the general form $e^{j(\lambda x + \omega t)}$. The solutions of equations (2.1)-(2.3) are in this case:

$$u(x,t) = [e\cos(\mu x) + f\sin(\mu x)]\cos(\omega t) \qquad \text{with} \quad \mu = \sqrt{\frac{\rho A \omega^2}{EA}}$$

$$v(x,t) = [a\cos(\lambda x) + b\cosh(\lambda x) + c\sin(\lambda x) + d\sinh(\lambda x)]\cos(\omega t) \qquad \text{with} \quad \lambda = \sqrt[4]{\frac{\rho A \omega^2}{EI}}$$

$$\theta(x,t) = [g\cos(\nu x) + h\sin(\nu x)]\cos(\omega t) \qquad \text{with} \quad \nu = \sqrt{\frac{\rho \omega^2}{G}} \qquad (2.4)$$

where the wave modes have been combined to give real motions and a, ... , h are real wave amplitudes. The beam supports left and right propagating modes of wavenumber $\pm \mu$ in compression, $\pm \lambda$ in bending, and $\pm \nu$ in torsion. In bending, there are also left and right evanescent modes of wavenumber $\pm j\lambda$ (which give rise to the cosh and sinh functions). On a free segment the amplitudes of different wave modes are constant for a steady-state harmonic motion. Their changes at boundaries will be discussed later; but for completeness, the limits of validity of this wave guide description should be discussed first.

Modification in the distributed properties of the continuous model

In a certain number of cases, the initial continuous model, equations (2.1)-(2.3), has to be modified to be an accurate representation of the structure. Actuators with a large spatial extension (which will be called distributed) modify the type of harmonic motions that can be present in the beam. The action of these actuators can be homogeneous,

corresponding to a closed linear feedback loop, or non-homogeneous if commands are input through distributed actuators. The non-homogenous case has to be used for the computation of the effect of distributed actuators or sensors on a controlled structure (see refs. [6] and [7]). However, in general the necessary modifications to the initial model are due to passive collocated effects so that only the homogeneous case is seen.

Prestress and predeformation are among the usual phenomena that can modify the behavior of the beam as a wave-guide. The initial model does not include a description of static stresses (e.g., due to cable tensions) and deformations (e.g., due to gravity) in the structure. However, a proper analysis of simplifying assumptions, and the use of a non-linear strain description, would show that these modify the beam wave-guide properties. For example, an axial tension introduces the homogeneous term $-T_u v^{ii}$ in equation (2.2) so that even for a compression of a few percent of the buckling load, significant changes in the bending behavior would be observed. These modifications are usually not available in standard softwares for the computation of approximate solutions of the continuous model, but this is the object of current research (ref. [32]).

Local damping is often introduced by the mean of constraining viscoelastic [8] and piezoelectric [9] layers. Due to damping, otherwise propagating waves have a spatial decay. As an example of modification due to damping, one can consider the damping of axial motions. Two mechanisms are possible: position rate damping ($F_u = C\,\dot{u}$), which corresponds to a damping mechanism linked to the external environment, such as a viscous foundation; and strain rate damping ($F_u = -C\,\dot{u}^{ii}$), which is more likely to represent an internal damping mechanism such as a constraining viscoelastic layer. In the case of strain rate damping, the wavenumbers of compression harmonic motions are:

$$\lambda_i = \pm\sqrt{\frac{\rho A\omega^2}{EA+jC\omega}} \qquad (2.5)$$

which are very similar to those of the usual beam (equation (2.4)) at low frequencies, but differ significantly for $C\omega > EA$.

Modifications of the beam behavior can in general be introduced in the closed form solutions, but the equivalent corrections of the approximate methods are rarely done. This constitutes an important limitation for the usual approximate models.

Point boundaries

The behavior of a structure formed of beams depends on the different beam segments described in the preceding paragraphs, but is also strongly conditioned by the behavior of boundary points such as beam tips, point actuators, or joints connecting different beams. At these points the amplitudes of different wave modes must be such that all the boundary conditions are met, even for transient motions. The boundary conditions are composed of continuity and equilibrium conditions. *Continuity of position*, which applies to axial and transverse motions, means for example that a clamped beam tip does not move or that the tips of two beams connected by a joint have the same position. *Continuity of slope*, which applies to bending motions, refers to the fact that when beam segments are connected by a rigid joint they have geometrically related slopes. *Moment equilibriums*, which apply to bending and torsion motions and couple them in some cases, are the moment equilibriums of each of the beam tips connected to a joint and the moment equilibrium of the joint itself. The usual moments present at a joint are: beam-tip moments due to bending or torsion, joint stiffness moments, inertial moments for massive joints, and external actuator moments. *Force equilibrium*, which applies to both compression and

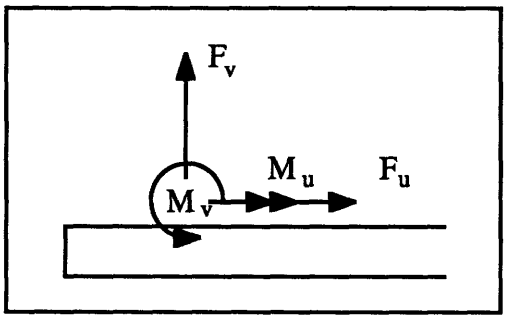

Figure 2.1. Local beam coordinates.

bending motions, is the force equilibrium of each joint which is subject to beam-tip forces due to compression and bending, inertia forces due to the joint mass, and external input forces.

In order to express the equilibriums, it is necessary to know the forces and moments transmitted by the beams. Using the standard local conventions for a beam (figure 2.1.), the forces that the beam exerts on a point located at the tip, and the moments exerted by the boundary on the beam tip are:

	left tip	right tip
$F_u =$	$EA\, u^{i}$	$-EA\, u^{i}$
$F_v =$	$-EI\, u^{iii}$	$EI\, u^{iii}$
$M_u =$	$GJ\, \theta^{i}$	$-GJ\, \theta^{i}$
$M_v =$	$EI\, u^{ii}$	$-EI\, u^{ii}$

(2.6)

The continuity and equilibrium conditions can then be simply expressed using a common global coordinate system.

Modes vs waves

In structural dynamics one usually uses modes as a specific basis of motions to describe the structural behavior. Modes are particular harmonic solutions of the equations of motion for which all the boundary conditions are met without the presence of an external harmonic excitation. In wave propagation terms they are standing waves. Until now, although some wave propagation terminology has been used, only possible harmonic motions and boundary conditions of the beam have been described so that the preceding paragraphs can be used to compute closed form frequency responses of the structure or closed form solutions for modes. The description in terms of waves and wave modes

would imply the use of an Eulerian point of view (a travelling description) and the expression of boundary conditions in terms of scattering coefficients. The link between the two approaches corresponds to the fact that wave modes are basic possible harmonic motions. For more details on the subject see [10] for example.

Modeshapes may be real or complex and have real or complex eigenvalues. In the latter case the modes are damped so that their amplitude diminishes with time.

The main characteristics of modes are: the time and space dependance of motion are decoupled for a mode so that one can consider non-dimensional time-invariant modeshapes and dimensional time-varying modal amplitudes; any displacement of the structure can be decomposed as a sum of modal responses (the approache to obtain accurate responses with a finite sum is the object of chapter V); as the modes are unforced responses they verify homogeneous equilibrium conditions at all points, so that forces and moments are continuous on any one dimensional part of the structure even at material discontinuities.

Example: Cantilever beam with midspan force actuator

The purpose of this example is to show an application of the analysis that has just been discussed to the computation of the exact open and closed loop frequency response of a beam (shown in figure 2.2.) with two free segments (1 and 2) and three different boundary points (O, A, and B).

The solution assumes that compression and torsion displacements are negligible. Section constants $EI = 1$ and $\rho A = 1$ are used for numerical simulations.

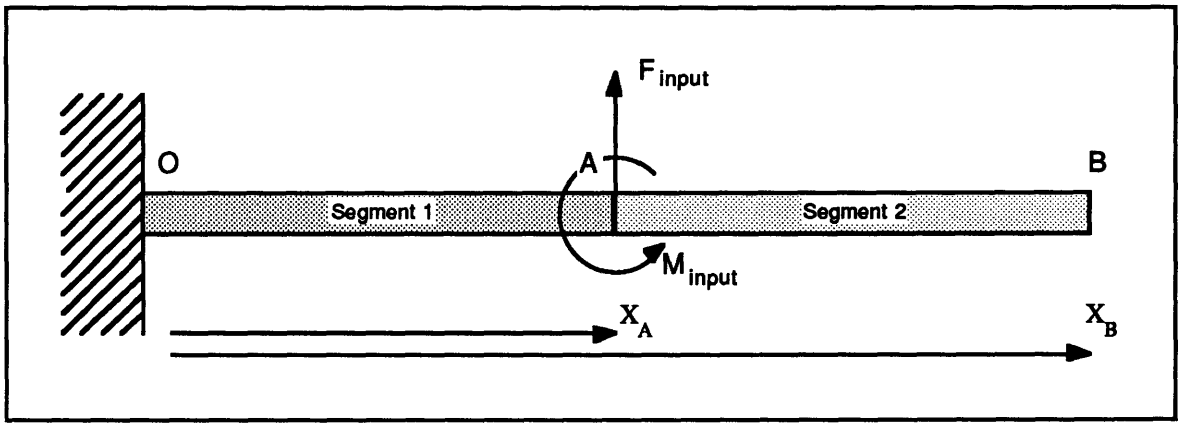

Figure 2.2. Cantilever beam with midspan actuator

Harmonic displacements of the two free segments are given according to (2.4) by:

$$v_1(x,t) = (a_1 \cos(\lambda x) + b_1 \, ch(\lambda x) + c_1 \sin(\lambda x) + d_1 \, sh(\lambda x)) \cos(\omega t)$$

$$v_2(x,t) = (a_2 \cos(\lambda x) + b_2 \, ch(\lambda x) + c_2 \sin(\lambda x) + d_2 \, sh(\lambda x)) \cos(\omega t)$$

$$\text{with} \quad \lambda = \sqrt[4]{\frac{\rho A \omega^2}{EI}} \tag{2.7}$$

The boundary conditions at O only constrain position and slope:

$$v_1(x_O,t) = 0 \qquad \overset{i}{v_1}(x_O,t) = 0 \tag{2.8}$$

The boundary conditions at B only constrain moment and force:

$$EI \overset{ii}{v_2}(x_B,t) = 0 \qquad EI \overset{iii}{v_2}(x_B,t) = 0 \tag{2.9}$$

At A the boundary conditions give rise to four constraints:

$$v_1(x_A,t) = v_2(x_A,t) \qquad \overset{i}{v_1}(x_A,t) = \overset{i}{v_2}(x_A,t)$$

$$EI \overset{iii}{v_1}(x_B,t) - EI \overset{iii}{v_1}(x_B,t) + F_{input} = 0$$

$$-EI \overset{ii}{v_1}(x_A,t) + EI \overset{ii}{v_2}(x_A,t) + M_{input} = 0 \tag{2.10}$$

Using (2.7) in (2.8)-(2.10) gives a set of linear equations that can be assembled in matrix form as:

$$\begin{bmatrix} 1 & 1 & 0 & 0 & 0 & 0 & 0 & 0 \\ 0 & 0 & 1 & 1 & 0 & 0 & 0 & 0 \\ c(\lambda x) & ch(\lambda x) & s(\lambda x) & sh(\lambda x) & -c(\lambda x) & -ch(\lambda x) & -s(\lambda x) & -sh(\lambda x) \\ -s(\lambda x) & sh(\lambda x) & c(\lambda x) & ch(\lambda x) & s(\lambda x) & -sh(\lambda x) & -c(\lambda x) & -ch(\lambda x) \\ -c(\lambda x) & ch(\lambda x) & -s(\lambda x) & sh(\lambda x) & c(\lambda x) & -ch(\lambda x) & s(\lambda x) & -sh(\lambda x) \\ s(\lambda x) & sh(\lambda x) & -c(\lambda x) & ch(\lambda x) & -s(\lambda x) & -sh(\lambda x) & c(\lambda x) & -ch(\lambda x) \\ 0 & 0 & 0 & 0 & c(\lambda x) & -ch(\lambda x) & s(\lambda x) & -sh(\lambda x) \\ 0 & 0 & 0 & 0 & -s(\lambda x) & -sh(\lambda x) & c(\lambda x) & -ch(\lambda x) \end{bmatrix} \begin{bmatrix} a_1 \\ b_1 \\ c_1 \\ d_1 \\ a_2 \\ b_2 \\ c_2 \\ d_2 \end{bmatrix} = \begin{bmatrix} 0 \\ 0 \\ 0 \\ 0 \\ M_{input}/\lambda^2 \\ -F_{input}/\lambda^3 \\ 0 \\ 0 \end{bmatrix} \quad (2.11)$$

For the remainder of the example, M_{input} will be assumed zero so that $\overset{ii}{v}_1(x_A,t) = \overset{ii}{v}_2(x_A,t)$. For an open-loop system, F_{input} represents a command or disturbance force entering the structure through the force actuator located at A. For a linear closed-loop system, F_{input} is the sum of an homogeneous term corresponding to the closed feedback loop, and an external excitation term corresponding to commands or disturbances. The homogeneous term depends on the time and space derivatives of the displacement at some set of points on the structure and/or integrated over some regions. As seen in (2.7), the displacement at a given frequency lies in a finite vector space so that the homogeneous forcing due to each of the base vectors of this vector space can be computed and assembled to form the columns of a compensator matrix K, which may depend on frequency if time derivatives of the displacement are involved. The forcing can therefore be described in the form:

$$F_{input} = K(\omega) [a_1\ b_1\ c_1\ d_1\ a_2\ b_2\ c_2\ d_2]^T + F_{command} \quad (2.12)$$

where the columns of $K(\omega)$ are the homogeneous forcings that would appear for a basic harmonic motion, the a_i, b_i, c_i ,d_i are the actual amplitudes of the basic motions, and $F_{command}$ is the external forcing.

The most usual form of $K(\omega)$ is a static feedback. For example:

$$K(\omega) = - k \, [0\ 0\ 0\ 0\ c(\lambda x_s)\ ch(\lambda x_s)\ s(\lambda x_s)\ sh(\lambda x_s)] \qquad (2.13)$$

is a static position feedback of a sensor located at x_s (between A and B). For $x_s = x_A$ the feedback is collocated and if k is positive real, it only acts as a spring. For $k<0$ the feedback loop is a negative spring, and, for $k = j\omega c$, the feedback act as a damper. Other general linear controllers can always be represented in the form (2.12), and for any given frequency it is possible to compute the exact (within the limits of the continuous idealized model) closed loop response of the structure.

Exact closed loop modes can be computed by solving for the singularities of the homogeneous part of (2.11). For an undamped system this is easily done by any root solver (e.g., Newton-Raphson algorithm) as one looks for the real roots of the determinant of the homogeneous part of (2.11). For damped systems the poles are complex so that the singularities must be searched out in the complex plane, which is much more difficult numerically. Finally, numerical conditioning would be a major issue if this method was to be used extensively. But it does provide in principle an exact solution to the open and closed-loop behavior of structures composed of beams.

2.2.2. Exact solutions of truss models

The choice of a description for the exact solution has a strong influence on the creation of approximate models. In this section, a general exact description of one-dimensional trusses will be introduced and two possible descriptions of the truss bay will

be given, so that approximate solutions can be derived in section 2.4. Exact solutions of continuous truss models have been used in different occasions and usually in a transfer matrix formalism (ref. [13] or [12]). As the objective is the creation of approximate methods in section 2.4., the following description only summarizes the essential points of the method. For more details one could refer to [13] or [14] which have similar treatments of the problem (although applied to wave-modes).

Truss beams considered here are formed by a certain number of identical (or almost identical) interconnected cells placed by translation along a single axis. Truss beams are similar to beams in the fact that one can use a single position variable to describe the whole truss (they have a mono-dimensional description), but they differ in that portions of the truss are similar only at periodically spaced points and not at all points. Because of this inherent periodicity, waves are only described as transmitted motions from one of these periodically spaced points to the next.

The choice of points at which the sustained harmonic motions are computed is arbitrary, but different choices lead to more or less accurate approximate methods. Placing the points with the cell periodicity simplifies the process when the truss is composed of many identical cells.

Having a set of points spaced along the truss, harmonic motions of the truss in the plane of these points can be described at each frequency as a finite number of displacements and slopes (u_i, of number p) corresponding to a finite set of forces and moments (F_i, also of number p). If the set fully describes truss motions it is possible to express the transmission of states from one point to its neighbor as a linear frequency-dependent matrix T_n (figure 2.3.).

T_n is called the transfer matrix from the states of position n to the states of position n+1. In most cases it can be computed exactly at each frequency by applying the methodology developed in section 2.2.1. to each of the free beam segments composing the bay and by properly modelling the boundary conditions at the joints. For cells connected in series, the transmission from one end to the other is given by :

$$\begin{bmatrix} u_N \\ F_N \end{bmatrix} = T_{n-1} \begin{bmatrix} u_{N-1} \\ F_{N-1} \end{bmatrix} = T_{n-1} \dots T_1 \begin{bmatrix} u_1 \\ F_1 \end{bmatrix} \qquad (2.14)$$

Computing the product $T_{N-1}...T_1$ can be difficult for large N but if the truss is actually periodic the T_i are identical and one can use their eigenvalue decomposition $T = U\Lambda V$ (where Λ is a diagonal matrix and $U=V^{-1}$) so that $T_{N-1}...T_1 = U\Lambda^{n-1}V$. Numerically the eigenvalues of T are often separated by several orders of magnitude so that using the eigenvalue decomposition is a sound numerical procedure which is much better conditioned than the direct product.

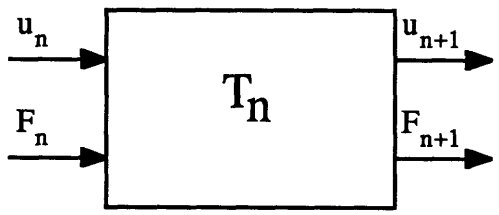

Figure 2.3. State transfer for a 1-D structure

At external boundaries, states are not transmitted but one has a set of boundary conditions (found by using the methodology of 2.2.1.).

$$B_1 \begin{bmatrix} u_1 \\ F_1 \end{bmatrix} = 0 \qquad B_N \begin{bmatrix} u_N \\ F_N \end{bmatrix} = 0 \qquad (2.15)$$

where B is a p by 2p matrix (p = size of u_i) which can be constant (clamped or free conditions, etc.) or frequency dependent (nodes linked by a beam, dynamic actuator, etc.).

Internal boundaries can be treated similarly and, if F_i (a set of either commanded or feedback forces and moments) corresponds to the input of the internal boundary, a matrix relationship of the following type can be found (where B is a 2p by 5p matrix):

$$B\begin{bmatrix} u_{N-1} \\ F_{N-1} \\ u_N \\ F_N \\ F_i \end{bmatrix} = 0 \qquad (2.16)$$

The transmission equations (2.14) and the boundary equations (2.15)-(2.16) define an over constrained problem if no command is input. The homogeneous part of this system has unforced non-zero solutions only at some particular frequencies of the s-plane and the associated motions are called modes in structural dynamics and standing waves in wave propagation theory. Modes are found by solving for singularities of the system (2.14)-(2.16), as was done in the example of the cantilever beam with midspan actuator (section 2.1.).

The bay can be described using many different approaches, two of which will be described in the following paragraphs. The development will use the truss-beam sample problem but could be easily generalized.

Joint-plane description of truss-beams

This approach, which is the classical approach to the problem, considers the bay shown on figure 2.4. The joints are taken as boundary points so that the states transmitted are states at these points. In some cases, as when defining an equivalent continuum, it is useful to use another linearly equivalent set of states (see section 2.4.2.) but the results linked to this approach do not change. For the 2-D truss shown, assuming pinned joints, the states are: two position coordinates and two associated forces at each node. The

moments are always zero so that they and their associated position states (the slopes) do not have to be considered.

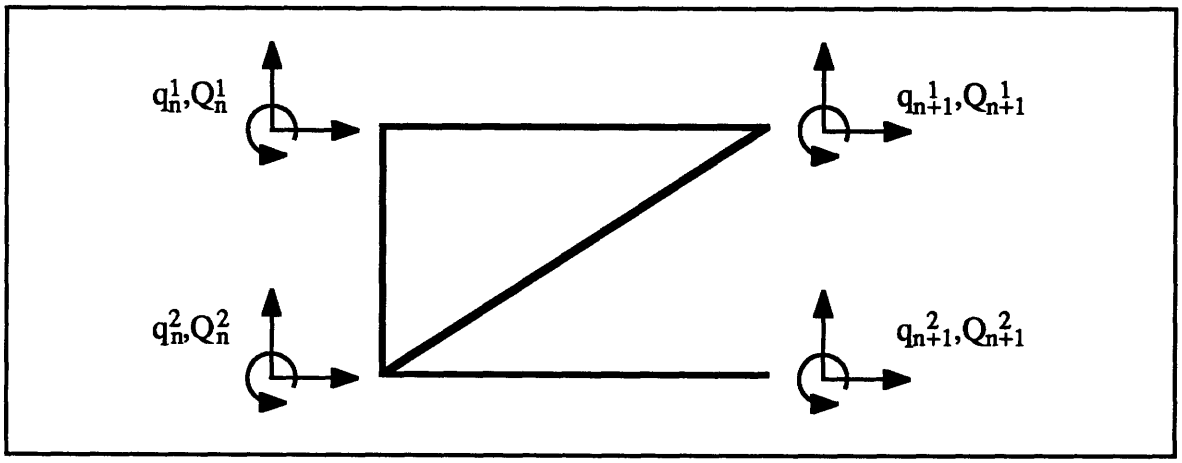

Figure 2.4. Joint-plane bay for the transfer matrix description of a truss-beam.

Therefore, on each side, there are 8 states, four positions and four forces. At any frequency the response of the bay is described by 24 independent coefficients (4 struts with 2 states for compression, and 4 states for bending according to (2.4)), and the boundary conditions at the four joints give rise to 16 constraints (8 on position and 8 on the moments). Therefore, if the states are known on one side of the cell, the states on the other side can be computed exactly at each frequency.

For clamped joints, the moments shown at each joint in figure 2.4. are non-zero, so that there are 12 transmitted states, but the problem is still solvable. If other joints (such as the one shown on figure 2.5.) are used, boundary conditions of moment equilibrium involve cross constraints between the states of two adjacent bays so that the formalism of the transfer matrix is much more difficult to use.

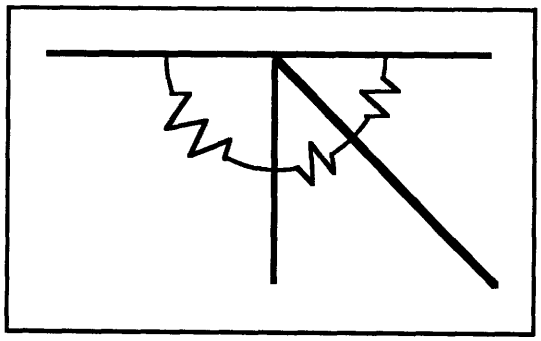

Figure 2.5. Stiff joint

Midbay-plane description of truss-beams

This approach, first introduced in [15], uses strut midspans as boundary points so that any discontinuity linked to joints is included in the computation of the transfer matrix and does not appear as a problematic behavior at the boundary points. For exact solutions this approach only reorganizes computations so that the transfer matrix methodology can be used with joints that are other than pinned or clamped. Irrespective of the type of joints there are 18 transmitted states (9 displacement and 9 moments) and 24 boundary conditions at the internal joints so that the 42 independent coefficients describing possible harmonic motions in each of the 7 beam segments are known at each frequency. Position continuity conditions at the upper and lower joints are:

$$v_1 = v_5 = u_4 = \frac{1}{\sqrt{2}}(u_2+v_2) \qquad u_1 = u_5 = v_4 = \frac{1}{\sqrt{2}}(u_2-v_2)$$

$$v_3 = v_7 = -u_4 = \frac{1}{\sqrt{2}}(u_6+v_6) \qquad u_3 = u_7 = v_4 = \frac{1}{\sqrt{2}}(u_6+v_6) \quad (2.17)$$

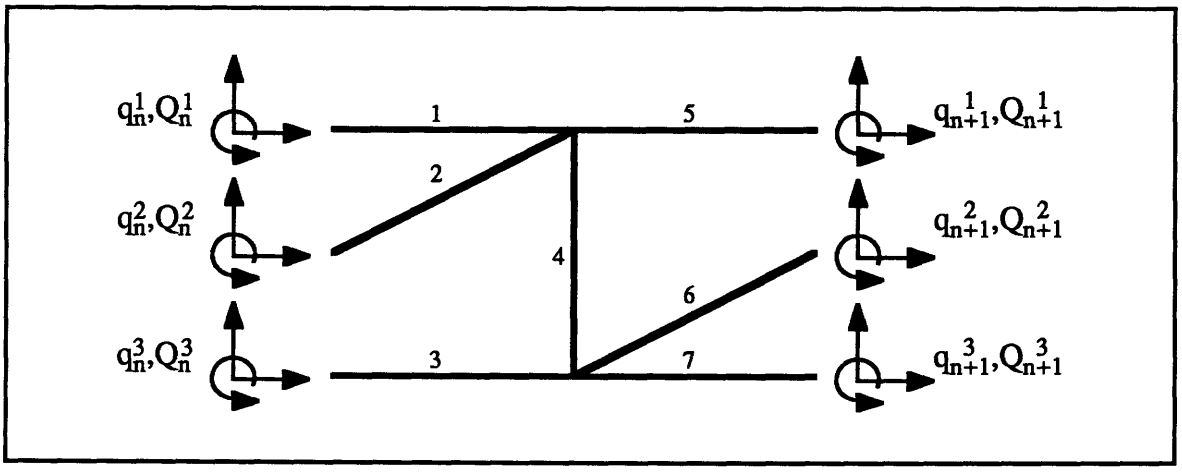

Figure 2.6. Midbay-plane transfer matrix description of a truss-beam.

where u is the axial and v the transverse beam displacement, and the indices correspond to the beam numbering shown on figure 2.6. Force equilibriums at the joints are:

$$
\begin{aligned}
&- EI\, v_1^{iii} + EI\, v_5^{iii} + EA\, u_4^{i} + \frac{1}{\sqrt{2}}(-EI\, v_2^{iii} + EA\, u_2^{i}) = 0 \\
&EA\, u_1^{i} - EA\, u_5^{i} + EI\, v_4^{iii} + \frac{1}{\sqrt{2}}(EI\, v_2^{iii} + EA\, u_2^{i}) = 0 \\
&- EI\, v_3^{iii} + EI\, v_7^{iii} - EA\, u_4^{i} + \frac{1}{\sqrt{2}}(EI\, v_6^{iii} - EA\, u_6^{i}) = 0 \\
&EA\, u_3^{i} - EA\, u_7^{i} - EI\, v_4^{iii} + \frac{1}{\sqrt{2}}(-EI\, v_6^{iii} - EA\, u_6^{i}) = 0
\end{aligned}
\qquad (2.18)
$$

Supposing the joint massless, moment equilibrium conditions for a joint with rotational joint rigidity k are, for each of the beam segments connected to the joint:

$$
\begin{aligned}
&EI\, v_1^{ii} + k\,(2v_1^{i} - v_2^{i} - v_5^{i}) = 0 \qquad && EI\, v_3^{ii} + k\,(2v_3^{i} - v_7^{i} - v_4^{i}) = 0 \\
&EI\, v_2^{ii} + k\,(2v_2^{i} - v_1^{i} - v_4^{i}) = 0 && EI\, v_6^{ii} + k\,(2v_6^{i} - v_7^{i} - v_4^{i}) = 0 \\
&EI\, v_5^{ii} + k\,(2v_5^{i} - v_1^{i} - v_4^{i}) = 0 && EI\, v_7^{ii} + k\,(2v_7^{i} - v_3^{i} - v_6^{i}) = 0 \\
&EI\, v_4^{ii} + k\,(2v_4^{i} - v_2^{i} - v_5^{i}) = 0 && EI\, v_4^{ii} + k\,(2v_4^{i} - v_3^{i} - v_6^{i}) = 0
\end{aligned}
\qquad (2.19)
$$

If the joints are clamped, these last 8 conditions are replaced by 6 slope continuitty and 2 moment equilibrium conditions. These conditions enable the analytical expression of the transfer matrix. Numerically this problem is inherently ill-conditioned. For example, the analysis cannot be performed for the truss beam sample problem without special precautions giving a better precision than the standard 16 digit precision.

The real advantages of this approach will be shown in section 2.4., where it is used to create approximate models.

2.3. Finite-element representation of beams: H-version versus P-version

2.3.1. Introduction

Having exact closed-form solutions of the response of beams, the objective is now to assess the validity of different approximate models. This section will consider simple beams, and determine the accuracy that can be expected for different levels of beam finite element refinement. Here the validity will be examined in the control sense (as defined in chapter I) although global integrated errors will sometimes be used.

When applying the finite element method to compute controlled structure dynamic response, one seeks to estimate the lower frequency eigenvalues and eigenfunctions of the structure. Usually an initial finite element model places nodes at structural junctions and uses elements such that at least the static response is described exactly. In many cases the model thus obtained needs to be refined to obtain accurate dynamic results. The FEM theory introduces two classical ways of refining the model: the h-version where the mesh is refined and the p-version where the order of the polynomials used as interpolating functions is increased. Hundreds of papers discuss the merits of the two approaches for different structures or physical phenomena but usually not for controlled structure applications. Reference [16] however, is a very useful discussion of the problem for structures, and [17] gives a sound basis for the proof of results seen in practice, although an important mathematical background is required to read it.

Actual modes, as they are unforced responses, satisfy force and moment equilibriums at all points. If only two parts of a structure are connected to a given point, forces and moments at that point will be continuous. The refinement of a finite element

model is done separately for each free segment or element of the initial model. The error in a modeshape estimate can be found by finding the size of the modeshape estimate projection on the space spanned by the exact modeshapes of other modes. For an h-refinement inexact discontinuities are present that imply more important components of the error on high frequency exact modes, than for a p-refinement which conserves continuity. So the p-refined modeshapes tend to be more accurate. In practice, this is balanced by the fact that h-refinements tend to capture more modes.

At boundary points of initial elements (which remain the same even if the model is refined), equilibrium conditions on force and moment, which govern the actual discontinuities of spatial derivatives of displacement, are never met exactly, since this cannot be imposed in the finite element method; for these points, the type of refinement does not make a difference. It is possible to impose strict compatibility conditions on the complete structure using an integrated force method (ref. [11]) or other similar approaches, but they are not of generalized use and would therefore be rather costly to implement on a realistic engineering basis.

For finite beam elements there are other reasons to use at least a partial p-refinement. The constraint of exact static response will not be met by the usual 2-node beam element (cubic interpolation) if the definition of static is extended to include uniformly accelerated motions (in translation and rotation), as is often done in the Component Mode Synthesis literature. A first p-refinement of the 2-node beam element would add inertia relief modes to the static modes already modelled, resulting in an element with quintic interpolation and an exact "static" response in the extended sense.

High order refinements are usually not needed, but some rules can be given for the eventual case where this would apply. the p-refinement also has, in general, the advantage of having a guaranteed monotonic convergence (consistent mass will always be assumed here). This guarantee comes from the fact that a p-refinement always includes the preceding model (this is called the inclusion property). But, when using usual 2-node beam elements

in an h-refinement, this property is also verified so that monotonic convergence is also guaranteed. In general, monotonic convergence is only guaranteed for refinements that include the non-refined model, but no other general consideration can be given. The monotonic convergence of point errors on the modeshapes is also guaranteed but may not be as quick as the global modeshape convergence.

In order to asses the accuracy of different beam elements, the addition of inertia relief modes to the standard beam element as a first step of p-refinement is discussed in section 2.3.2. In section 2.3.3., errors in the prediction of modeshapes are studied for a simple beam configuration using the control-approach error definition. Finally, conclusions on the expected accuracies of finite element models are drawn in section 2.3.4.

2.3.2. An 18 dof beam element

As a first step to a p-refinement this section discusses the creation of a 18 dof beam element that could be used without restrictions in a 3-D finite element code such as NASTRAN.

The usual 12-dof, 3-D, 2-node beam element, which represents exactly the static response of a Bernouilli-Euler beam, uses a set of 12 shape functions:

Bending (2 axes)	Compression	Torsion
$v_1(s) = 2\,s^3 - 3\,s^2 + 1$	$u_1(s) = -\,s + 1$	$\theta_1(s) = -\,s + 1$
$v_2(s) = -2\,s^3 + 3\,s^2$	$u_2(s) = s$	$\theta_2(s) = s$
$v_3(s) = s^3 - 2\,s^2 + s$		
$v_4(s) = s^3 - s^2$		

where s is the non-dimensional local coordinate along the element (which varies from 0 at node 1 to 1 at node 2), u_1, v_1 and u_2, v_2 correspond to unity axial and transverse

displacements at nodes 1 and 2 respectively, v_3, θ_1 and v_4, θ_2 correspond to unity torsion angle and bending slope at nodes 1 and 2, respectively.

For a p-refinement of this element, the solution depends only on the functional space spanned by the interpolating functions, but the added shape functions should be chosen so as to simplify the mixed use of the initial and refined elements by keeping unchanged the interpretation of the 12 initial functions in terms of unitary displacements at the boundary nodes. Here the shape functions have also been chosen to have an interpretation in terms of midspan displacements, and take the following forms in terms of the non-dimensional coordinate s:

Bending (2 axes)	Compression	Torsion
$v_5(s) = 16\ s^4 - 32\ s^3 - 16\ s^2$	$u_3(s) = -2s^2 + 2s$	$\theta_3(s) = -2s^2 + 2s$
$v_6(s) = 16\ s^5 - 40\ s^4 + 32\ s^3 - 8\ s^2$		

where u_3 and v_5 correspond to unity axial and transverse midspan displacement, the end nodes being fixed; θ_3 and v_6 correspond to unity torsional and transverse midspan slopes, the end nodes being fixed.

The addition of these higher order shape functions enables the exact description of inertia relief modes. A detailed definition of inertia relief modes is given in chapter V but, as an example where their influence is seen, one can consider the steady-state response of a free-free beam with a constant load at one point. The beam undergoes an infinite rigid body motion and a finite constant flexible deformation, which is called the inertia relief deformation and corresponds to the fact that the structure must be stressed so that the external force applied at one point results in forces applied at all points which induce the rigid-body motion of all the structure. Inertia relief modes of a beam are quadratic polynomials in compression and torsion, and quintic polynomials in bending, so that the new element describes them exactly.

Using these shape functions the corresponding mass and stiffness matrices have been derived and are shown on figure 2.7.

To develop higher order p-refined general elements similar approaches could be used, introducing more intermediate nodes and their associated shape functions, but it is obvious that this would require a full automation within the finite element code, which is not generally available at the present time.

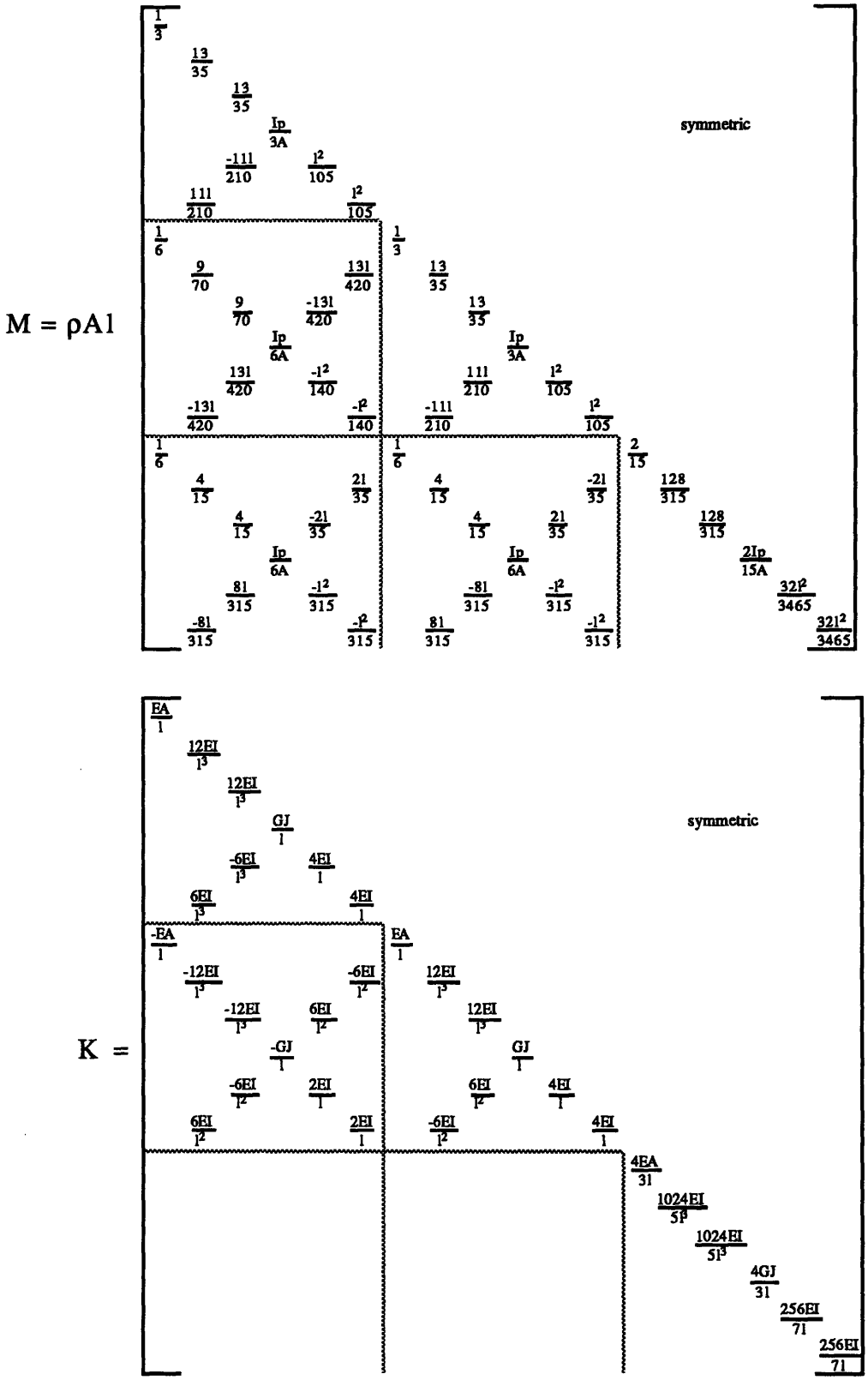

Figure 2.7. Mass and stiffness matrices for the 18 dof beam element. Degrees of freedom: u,v,w,θ_u,θ_v,θ_w for left, right, and phantom nodes

2.3.3. Accuracy of models of controlled beams

Having defined the exact solution and the different refinement levels of finite element beam models, the problem is now to determine the accuracy of different approximate solutions in the sense of control applications (as described in chapter I).

Figure 2.8. summarizes the characteristics of the several current point actuators and sensors. The force actuators and position, velocity, or acceleration sensors (cases a and c) will be accurately modelled if the point displacements are accurate. Differential force actuators and axial strain sensors (case b) will be as accurate as the integrated axial strain which is equal to the difference of the displacements at the two extremities of the sensor/actuator. Similarly for case d the slope at the actuator/sensor point determines the accuracy and for case e the integrated curvature (equal to the slope difference) must be accurate over the sensor/actuator location.

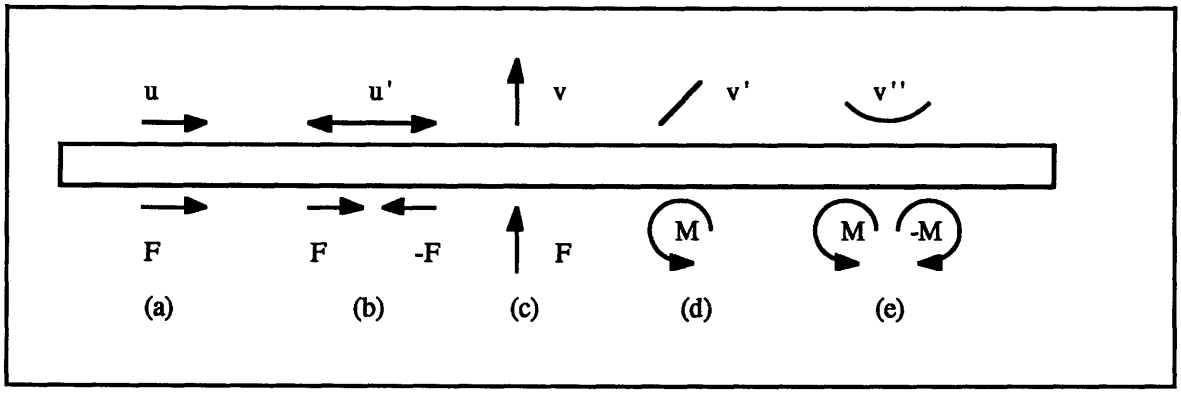

Figure 2.8. Typical structural sensors and actuators.

So for the representation of typical sensors and actuators considered in figure 2.8., the accuracy depends on estimated point values of axial displacement and transverse displacement and slope. In order to assess the accuracy of different finite elements of a beam, figures 2.9. and 2.10. compare the exact and estimated response for a beam in

bending and compression. Torsion follows the same partial derivative equation as compression and has the same shape-functions so that its case, when non-dimensionalized, corresponds exactly to compression and will therefore not be considered.

Figure 2.9. considers the axial motions of the tip of a free-free beam undergoing a collocated harmonic axial forcing at the tip. Figure 2.10. compares the transverse motions of the cantilevered beam with an intermediate collocated force actuation (the example of figure 2.2.. with $x_A = .5\ x_B$). In both cases the motions are undamped so that differences in the height of the spikes are due to numerical discretization of the frequency axis.

The first characteristic of these plots is that as expected the static behavior of the structure is well represented. In figure 2.9., where a rigid body mode is involved, only the quadratic element captures exactly the static response, as it includes inertia relief modes. For other models the inertia relief flexible deformation is not exactly represented, and the difference between the exact and estimated transfer functions tends to a finite error at DC (as the response is infinite the *relative* error does go to zero). In figure 2.9., this results in a much better estimate of the low frequency behavior: at a normalized frequency of 1, the linear element has a 13% relative error, the 2 linear a 3%, and the quadratic a .07%. This effect is also seen in the accuracy of the first zero location.

The estimates of the first resonance are poor in figure 2.9. For one and two linear elements, the relative frequency error is 10%, and for four elements still 3% (two quadratic elements, with the same 5 dof, have only .5% error). This poor accuracy of the linear interpolation functions is seldom a limitation, since resonant frequencies in compression (and torsion) are in most structures decades above the frequency range of interest.

In bending, the frequencies of interest often correspond to wave modes that are not well approximated by the cubic interpolation functions. As shown in figure 2.10., the initial finite element model, which uses one cubic element for each of the beam segments, is fine enough to represent the first two modes but is inaccurate afterwards. The refinement is done seperately for each of the two initial elements by a p- and an h-refinement. As

expected after the heuristic arguments of the introduction, the figure shows that the p-refinement (2 quintic elements) gives a better estimate of the low frequency response (the 4^{th} mode is much better captured). At higher frequencies (not shown on the figure) the h-refinement (4 cubic elements) captures a few more modes.

Although the frequency estimates for the first modes of p-refined models tend to be more accurate, the trend on modeshapes may not be true for control applications. This can be seen by comparing modeshapes or, equivalently, residues. The exact and approximate first modeshape (and first three spatial derivatives, plotted as transverse displacements) of a free-free beam in bending are plotted in figure 2.11. Although the modeshapes of quintic elements are closer in a spatial L_2 sense to real modeshapes, the tip values of all the spatial derivatives of the displacement are better approximated by the two cubic elements. Therefore if actuators and sensors are located near the tips, the relative error in an estimated transfer-function will in fact be smaller for the h-refined element, although a structural dynamicist would consider the model to be less accurate.

In conclusion, the value of the two different refinements depends on the model objective. The p-refinement will tend to give fewer but usually more accurate modes than the h-refinement. In choosing a type of refinement, one should not forget that innacuracies in the solution estimate of the continuous idealized model are of no importance if they are much smaller than the discrepancies between the real stucture and the idealized model. So, the h-refinement, beeing often easier to implement, is the practical solution in cases with no hard limit on the number of degrees of freedom and no extreme confidence in the continuous idealized model.

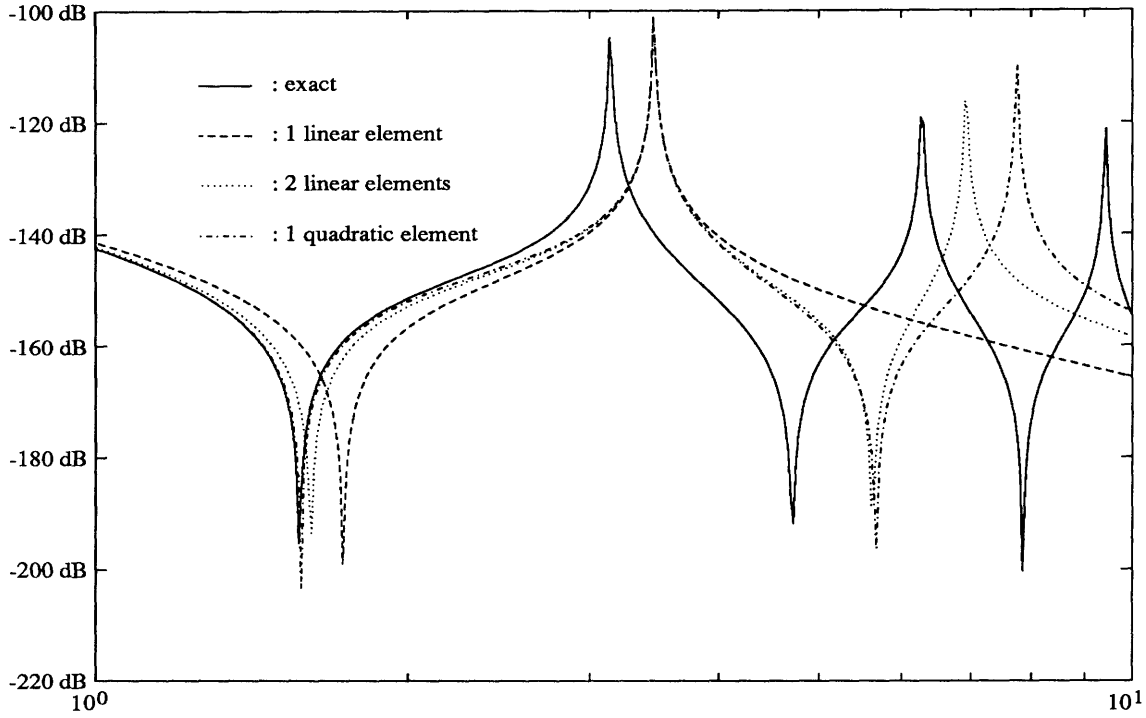

Figure 2.9. Amplitude of the tip displacement of free-free beam subject to an axial force at the same point as function of the forcing frequency. Exact and approximate solutions.

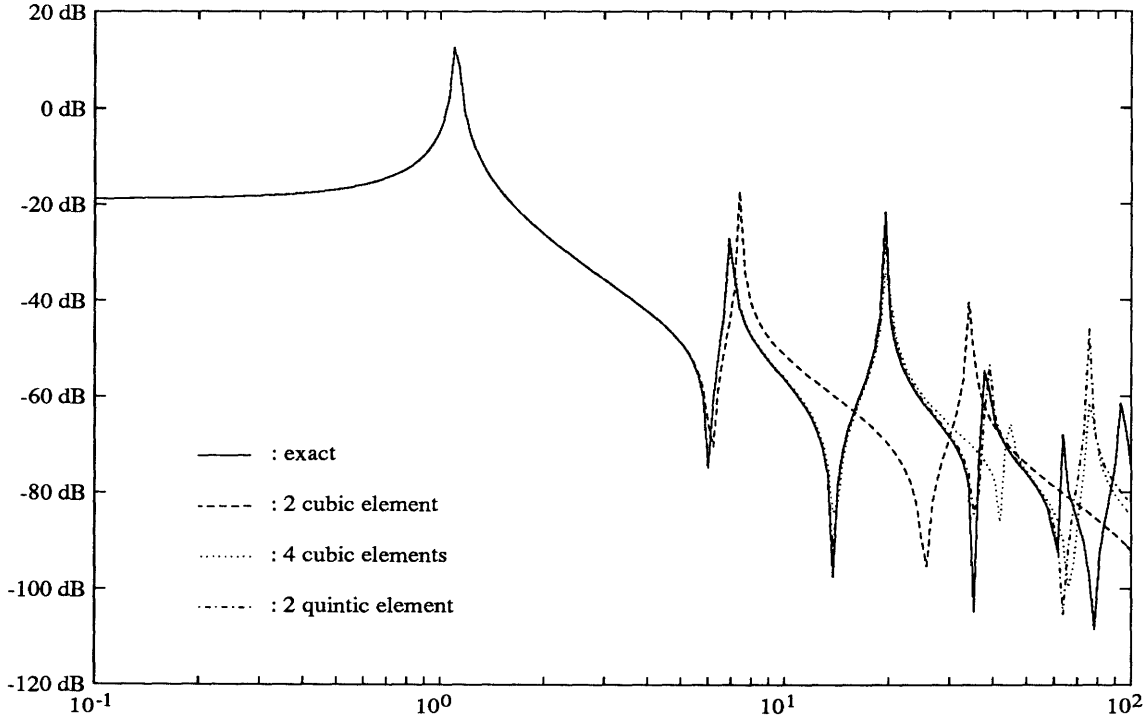

Figure 2.10. Amplitude of the tip vertical displacement of a cantilever beam subject to vertical forcing as a function of the forcing frequency Exact and approximate solutions.

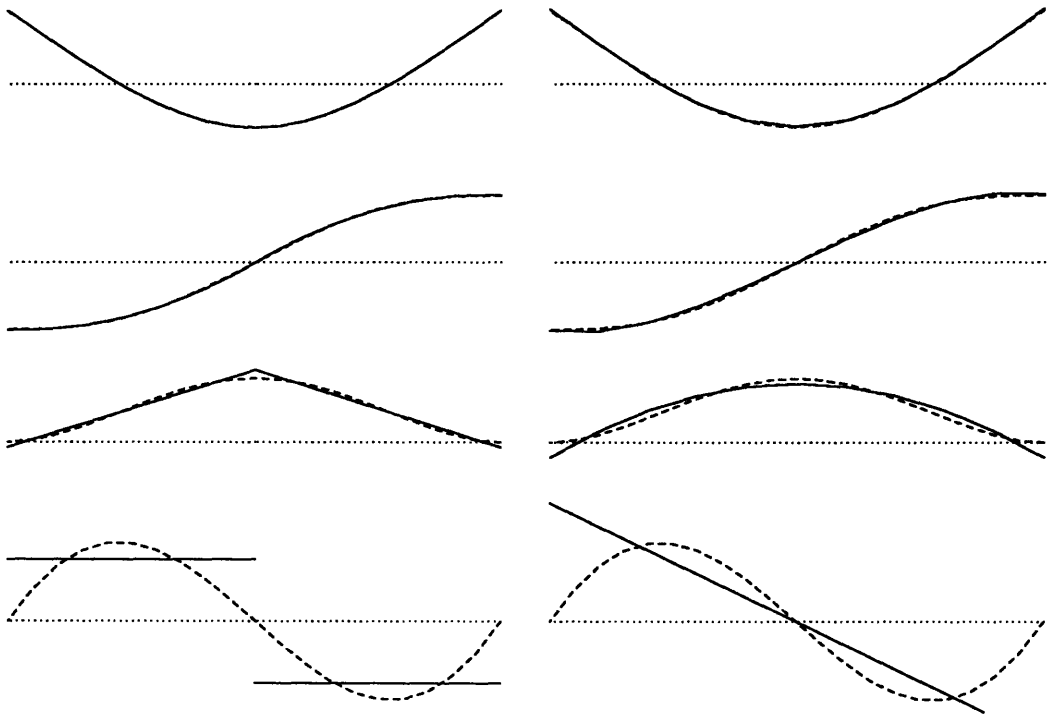

Figure 2.11. 1st mode position and curvature shapes of a free-free beam in bending. Left: 2 cubic elements, right: 1 quintic element, dashed : exact.

The extension to trusses of these considerations made for beams can be done by considering separately the beam elements of the truss (as the accuracy of the each element is a sufficient condition for the accuracy of the complete model). The accuracy of an element is limited in frequency: if the harmonic motions that it must represent have too short wavelengths the element will be inaccurate and should be refined. In practice, if the wavelength is twice the element length (which happens at the pinned-pinned mode frequency) significant differences begin to appear, so that a refinement may be needed.

In the case of the initial interferometer model (introduced in chapter I), a wavelength of two element lengths (50 cm) would be found around 8500 Hz in compression, but around 200 Hz in bending. So, as is usually true for truss-structures, the compression is very accurately modelled. However, if bending influences the global behavior, the convergence of the model can be expected to be inaccurate above 200 Hz.

The exact influence of insufficient refinement is also strongly dependent on the influence of the mismodelled phenomena on the modeshape characteristics. A good indicator of this influence is the relative amount of energy linked to the inaccurately modelled phenomena. For the interferometer, modes below 100 Hz have less than 1% energy in bending, so that modelling bending has almost no influence, at higher frequencies bending energy is a few percent so that inaccurate modelling of the quasistatic bending and of the local bending resonance can be expected and has been shown to be significant, above 100 Hz because of inaccurate modelling of static bending, and above 200 Hz because of insufficient mesh refinement.

2.4. Modelling truss-beams

2.4.1. Introduction

While the previous section considered the model accuracy for simple beams, the results can be extended to the case of trusses by considering the accuracy of the model of each strut. This section will introduce different truss-beam models, consider their accuracy, and show the main causes for the existence of dicrepancies between the response of the continuous idealized model and the corresponding finite element model.

The first step in the computation of an approximate solution is to introduce *kinematic assumptions* that describe the possible motions of the structure included in the model (Ritz or FEM shapes).

The second step is the introduction of *simplifying assumptions* that will enable a reduction of unnecessary degrees of freedom. The neglected degrees of freedom can either be set to zero (neglecting axial motions for example) or statically condensed, if the considered deformation behaves quasistatically. The difficulty associated with a valid static

reduction is that in many cases the degrees of freedom that should be condensed are not those of the initial description of the structure, but rather the degrees of freedom of a new description found by a linear, non-singular transformation of the initial degrees of freedom. For example, in the truss beam sample problem, the extension of the vertical strut can be considered as quasistatic but the vertical displacements of the two nodes at the extremities of the strut cannot. The main advantage of equivalent continuum ideas is to introduce a description where good simplifying assumptions can be made.

Finally, the *dynamic response* is computed and can be reexpanded to a form using all the initial degrees of freedom by inverting the expressions used at the simplifying stage.

These steps are discussed in the following sections, for the joint-plane approach, from which equivalent continuum models are derived, and for the midbay-plane approach that enables a low cost model accurate at higher frequencies. The discussion of the classical approach assumes that the reader is familiar with the construction of equivalent continuum models by comparison of energies (if such is not the case, [18] and [19] document the process in detail). In section 2.4.4. the accuracy of these models is compared using the truss-beam sample problem, and discrepancies are shown to correspond to frequencies where bending motions become important.

2.4.2. Joint-plane bay, equivalent continuum models

The classical approach considers a bay limited by joint points, as was shown in figure 2.4. For equivalent continua it is necessary to define relations between the displacements of the truss and those of the continuum. The linkage is made using Taylor series expansions of the continuum displacements and matching truss and continuum displacements at truss joints. The expression of truss displacement in terms of continuum displacment is, therefore, only meaningful at joints, which is a hard limitation on the accuracy of equivalent continuum models. It should be clear that this step is essential in the

use of the method for anything other than a conceptual model, since it links displacement and therefore modal information between the two models. In most cases, including the case of equivalent continuum approaches, the kinematic assumptions are that the motions for each individual strut are those of a standard 2-node static finite element, which (as shown in 2.3.2.) are cubic polynomials for transverse displacements and linear functions for axial and torsional displacements.

The dynamics of the model are defined as those of an initial finite element model with 1 cubic element per strut. The kinetic and strain energy estimates of an equivalent continuum bay-element are equated to this estimate using the kinematic assumptions. The equivalent continuum properties are fixed by this equation and the continuum beam element models the same dynamics as the initial model if no simplification is done.

After the definition of the dynamics, the model can be simplified or solved directly. No easy simplification can be done on the model with one element per strut, so that by changing the definition of degrees of freedom one simplifies the equivalent continuum form. Three types of simplifications are performed. To describe the truss as a series of repeated continuum bay-elements, *compatibility conditions* must be imposed with no other justification than the final model accuracy. *Model reductions* are performed by condensation of a certain number of degrees of freedom. As stated before, this is justified if the behavior of these degrees of freedom can be accurately modelled as quasistatic in the frequency range of interest. Finally, *dynamic assumptions* can be introduced which neglect or use different values for coupling terms in the stiffness and mass matrices (this is needed if one wants an equivalent beam in terms of equivalent cross-section properties: density, section area, section inertia, etc.). These assumptions are valid in many cases although no general justification exists.

Using this approach, the frequency limit of accuracy is linked to the proximity of local strut resonances, and refined models, such as the one proposed in section 2.4.3., are needed to get accurate results even below the actual local strut resonance frequency.

2.4.3. Midbay-plane model

This approach considers the bay shown on figure 2.6. as the repeated truss element. The initial modeled kinematics are those of 2-node elements for each strut of the bay, which corresponds to two elements per strut in the joint-plane description. As will be shown in chapter IV (in the study of the classical bay dynamics) this model captures accurately the first resonances of the truss members, so that truss dynamics found with the model used here are accurate up to and above the first local strut resonances.

As for the equivalent continuum methods, the real interest of this new approach lies in the simplifying assumptions that can be made. The degrees of freedom associated with joint nodes of the bays shown as circles in figure 2.12. are internal degrees of freedom that

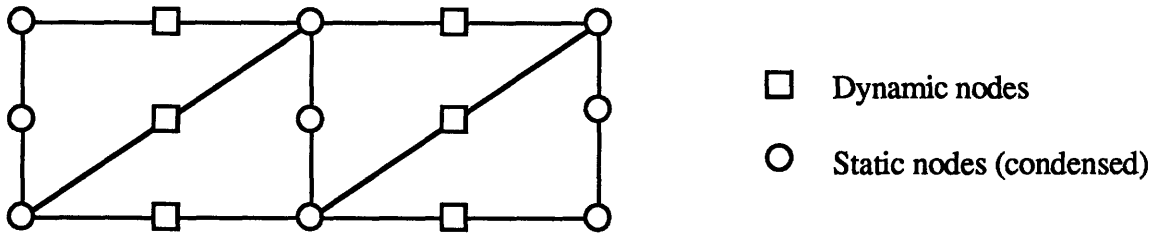

Figure 2.12. Dynamic and static nodes for a truss-beam model using the new approach.

can be statically condensed with almost no loss of accuracy in the frequency range of interest, which includes the first local resonances. The physical reason is that the joints are geometrically stiff, therefore fixing the states of strut midspans induces high frequency dynamics on the joint which, at low frequencies, are seen as a quasistatic behavior. The remaining dynamic degrees of freedom shown on figure 2.12. form a set complete enough

to represent accurately the truss dynamics up to the frequency where longeron and diagonal bending motions have an important effect. The number of active degrees of freedom is in this model slightly larger than for the equivalent continuum model, but the refinement is in different cases necessary to have accuracy in the full frequency range of interest.

On the truss beam sample problem, condensation of the joint degrees of freedom changed the approximate modal frequencies (up to and including the local modes) by less than .1% in both the pinned and clamped joint cases; it changed the modeshapes by only a few percent for an Euclidian norm on the nodal displacements.

The definite advantage of this approach compared to the classical method is that linear joint behaviors can be introduced easily and without increasing the size of the dynamic problem. Since it has been found that the joints behave quasistatically in the two extreme cases of the pinned and the clamped joint, one assume that they will still do so in the intermediate cases of joints with linear rotational stiffness. The correction of joint behavior will only appear as a correction on the mass and stiffness matrix of the dynamic degrees of freedom, so that the model cost is increased only by the computation of the correction. For other linear joints or non-linear joints approximated by describing functions, the quasistatic joint behavior would have to be assessed, but the method definitely provides a very effective tool to get a first estimate of the dynamic behavior of a truss with non-trivial joint behavior.

The importance of modelling rotational rigidity at joints depends partially on the energy stored in bending, and the new approach gives much more accurate estimates of the strut bending behavior so that even if joint models were possible in the classical approach, the midbay-plane model would be much more accurate without using many more dynamic degrees of freedom.

2.4.4. Comparison of results and validity ranges

As a mean of assessing the validity range of the different models, the truss-beam sample problem (see description made in section 1.3.) will be used. Figure 2.13. shows modal frequencies of three models of the truss-beam.

The first set of frequencies corresponds to a Bernoulli-Euler beam with a first mode matched to the actual first frequency of the truss, which is the result of a simple equivalent continuum modelling approach. For this model even the second mode is innacurate. For other truss configurations it could match more of the behavior, but when bending effects due to clamped joints or resonant struts are present no agreement can be expected. The second set of frequencies corresponds to a model with one element per strut, which is the limiting performance achievable by equivalent continuum approaches. The first and second modes are good, but not the following ones. The bending half-wavelength is the length of the diagonal element at 103.5 Hz, so that significant influence of diagonal strut resonance should be, and indeed is, seen above that frequency. The third set of frequencies corresponds to a model with two elements per strut, which is the limiting performance of

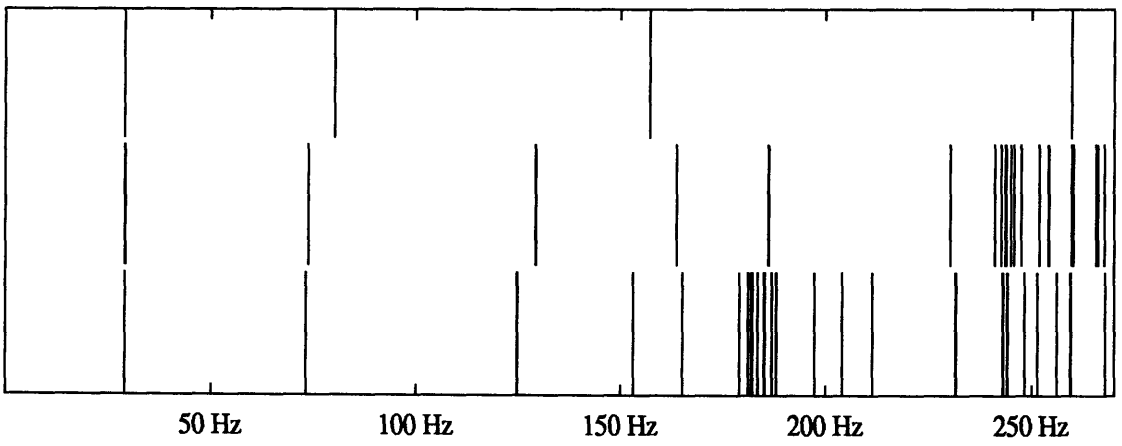

Figure 2.13. Modal frequencies of the truss beam models: Bernouilli-Euler beam, 1 element per strut, 2 element per strut.

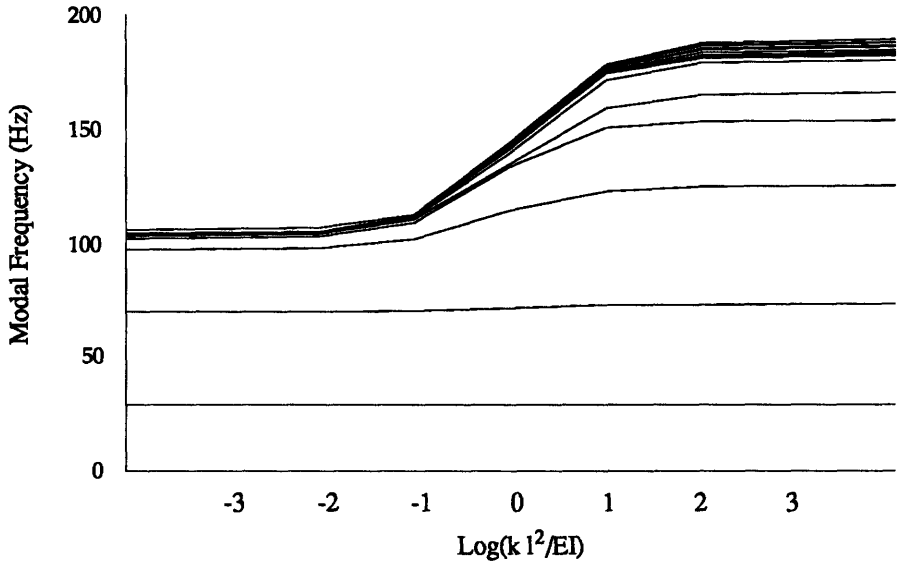

Figure 2.14. Effect of joint rotational stiffness on modal frequencies of the truss-beam.

the midbay-plane modelling approach. For most purposes, accuracy can be expected in the frequency range of interest (0 to 200 Hz). The presence of internal degrees of freedom on each free segment (nodes at strut midspans) gives a good *a priori* confidence in the agreement that is effectively observed. The accuracy of the model will be confirmed by the study of bay resonances in chapter IV.

As an application of the new method, the evolution of modal frequencies of the truss-beam sample problem was computed as a function of joint rotational stiffness and is plotted on figure 2.14. The first two modes are almost independent of joint stiffness (.5% and 2.5% variation in frequency): they are global modes that would be well predicted by both the classical and the new approach. The following modes show a much heavier dependance on joint properties(>25% variation in frequency); bending influences the truss behavior and therefore the classical equivalent continuum method would give innacurate results. The micropolar equivalent continuum developed by A.K. Noor [15] would

probably give acceptable results for the third mode but not afterwards, since the subsequent modes involve local resonances of the bays that are not accurately described by the model with one element per strut.

CHAPTER III

CORRELATION WITH EXPERIMENTAL RESULTS

3.1. Introduction

The purpose of all models is to give a good representation of actual physical phenomena. In structural dynamics applied to controlled structures one is essentially interested in the low frequency dynamics of the structure, with a special interest in a good representation of modal frequencies and modal residues linked to the different sensors and actuators, or in other words, one is interested in good representations of the input/output transfer functions. The construction of the structure dynamic model is one of the most important steps in the control design, since it conditions the validity of any control methodology that may be applied.

In chapter II, so that finite element solutions could be of effective use, the size and form a finite element model should have to be a good representation of the continuous idealized model of the structure was discussed. This chapter will: give a better understanding of the different parameters that enter the definition of the continuous idealization, show how different updates of this conceptual model can be introduced using measured data to get a better estimate of the response, and list some of the errors that are often present in this idealized model.

For truss structures many testbeds (refs. [21]-[23]) give examples of comparisons between models and experiments. In this chapter the interferometer testbed and the Γ-truss (both described section 1.3.) will be used as examples to support different considerations.

Section 3.2. discusses the methodology usually applied in the modelling approach: construction of an initial model from hardware specifications, update using component properties measurements, and update using structural dynamic measurements.

Section 3.3. reviews usual modelling errors focusing on both causes and effects.

3.2. Methodology

This section discusses the standard steps in the creation and update of structural dynamic models, and the framework is illustrated by the case of the interferometer and of the Γ-truss testbeds.

Initial model

Before a structure is built, an initial finite element model is usually created based on the hardware specifications. The normal procedure is to create a detailed continuous model describing the structure as an assembly of components (beams, plates, joints, ...) with precise local properties (stiffness, densities) and simple behavior descriptions in the form of partial derivative equations. In the model, assemblies (struts composed of different connected parts) should be described as different parts.

As the continuous solution is not computable with available analytical tools, one usually creates from the continuous idealized model a detailed finite element model, as was done in chapter II. This model has typically many more degrees of freedom than acceptable or useful for the dynamic model so that a static condensation of many of the degrees of freedom should be performed.

For the Γ-truss, the model was reduced from 1900 dof to 216 dynamic dof. For the interferometer testbed, the reduction was done as an initial step before assembly of the model. Each strut was described by a 48 dof model which was condensed to 12 so that

equivalent properties (matching the mass and stiffness matrix diagonal elements) could be computed and incorporated in the model as one strut element. This process reduced an initial model that would have had 26424 dof to a 1368 dof model.

The accuracy of this initial model is a central issue since it is the only working tool for control designers, as long as no update is performed using experimentally obtained data. Many assumptions are usually made for the creation of this initial model concerning the phenomena that are and should be modelled, and these will be discussed in more details in section 3.4. However, assuming that the structure is built according to the specifications and that there is no major unmodelled dynamic effect (e.g. suspension effects), the usual accuracy that can be expected is less than 10 % percent error for modal frequencies and an acceptable accuracy for modeshapes (no phase error far from nodes and global shape agreement, with node meaning "point where the quantity of interest is zero). This of course assumes that the finite element model gives a proper solution of the underlying continuous model, as was discussed in chapter II.

The accuracy of the modeshapes is heavily dependent on modal density: the sensitivity to perturbations in the structure is inversely proportional to modal frequency separation (see section 1.2.2.), so that the higher the modal density the less confident one can be in the modeshapes. In the limiting case of modes having identical frequencies, individual modeshapes are not defined but span a subspace. Reasons for the presence of high modal density, at low frequncies, will be analyzed in chapter IV, but it is generally caused either by approximate symmetry or by decoupled local vibration.

For the Γ-truss, the identification of the first two modes was not valid in the initial model: their proximity, coupled with a inaccurate stiffness estimate, induced a significant modification of the modeshapes, which caused a phase error between the sensor and the actuator location.

The sensitivity due to high modal density makes both analytical and experimental measurements inaccurate, so it is always difficult to analyze. The consequences on MIMO

controller stability and performance are not completely known, so no general conclusions can be drawn in terms of the influence of such perturbations on controlled structure characteristics. Damping, though, dimishes the importance of modelling errors by augmenting the modal overlap (see chapter IV).

No general rule can be given on the accuracy of point informations of a model, but some of the following considerations may help. Continuous models are able to represent the response of the structure and it is possible to create finite element models that give accurate estimates of the low frequency modes of the continuous idealized model (as seen in chapter II). If the material properties are well known, if the modes are well separated (for example, relative separation greater than 15%), and if no omission has occured in the modelled dynamic phenomena, the continuous model underlying the finite element model can be expected to give modal frequencies with less than 10 % error and all the major dynamic characteristics of the response, even though zeros (i.e. transfer-function phases) could be very inaccurate. The accuracy of the finite element model is limited in the high frequencies by the kinematic assumptions made on the structural behavior (mesh and element type of the finite element model) as these assumptions put a upper limit on the wavenumbers that can be accurately represented. Under the previous assumptions, and for frequencies where displacements can be considered quasistatic over an element length, one can expect local results to be accurate if they are not near nodes. Where nodes are points at which the quantity of interest is zero, so that nodes of displacement, slope and curvature are different points.

Updating with component measurements

The first possible update of the initial model is the inclusion of measured component properties. Once the structure is built, but not necessarily assembled, it is often relatively easy to measure actual properties of components, such as mass and stiffness distributions of the struts composing a truss. Using these measurements the model can be

corrected. This step is clearly desirable and is probably the only affordable update that can be done for a structure which could not be fully tested before its first real use; but it can be very tricky: the definition of boundary conditions for the element test is essential. In the component test a distinction must be made between the measurement and the parameter that will be used to update the model of the real structure, and careful attention must be paid to get results that can be extrapolated to the real structure. Usually one measures stiffness and mass distribution properties.

The struts of the interferometer are formed of aluminum tubes tightly screwed to aluminum ball joints. The initial guess for the strut properties was based on a detailed model of the strut. The aluminum tube and the screws were modelled as beams and the ball joints as rigid bodies. This model gave an axial short strut stiffness EA/l = 12.83 N/μm (which was later measured as 12.9 N/μm). The assumption of rigid aluminum ball joints was an error that resulted in an axial stiffness overestimated by 12% and gave frequencies for the first 20 modes overestimated by approximately 6 %. A first test with the ball joints replaced by aluminum fittings gave an estimate of the axial stiffness EA/l = 10.5 N/μm, but this component test did not include the real joint stiffness so that the estimated modal frequencies were under the actual ones. A test with a real ball joint at one end gave an estimated axial stiffness EA/l = 11.2 N/μm. This test included the real joint stiffness, and the corresponding last update gave frequencies of the first 12 modes within 2% of the actual ones (see section 3.3. and table 3.2. for further details). At that point, the remaining uncertainty in the real stiffness distribution, still accounted for more than the measured error in frequency.

Errors in modelling the mass distribution have a strong influence on local bending motions. For the first twelve of modes of the interferometer, which are characterized by axial strut motions, uncertainty in the mass distribution could account for up to about .5% error in the modal frequencies. At higher frequencies bending motions having more influence, and errors could go up to 5% or more after the 20^{th} mode.

In general the component test update should be considered with caution and cross-checked with global structural dynamic measurements. The failure to do so might lead to the update of some properties, while others having a comparable influence are not updated, so that the global change could be meaningless.

Updating with structural dynamic measurements

The first difficulty when updating with structural dynamic measurements is with the generation of the measurements. The object of this analysis is not to give a detailed review of all the difficulties encountered in a structural dynamic identification, and textbooks such as references [24] and [25] have much more information than could be given here. In practice, modal frequencies can be measured quite accurately but damping and modeshapes measurements should be considered with much more caution. Nevertheless, assuming that accurate modal characteristics are available, the question is how to update the initial model to match the actual properties better. No generally accepted method is available for that update, so a number of references corresponding to different methods should be cited: [26]-[29].

The first step of the update, and also the one where engineering judgement has the most influence, is the determination of the form of the error. The errors that can be handled by an update can lie in the mass or the stiffness distributions, they can be global (parameter, such as Young's modulus, incorrectly estimated over the whole structure) or local (one particular strut is less stiff). Global errors are the easiest to handle, but there exist some ways of characterizing local errors (refs. [27] and [28]) within a restricted error-form framework. The restriction of the type of local and global errors is necessary since there are never enough measurements to deterministically update all the parameters of the model. Of course this restriction itself introduces an arbitrariness which may be the source of error (see ref. [30]).

The second step is the determination of what is expected to match. Obviously, modal frequencies should match, but for modeshapes the question is unclear since measurements and modelled modeshapes do not have the same forms. As seen in section 1.2.1., different methods to define the agreement can be used and give different results (also see refs. [27] and [29]).

Finally, the update can be done in an exact approach (matching exactly a finite number of characteristics), or in an optimal sense (minimizing a cost that includes all the "important" parameters of the problem). In the optimal case, one computes different complete solutions, or more efficiently makes a mixed use of complete solutions and of sensitivities to different parameters found using the perturbation method.

In both cases the method gives a new model that matches characteristics considered important. But wether this model is a better approximation of reality depends essentially on the definition of "better", or, in other words, on the intended use of the model. For further details on the characterization of model error see section 1.2.1.

3.3. Review of usual modelling errors

In the modelling process several modelling errors are usually made because of inexact assumptions about the structure. Errors can be voluntary (neglected suspension, neglected prestress ...) or involuntary (geometric reality differs from engineering drawings, ...). The engineering problem is to assess which of these errors should be corrected to get a good model. Errors can be categorized according to their causes or their effects, and the object of this section is to give a list of these categories, supported by examples found during the modelling of the interferometer testbed.

The main cause of error is human: bad measurements, bad acquisition of numerical parameters for the model, discrepancies between engineering specifications and actual

hardware, etc. are well known to all engineers but have no cure and no predictable effects in general. Other essential causes of error, which will be further detailed, are unmodelled geometric reality, inaccurate estimation of the model solution, unmodelled phenomena, and non-linearities. The effects can be of many types, but the following categories will be used as subsections: biased and unbiased global errors, local errors, neglected stiffness and resonances, and other unmodelled phenomena.

Biased global errors

Biased errors in the estimation of global parameters cause the model to give consistently under or overestimated modal frequencies and induce changes in the modeshapes that affect all the structure. The amplitude of model errors is closely related to the relative error in the strain and kinetic energy estimation: if for a given mode 99% of the energy is due to compression, a percent error in the transverse moment of inertia will have almost no effect (see expression of the first order perturbation in section 1.2.2.), but a percent error in the axial stiffness will induce almost a percent error on the frequency squared ($\sqrt{1.01}$ error on the frequency). The effect on modeshapes is essentially dependent on whether or not the modelled mass and stiffness matrices can be considered as proportional to the actual ones. For a truss structure dominated by axial motions, an error in the strut axial stiffness is proportional, so estimated modeshapes are correct, but an error in bending is not proportional, so modeshapes will change for modes influenced by bending. Modal frequency separation is an important factor for the general accuracy of all models but in the case of global errors its influence tends to be small. The following paragraphs describe some of the factors that cause biased global errors.

Innacuracies of global property estimates, such as axial strut stiffness for trusses, are usual and should be corrected (with component measurements) during the update (as detailed in section 3.2.). Table 3.2. gives the variations of the estimate due to the use of different values of the strut axial stiffness (as discussed in section 3.2.). The first column

gives measured frequencies (the presense of the modes in parenthesis is deduced from the finite element model, suspension modes are not included see table 3.3. which focuses on this problem), and the last two give the relative error in the frequency estimate for axial stiffness EA/l = 12.83 N/mm and 11.2 N/mm respectively. For the first twelve modes which are characterized by the same first bending mode of the legs, the frequencies squared all decreased by about 6.5% between the first and the second approximate model. For the following modes, bending has more influence and the frequency shift is smaller. The change of stiffness and mass distribution is basically proportional for the first twelve modes, so that the sensitivities of the modeshapes to the change of modelled axial stiffness are below .1%, but for modes 13 to 20, bending becomes more important and the sensitivities go up to 3%.

Table 3.2. Measured modal frequencies of the naked interferometer testbed, and relative error on modal frequency for strut axial stiffness EA/l = 12.83 N/mm and 11.2 N/mm.

ω_{meas} (Hz)	$\Delta\omega_{E1}$ (%)	$\Delta\omega_{E2}$ (%)	ω_{meas} (Hz)	$\Delta\omega_{E1}$ (%)	$\Delta\omega_{E2}$ (%)
35.10	5.73	2.30	55.20	4.64	1.36
(35.10)	5.73	2.30	55.60	4.59	1.30
38.90	6.98	3.42	100.80	6.19	3.80
39.40	5.62	2.11	101.70	5.25	2.88
(39.40)	5.81	2.29	102.00	4.96	2.58
43.30	6.27	2.80	105.50	6.27	2.72
43.70	5.39	1.96	111.00	5.96	2.57
(43.70)	5.39	1.96	111.50	5.49	2.11
52.10	5.56	2.13	112.50	4.38	2.16
54.70	5.60	2.28	112.50	6.37	3.54

Non-uniform distribution of some properties can lead to biased global errors of unknown amplitude. For the interferometer, strut misalignment always leads to a smaller

apparent axial stiffness. As a simple way to prove this, one can consider a segment with two half struts separated by a ball joint. If the junction points of the struts with the joint are offset from the nominal straight line, with the struts remaining straight but not following the nominal direction, a coupling between compression and bending motions is introduced resulting in apparently lower axial stiffness. For 1° rotation of the connection points on the joint, the axial stiffness is reduced by .5%, and for 2° by almost 2%. A 2% overestimate of the mean axial stiffness would result here in approximately 1% error in frequency, but there is no way to measure the real mean stiffness so this error has to be considered generic and may be used in updates with structural dynamic measurements.

Prestress and predeformation also modify the behavior in sometimes biased manners. For example, pretensioning cables in a truss will lower the bending frequency of the struts so that the influence of bending motions increases with pretension. General tools to include these effects are not readily available, but it would be possible to introduce in a finite element code an automatic correction for initial structural modifications.

Unbiased global errors

Unbiased global errors are global errors for which the best estimate is zero. This usually means that some structural properties are not or cannot be known with a better precision than that used in the model. Such properties include initial estimates of component material properties, which can be updated through component tests, and distributed geometrical properties of nominally identical components, which cannot usually be updated.

Unbiased global errors can be corrected either by measuring estimated properties (the error is then biased until the model is corrected), or by updating the model through structural dynamic measurements (as described in section 3.2.). In the later case the process is not unique, so careful attention must be paid to the physical significance of the solution (see ref. [30]).

Local errors

This type of error groups all the cases for which voluntarily or involuntarily a part of the structure (one or a few struts of a truss for example) is very different from the model description. The effect of such modelling errors depends essentially of two factors: the relative amount of strain and kinetic energy energy found in the mismodelled part compared to global strain and kinetic energies, and the modal frequency separation which is related to the minimal variation in the energy distribution needed to get significant changes in the modeshapes.

Using the definition of the first perturbation (given in section 1.2.2.), one could prove that if the relative error in energy is small (so that $|-\omega^2 \phi^T M^{(1)} \phi + \phi^T K^{(1)} \phi| < .1\ m\omega^2$) and the frequency separation is important ($|\omega_i^2 - \omega_j^2| > .1\ \omega_i^2$), the sensitivities to the perturbation are small ($c_{ij} < .01$). For the interferometer unmodelled active struts, with a third of the nominal axial stiffness, where present in the structure. Placing an active strut in the middle of a leg, the resulting relative error in energy was, for the first 20 modes, less than .5% for the kinetic energy and less than 3% for the strain energy , so that the perturbation should only be noticeable for the degenerated modes. The actual perturbation analysis gave modeshape sensitivities of less than 2% except for almost degenerated modes for which the analysis is not valid.

Obviously local errors that have a significant influence should be corrected, but it is often hard to pinpoint involuntary errors. Some attempts ([28]) have been made to identify such errors from measured modal data, but these cannot to date be used as general tools.

Unmodelled stiffness and resonances

Three important cases fall in this category: internal resonances, suspension effects, and unmodelled resonances.

Internal resonances of continuous systems produce modelling errors when the resonances are near or in the bandwidth of interest and the form chosen for the finite element solution is not able to represent them (see chapter II). An example, often used in this report (chapters II and IV), is the bending resonance of struts in truss structures. For the interferometer testbed, local resonances appear a little above 200 Hz and significant errors due to inaccurate modelling of bending can be expected down to 100 Hz (at that frequency bending represents more than 5% of the strain energy, and wavelengths in the struts are of the order of two strut lengths).

Suspension effects are an major difficulty of ground testing, as the stiffness of the suspension may have some non-negligible effects. The Γ-truss, for example, was cantilevered from a large isolation mass supported by air-bags, but although the mass largely outweighed the truss, rotational inertia effects were important and a model of the support was necessary to get good agreement between measured and estimated modeshapes.

For the testing of proposed space based structures, the ideal suspension induces very low frequency modes with an almost rigid structure. Passive solutions to this problem use very soft springs. However, as was found for the interferometer testbed, long soft springs have high levels of internal axial resonances (i.e. surge modes of the suspension), so that a trade-off must be made between low rigidity and low levels of internal resonance. Table 3.3. gives measured and predicted modal frequencies for the interferometer (the predicted frequencies are those of the second update considered in table 3.2.). The surge modes of the suspension, which appear clearly in the testing, where not modelled. This resulted in a misinterpretation of the measured results. The testing also missed many of the almost degenerated modes of the structure, but a multi-input experiment would have been necessary to separate these, so that the model gives some essential information about the structure which could not be seen during the single actuator testing.

Table 3.3. Measured modal frequencies of the naked interferometer testbed, compared with the predictions of a model without suspension.

$\omega_{measured}$	$\omega_{predicted}$	$\omega_{measured}$	$\omega_{predicted}$
31.35	suspension	55.20	55.95
31.75	suspension	missed	56.32
35.10	35.91	62.70	suspension
missed	35.91	63.40	suspension
38.90	40.23	94.10	suspension
39.40	40.23	94.80	suspension
missed	40.30	95.00	suspension
43.30	44.51	100.80	104.63
43.70	44.56	101.70	104.63
missed	44.56	102.00	104.63
52.10	53.21	105.50	108.36
54.70	55.95	111.00	113.85

Other unmodelled phenomena

The list here could be very long so only usual and well known cases are treated.

Damping is almost never modelled initially, and is added for control purposes as modal damping on the undamped estimated modes. This is accurate, if proportional damping is a good hypothesis, and damping levels can be estimated from measurements (measured damping levels should be taken with caution as 100% errors are usual). But in any case, initial models of damping would be hard to introduce since many real unintentional damping mechanisms are not well understood. For example, wires add significant damping to testbeds. Damping treatments are better understood, and can be modelled with high fidelity, though usually requiring the introduction of additional states. Modelling and study of proportional and non-proportional damping mechanisms is certainly of major importance for future developments of controlled structure technologies.

Non-linearities (ref. [31]), which occur for trusses essentially at joints and in cables, can be sources of errors. The main effects of small non-linearities are amplitude dependence and non-harmonic response, which are difficult to deal with and much more work is needed on the subject.

Gravity is an important factor in the use of ground tests as update bases for space structure models. The modification of behavior due to gravity can be important and should be taken into account, but little work has been done to date on the subject ([32] is in preparation)

CHAPTER IV

HIGH MODAL DENSITY

4.1. Introduction

One of the most challenging difficulties in future space structures is their high modal density. Due to stringent mass and stiffness requirements, they will tend to have a fair portion of their mass distributed over large areas, which induces low frequency and often very closely spaced resonances. As seen in chapter I, the sensitivity of modeshapes characteristics to perturbations is inversely proportional to the relative modal frequency separation, so that the characterization of structural response by the use of modeshapes becomes more and more difficult when modal density increases. As high sensitivity implies high influence of modelling errors, it is essential, for control and identification purposes, to study the porperties of structures with high modal density. An assessment of the exact influence of errors in the estimation of modal characteristics on the actual input-output response should then be possible.

The limiting case of high modal density is modal degeneration where different modes have the same frequency. The appearance of degeneration is always linked to uncoupled vibrations, which may be linked to symmetry or local vibration. This chapter will study the general properties of degeneration due to symmetry and the effects of near degeneration due to substructure vibration. In the case of the truss-beam sample problem (described in section 1.3), this will present a clearer picture of the properties of almost degenerated modes and, in one case, show how damping has a desensitizing influence that increases with modal density.

In section 4.2., algebraic properties of symmetric structures will be used to gain a better understanding of their dynamics. The decomposition of modes into symmetry types and the cases of symmetry imposed degeneration will be treated. Two examples, a simple triangle of beams and the interferometer testbed, will be used to show typical conclusions that can be drawn.

In section 4.3., the case of substructure vibration will be examined. For the truss-beam sample problem, in the case of clamped joints where the structure seems fully coupled, the conjecture that degenerated modes correspond to the vibration of uncoupled substructures will be confirmed by finding a small perturbation inducing modal localization. The effect of diagonal strut vibration, which characterizes the modes subject to localization, will then be analyzed as the effect of distributed proof-mass dampers. Using this point of view the desensitizing influence damping on the response in terms of transfer functions will be shown, giving a better perspective on real characteristics of the structure, than the highly sensitive modal description.

4.2. Degeneration due to symmetry

4.2.1. Theoretical results

Symmetric structures have dynamic properties that can be deduced from the algebraic properties of the group of transformations that leave them invariant. This fact is well known in quantum mechanics where group theory plays a leading role. But the application of such considerations to structural mechanics is rather unusual (see ref. [33]). This section details essential results in this field so that the reader may understand the main implications of the theory and apply them to simple cases. To be used these results necessitate the knowledge of a number of definitions that will be given in the following

paragraphs. In practice, the most useful information is found in character tables, such as 4.1., which will be analyzed as the different critical ideas are introduced.

Table 4.1. Character table of T, tetrahedral group with no reflections.

T	E	8C3	3 C_2
A	1	1	1
E	2	-1	2
T	3	0	-1

V, *the vector space of possible deformations* is the space of functions that mathematically represent the deformations and motions that can affect the structure. If the structure is represented by a discretized model, V is a m-dimensional real vector-space, $V=R^m$, where m is the number of degrees of freedom of the discretized model. In further developments the model will always be assumed discrete but all results still hold for continuous cases with minor modifications.

One says that a structure is symmetric if there is a set of isometric transformations that leave the structure invariant. An isometric transformation (such as a rotation or a symmetry) is a transformation that leaves lengths unchanged. The structure is left invariant if the structures before and after the transformation cannot be distinguished. For the mathematical discretized model each physical transformation is represented by a matrix, and carrying out the transformation is done by multiplying the state vector on the left by the matrix. The isometric operations leaving a structure invariant always form a group, called G, *the group of symmetry of the structure*. The name of the group is given in the upper left cell of the character tables (here T for tetrahedral). The structure group of symmetry does not depend on a particular basis chosen to describe the motions of the structure and certain

dynamic characteristics of the structure can be deduced from the mathematical structure of the group.

Groups are formed of *elements*, σ, wich are listed in the first row of the character table (in table 4.1., E is the indentity; there are 8 rotations of $2\pi/3$, noted as 8 C_3; and 3 rotations of π, noted as 3 C_2). For a given space of possible motions (V or any of its subspace for which it makes sense) a *representation* of the group is the set of isometric transformation matrices, σ_V, associated with each of the group elements, which carry out the group operations on the considered vector space. The transformation matrices (σ_V) depend on choices of basis that can be done, but the algebraic structure of the group they form is fixed.

The *character* of a matrix element of a representation is the trace (i.e. the sum of the diagonal elements) of the transformation matrix. Although the matrices that form the representation are dependent on specific choices of basis, their characters are invariant and contain the important information about the algebraic properties of the representation. For groups composed of a finite number of elements, the characters of the elements of an associated representation cannot be arbitrary: the vector formed by the characters of each of the matrices in the representation (vector of the $tr(\sigma_V)$) is a linear combination (with positive integer coefficients) of a small number of minimal character vectors ($\chi_i(\sigma)$). The minimal character vectors are character vectors of *minimal representations*, defined as representations such that no change of basis exists that gives to all the group element matrices a block diagonal form other than the "one block per matrix". Character tables give a list of all the minimal representations of a given group. Their names are listed in the first column of the table with the standard convention that A designs a one-dimensional representation, E a 2-D, and T a 3-D. Then, for each minimal representation, the characters of the matrix elements of the minimal representation ($\chi_i(\sigma)$) are given in the rest of the table. The construction of character tables is difficult and usually not necessary since they are widely available in standard texts on group theory (see ref. [33] for example).

The expression of the characters as a linear combination of minimal characters is called a decomposition and corresponds to another very important property: a change of basis exist, for which all the matrices of the representation have a common block diagonal form.

The dynamics of the structure are, for a discretized model, characterized by a mass and a stiffness matrices. The fact that the transformation matrices of a representation (the σ_V) leave the structure invariant implies that all these matrices commute with M and K: $M\sigma_V = M\sigma_V$, $\sigma_V K = K\sigma_V$. This property of commutation with a group of matrices having a particular block diagonal form imposes a block diagonal form to K and M.

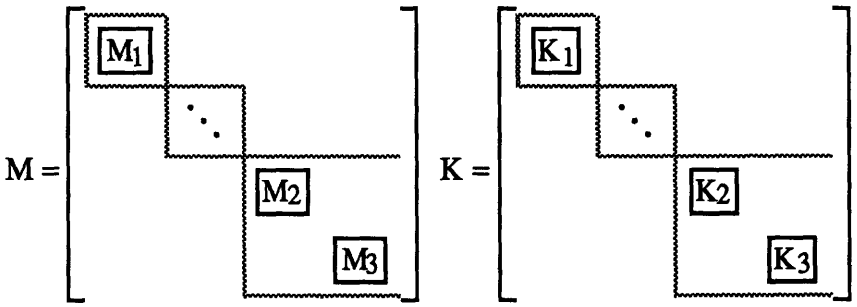

Figure 4.1. Block decomposition of the mass and stiffness matrices of a symmetric structure according to symmetry types.

In the basis where all the σ_V are block-diagonal K and M are also block diagonal (see figure 4.1.) and each block of K and M is associated with a single minimal representation so that the base vectors of each block have common properties which are usually refered to as *symmetry types* (the most familiar symmetry types are symmetric and antisymmetric behaviors for a beam). In many cases the block has a dimension much greater than the minimal representation it is associated with, but its base vectors can be divided in subsets such that the representation of the group for each subset is the minimal representation associated with the block. The decomposition in block diagonal form can be obtained by application of simple formulas that give the projections on the subspaces of each symmetry type:

$$\pi_i = \frac{h_i}{h} \sum_{\sigma \in G} \chi_i(\sigma)\, \sigma_v \qquad (4.1)$$

where π_i is the projection of V on the subspace of vectors of the i^{th} symmetry type (corresponding to the i^{th} minimal representation of the group as given by the character table). h_i is the dimension of the i^{th} minimal representation (also equal to the character of the identity) and h is the number of elements in the group. $\chi_i(\sigma)$ is the character of the element σ in the i^{th} minimal representation of the group, which is found at the intersection of the i^{th} row and of the column corresponding to σ in the character table. σ_v is the matrix associated with σ in the representation of the group on V.

The dimension of each block, or number of vectors of each symmetry type is found by applying the following formula derived from orthogonality conditions on the character vectors (with the same notations as (4.1)):

$$\dim(U_i) = \frac{h_i}{h} \sum_{\sigma \in G} \mathrm{tr}(\sigma_v)\, \chi_i(\sigma) \qquad (4.2)$$

Now that all these properties have been introduced, the main useful results that are derived from this theory are:

All the modes of a structure have a symmetry type. This is quite obvious since K and M are decomposed in a block diagonal form with the base vectors of each block having a common symmetry type. For a non-symmetric structure, the group of symmetry only contains the identity so that a symmetry type has no characteristics. Otherwise, geometrical characteristics of the different symmetry types are found by considering the spaces onto which the π_i project. Familiar characteristics are symmetric and antisymmetric, but more interesting properties exist for more complex symmetries (see the examples treated in 4.2.2. and 4.2.3.). Consequently *the number of modes of a given symmetry type is given*

by the dimension of the subspace of that symmetry type: $\dim(U_i)$ which is found using (4.2).

The modes of a symmetry type have at least multiplicity h_i (the dimension of the minimal representation associated with the symmetry type). This result is very important since it governs the degeneration of modes at low frequencies. At low frequencies it is very unusual to have two different modes of different or identical symmetry type at the same frequency. Therefore, the degeneration of low frequency modes is almost always the multiplicity of their symmetry type (it cannot be less but could eventually be more).

The application of these results to the "a priori" analysis of the response of a symmetric structure enables: the characterization of geometrical properties of different modes by the decomposition into symmetry types, and the knowledge of the number and degeneration number of modes of each symmetry type for a discretized model.

4.2.2. Example: Trifold symmetry

This first example considers an equilateral triangle formed of three beams connected at their vertices by rigid joints fixed in translation. The simplest discretized model of this structure uses a 2 node beam element for each beam and assumes planar motions. This model, which gives a good idea of the first three planar modes of the structure, considers one degree of freedom for the rotation of the each of the 3 joints: $V = R^3$.

The structure is invariant by the identity transformation (called E), by rotations of $\pm 2\pi/3$ (called C_{-3} and C_{+3}), and by reflections about the beam medians (called R_1, R_2, and R_3). The elements of the representation of the group on V are the following matrices:

$$E=\begin{bmatrix}1&0&0\\0&1&0\\0&0&1\end{bmatrix} \qquad C_3=\begin{bmatrix}0&0&1\\1&0&0\\0&1&0\end{bmatrix} \quad C_{-3}=\begin{bmatrix}0&1&0\\0&0&1\\1&0&0\end{bmatrix}$$

$$R_1=\begin{bmatrix}1&0&0\\0&0&1\\0&1&0\end{bmatrix} \qquad R_2=\begin{bmatrix}0&0&1\\0&1&0\\1&0&0\end{bmatrix} \quad R_3=\begin{bmatrix}0&1&0\\1&0&0\\0&0&1\end{bmatrix} \tag{4.3}$$

The character table of this trifold cyclic group, which includes both rotations and reflections, is given in table 4.2.

Table 4.2. Character table of the trifold symmetry group, C_{3v}.

C_{3v}	E	2C3	3R3
A_1	1	1	1
A_2	1	1	-1
E	2	-1	0

As do all cyclic groups, C_{3v} has minimal representations of dimensions 1 and 2. Higher dimensions are very unusual and are found for more elaborate symmetric structures as tetrahedrons, but never for cyclic structures. From this character table the projections on the symmetry types of the representation can be computed using (4.1):

$$\pi_1=\frac{1}{3}\begin{bmatrix}1&1&1\\1&1&1\\1&1&1\end{bmatrix} \quad \pi_2=\begin{bmatrix}0&0&0\\0&0&0\\0&0&0\end{bmatrix} \quad \pi_3=\frac{1}{3}\begin{bmatrix}2&-1&-1\\-1&2&-1\\-1&-1&2\end{bmatrix} \tag{4.4}$$

For any displacement u, $\pi_1 u$ will be proportional to $[1\ 1\ 1]^T$, so the first symmetry type of this representation is characterized by equal rotations of the 3 joints. The second type is never observed and a further analysis would show that it corresponds to equal axial

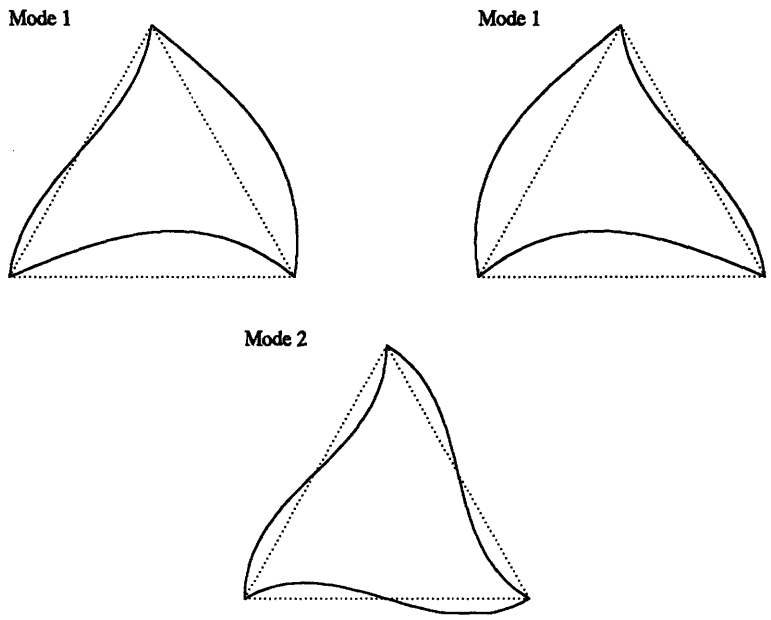

Figure 4.2. First modes of a triangle of beams.

motions of the beams which are not modelled here. π_3 projects on a subspace of dimension 2 whose base vectors (any two column of π_3) are characterized by two joint angles being equal and the third double and opposite, so that a type 3 mode will be a linear combination of two such vectors. As pointed out earlier the modes of the structure will have either one of these symmetry types and, for the case of π_3, they will be double modes since the minimal representation is 2 dimensional. The number of modes of each type is found easily using (4.2):

$$\dim(U_1) = \frac{1}{6}(1x3 + 1x(0+0+0) + 1x(1+1+1)) = 1$$

$$\dim(U_2) = \frac{1}{6}(1x3 + 1x(0+0+0) - 1x(1+1+1)) = 0$$

$$\dim(U_3) = \frac{2}{6}(2x3 - 1x(0+0+0) + 0x(1+1+1)) = 2 \qquad (4.5)$$

Computation of the modal response of the structure gives the results shown in figure 4.2.. As predicted by (4.5) there is a double mode of symmetry type 3 and a single mode of symmetry type 1. If a more elaborate model able to represent more modes were

used, the decomposition in symmetry type could still be easily done, and the response would be composed of single type 1 modes and double type 3 modes. Type 2 modes correspond to equal axial motions of the beams, which here are uncoupled, so that a case of triple degeneration appears. Degeneration not due to symmetry is always due to uncoupling, but the uncoupling may be difficult to handle. Section 4.3. will describe an interesting case of uncoupling of local vibrations.

4.2.3. Example: Tetrahedral symmetry

The trifold symmetry example treated in the preceding section was rather simple. Here, the purpose of the analysis is to help understand the modal properties of the naked interferometer testbed, which has a tetrahedral shape. The structure is not exactly symmetric because of differences in the lacing of the different truss legs and this will appear as near degeneration, which is even easier to handle.

The first clump of 12 modes is characterized by the bending of each leg in a first beam bending mode shape, so a discretized model of these modes will include for each leg a displacement degree of freedom in the 2 transverse directions, and $V = R^{12}$. For the projections onto symmetry types, the first 6 dof correspond to the local z axis (pointed towards the center of the tetrahedron), and the other 6 dof correspond to local y direction (orthogonal to the leg axis and the z direction). The group of symmetry of the structure is T_d, the tetrahedral group with reflections. T_d has 24 elements: E the identity, 8 C_3 rotations of $2\pi/3$, 3 C_2 rotations of π, 6 S_4 reflections, 6 S_d rotations coupled with a reflexion. The character table of T_d is given in table 4.3.

Table 4.3. Character table of the tetrahedral group T_d.

T_d	E	8 C3	3 C_2	6 S_4	6 S_d
A_1	1	1	1	1	1
A_2	1	1	1	-1	-1
E	2	-1	2	0	0
T_1	3	0	-1	1	-1
T_2	3	0	-1	-1	1

The projection operators of possible displacements onto the different symmetry types can be computed using (4.1). They have the following matrix expression for the chosen form of the vector space of possible displacements.

$$\pi_1 = \frac{1}{24}\begin{bmatrix} 4 & 4 & 4 & 4 & 4 & 4 & 0 & 0 & 0 & 0 & 0 & 0 \\ 4 & 4 & 4 & 4 & 4 & 4 & 0 & 0 & 0 & 0 & 0 & 0 \\ 4 & 4 & 4 & 4 & 4 & 4 & 0 & 0 & 0 & 0 & 0 & 0 \\ 4 & 4 & 4 & 4 & 4 & 4 & 0 & 0 & 0 & 0 & 0 & 0 \\ 4 & 4 & 4 & 4 & 4 & 4 & 0 & 0 & 0 & 0 & 0 & 0 \\ 4 & 4 & 4 & 4 & 4 & 4 & 0 & 0 & 0 & 0 & 0 & 0 \\ 0 & 0 & 0 & 0 & 0 & 0 & 0 & 0 & 0 & 0 & 0 & 0 \\ 0 & 0 & 0 & 0 & 0 & 0 & 0 & 0 & 0 & 0 & 0 & 0 \\ 0 & 0 & 0 & 0 & 0 & 0 & 0 & 0 & 0 & 0 & 0 & 0 \\ 0 & 0 & 0 & 0 & 0 & 0 & 0 & 0 & 0 & 0 & 0 & 0 \\ 0 & 0 & 0 & 0 & 0 & 0 & 0 & 0 & 0 & 0 & 0 & 0 \\ 0 & 0 & 0 & 0 & 0 & 0 & 0 & 0 & 0 & 0 & 0 & 0 \end{bmatrix} \qquad \pi_2 = \frac{1}{24}\begin{bmatrix} 0 & 0 & 0 & 0 & 0 & 0 & 0 & 0 & 0 & 0 & 0 & 0 \\ 0 & 0 & 0 & 0 & 0 & 0 & 0 & 0 & 0 & 0 & 0 & 0 \\ 0 & 0 & 0 & 0 & 0 & 0 & 0 & 0 & 0 & 0 & 0 & 0 \\ 0 & 0 & 0 & 0 & 0 & 0 & 0 & 0 & 0 & 0 & 0 & 0 \\ 0 & 0 & 0 & 0 & 0 & 0 & 0 & 0 & 0 & 0 & 0 & 0 \\ 0 & 0 & 0 & 0 & 0 & 0 & 0 & 0 & 0 & 0 & 0 & 0 \\ 0 & 0 & 0 & 0 & 0 & 0 & 0 & 0 & 0 & 0 & 0 & 0 \\ 0 & 0 & 0 & 0 & 0 & 0 & 0 & 0 & 0 & 0 & 0 & 0 \\ 0 & 0 & 0 & 0 & 0 & 0 & 0 & 0 & 0 & 0 & 0 & 0 \\ 0 & 0 & 0 & 0 & 0 & 0 & 0 & 0 & 0 & 0 & 0 & 0 \\ 0 & 0 & 0 & 0 & 0 & 0 & 0 & 0 & 0 & 0 & 0 & 0 \\ 0 & 0 & 0 & 0 & 0 & 0 & 0 & 0 & 0 & 0 & 0 & 0 \end{bmatrix}$$

$$\pi_3 = \frac{1}{24}\begin{bmatrix} 8 & -4 & -4 & -4 & -4 & 8 & 0 & 0 & 0 & 0 & 0 & 0 \\ -4 & 8 & -4 & 8 & -4 & -4 & 0 & 0 & 0 & 0 & 0 & 0 \\ -4 & -4 & 8 & -4 & 8 & -4 & 0 & 0 & 0 & 0 & 0 & 0 \\ -4 & 8 & -4 & 8 & -4 & -4 & 0 & 0 & 0 & 0 & 0 & 0 \\ -4 & -4 & 8 & -4 & 8 & -4 & 0 & 0 & 0 & 0 & 0 & 0 \\ 8 & -4 & -4 & -4 & -4 & 8 & 0 & 0 & 0 & 0 & 0 & 0 \\ 0 & 0 & 0 & 0 & 0 & 0 & 0 & 0 & 0 & 0 & 0 & 0 \\ 0 & 0 & 0 & 0 & 0 & 0 & 0 & 0 & 0 & 0 & 0 & 0 \\ 0 & 0 & 0 & 0 & 0 & 0 & 0 & 0 & 0 & 0 & 0 & 0 \\ 0 & 0 & 0 & 0 & 0 & 0 & 0 & 0 & 0 & 0 & 0 & 0 \\ 0 & 0 & 0 & 0 & 0 & 0 & 0 & 0 & 0 & 0 & 0 & 0 \\ 0 & 0 & 0 & 0 & 0 & 0 & 0 & 0 & 0 & 0 & 0 & 0 \end{bmatrix} \qquad \pi_4 = \frac{1}{24}\begin{bmatrix} 0 & 0 & 0 & 0 & 0 & 0 & 0 & 0 & 0 & 0 & 0 & 0 \\ 0 & 0 & 0 & 0 & 0 & 0 & 0 & 0 & 0 & 0 & 0 & 0 \\ 0 & 0 & 0 & 0 & 0 & 0 & 0 & 0 & 0 & 0 & 0 & 0 \\ 0 & 0 & 0 & 0 & 0 & 0 & 0 & 0 & 0 & 0 & 0 & 0 \\ 0 & 0 & 0 & 0 & 0 & 0 & 0 & 0 & 0 & 0 & 0 & 0 \\ 0 & 0 & 0 & 0 & 0 & 0 & 0 & 0 & 0 & 0 & 0 & 0 \\ 0 & 0 & 0 & 0 & 0 & 0 & 12 & 6 & 6 & -6 & 6 & 0 \\ 0 & 0 & 0 & 0 & 0 & 0 & 6 & 12 & 6 & 0 & -6 & 6 \\ 0 & 0 & 0 & 0 & 0 & 0 & 6 & 6 & 12 & 6 & 0 & -6 \\ 0 & 0 & 0 & 0 & 0 & 0 & -6 & 0 & 6 & 12 & -6 & -6 \\ 0 & 0 & 0 & 0 & 0 & 0 & 6 & -6 & 0 & -6 & 12 & -6 \\ 0 & 0 & 0 & 0 & 0 & 0 & 0 & 6 & -6 & -6 & -6 & 12 \end{bmatrix}$$

$$\pi_5 = \frac{1}{24}\begin{bmatrix} 12 & 0 & 0 & 0 & 0 & -12 & 0 & 0 & 0 & 0 & 0 & 0 \\ 0 & 12 & 0 & -12 & 0 & 0 & 0 & 0 & 0 & 0 & 0 & 0 \\ 0 & 0 & 12 & 0 & -12 & 0 & 0 & 0 & 0 & 0 & 0 & 0 \\ 0 & -12 & 0 & 12 & 0 & 0 & 0 & 0 & 0 & 0 & 0 & 0 \\ 0 & 0 & -12 & 0 & 12 & 0 & 0 & 0 & 0 & 0 & 0 & 0 \\ -12 & 0 & 0 & 0 & 0 & 12 & 0 & 0 & 0 & 0 & 0 & 0 \\ 0 & 0 & 0 & 0 & 0 & 0 & 12 & -6 & -6 & 6 & -6 & 0 \\ 0 & 0 & 0 & 0 & 0 & 0 & -6 & 12 & -6 & 0 & 6 & -6 \\ 0 & 0 & 0 & 0 & 0 & 0 & -6 & -6 & 12 & -6 & 0 & 6 \\ 0 & 0 & 0 & 0 & 0 & 0 & 6 & 0 & -6 & 12 & 6 & 6 \\ 0 & 0 & 0 & 0 & 0 & 0 & -6 & 6 & 0 & 6 & 12 & 6 \\ 0 & 0 & 0 & 0 & 0 & 0 & 0 & -6 & 6 & 6 & 6 & 12 \end{bmatrix}$$

π_1 only has non-zero terms for the local z degrees of freedom so that modes of the first type correspond to breathing modes with all the legs bent towards the center of the tetrahedron (equal displacement in the local z direction). Type 2 modes correspond to equal axial motions in the legs, which have not been represented in the choice of V. As for type 1, type 3 modes have displacement only in the local z direction. Type three modes also are double modes. Similarly, type 4 modes are triple modes characterized by motions in the local y direction, and 5 are triple modes with coupled y and z displacements.

Using formula (4.2), one finds the number of modes of each type that will be found in the first twelve modes of the interferometer testbed.

$$\dim(U_1) = \frac{1}{24}(1\times12 + 1\times0 + 1\times0 + 1\times0 + 1\times12) = 1$$

$$\dim(U_2) = \frac{1}{24}(1\times12 + 1\times0 + 1\times0 + 1\times0 - 1\times12) = 0$$

$$\dim(U_3) = \frac{2}{24}(2\times12 - 1\times0 + 2\times0 + 0\times0 - 0\times12) = 2$$

$$\dim(U_4) = \frac{3}{24}(3\times12 + 0\times0 - 1\times0 + 1\times0 - 1\times12) = 3$$

$$\dim(U_5) = \frac{3}{24}(3\times12 + 0\times0 - 1\times0 - 1\times0 + 1\times12) = 6$$

These conclusions on the type and number of the modes composing the first clump of twelve modes of the interferometer have been checked for both the analytical predictions and experimental measurements (see table 4.4.). For the numerical estimate, results are almost perfect, and the small non-degeneration of the triple modes is explained by the small non-symmetry of the truss lacing. For experimental measurements all mode shapes are not available, but all the measured modes have a very strong component on the symmetry type predicted by the theory, which is the best that can be hoped for with the quality of modeshape measurements available. The use of the prediction of degeneration enabled a clear identification of the frequencies of unmeasured modes and the eviction of unknown modes later identified as suspension resonance modes.

Table 4.4. Measured and estimated 12 first modal frequencies of the naked interferometer testbed, and classification by type.

F_{meas} (Hz)	F_{pred} (Hz)	Type	F_{meas} (Hz)	F_{pred} (Hz)	Type
31.35	-	suspension	43.70	44.56	type 5
31.75	-	suspension	-	44.56	type 5
35.10	35.91	type 3	52.10	53.21	type 1
-	35.91	type 3	54.70	55.95	type 5
38.90	40.23	type 4	55.20	55.95	type 5
39.40	40.23	type 4	-	56.32	type 5
-	40.30	type 4	62.70	-	suspension
43.30	44.51	type 5	63.40	-	suspension

4.3. Degeneration due to uncoupling

4.3.1. Introduction

By definition, modes are uncoupled. So the dynamics of degenerated modes correspond to a juxtaposition of uncoupled oscillators. In section 4.2., the presence of different uncoupled harmonic motions at one frequency was related to the symmetry properties of the structure. However, if the structure does not present a symmetry implying degeneration of some modes, what does the mathematical uncoupling physically represent? If one omits cases of decoupled motions (such as bending and torsion in a beam), it seems that degeneration can only be due to substructure vibration. For a really degenerated mode, there would be two substructures, having uncoupled harmonic motions at a given frequency. In particular one substructure could be moving and the other be still. The appearance of such modes (called localization) was studied in physics, where it applies to

lightly disordered crystals (see ref. [34]), and in mechanics for several different structures (refs. [35]-[37]).

For mono-coupled mono-dimensional structures with light substructure coupling, perturbations in the periodicity of the structure have been proven to localize modes. The conjecture of the present analysis is that even for multicoupled structures with degenerated modes some, but not all, arbitrarily small perturbations result in modal localization. No proof is known for this conjecture, but, for the truss-beam sample problem with clamped joints, perturbations of the local resonances indeed results in modal localization.

The objective of this section is to analyze the properties of degenerated modes linked to local vibrations. First, a characterization of the local vibration modes of the truss beam-sample problem is given. Then the classic high sensitivity of modeshapes is shown by the introduction of a localizing perturbation. Finally, the desensitizing effect of damping on the actual input-output response is considered.

In section 4.3.2., a study of the bay dynamics shows the importance of the diagonal strut resonance and the minimum complexity of a finite element model needed to model local resonances. The modal response of the truss is then be analyzed, and the first set of highly dense modes (called local modes) related to the resonance of diagonal members. Aapplying the conjecture in section 4.3.3., a particular small perturbation that localizes the normal modes of the structure is found. The poor significance of normal modes in presence of damping is then be shown, considering the filtering properties of local resonances for a damped truss.

4.3.2. Frequency response up to the resonance of the diagonals

In 2.4.4., the frequency response of the truss-beam sample problem has already been analyzed and shown to be accurately represented by a model with two elements per

strut. Here in order to get a better understanding of this structure, analysies of the modeshapes have to be done. First, a study of the bay and of how different models capture its dynamics will give a good understanding of its characteristics, then the shape characteristics of the truss-beam modes will be analyzed.

Characteristics of bay vibration

Considering a single bay with joints fixed in translation, the simplest model (which would be used by an equivalent continuum method) uses one 2-node quasistatic element for each strut. A refined model would at least consider 2 quasistatic elements for the diagonal strut: its frequency of half wavelength for strut length is 103 Hz, and the bandwidth of interest goes up to 200 Hz. The first mode estimate for these two models and for two others (diagonal strut modelled by one quintic element, and all struts modelled by 4 quintic elements to get an almost exact response) are plotted on figure 4.3., where the modeshape, and the curvature along the struts plotted as a transverse displacement, are shown for each model.

In model (a), the middle strut does not have internal dynamic degrees of freedom so that the first bay mode cannot be characterized by the resonance of this strut. The two curvature nodes of this strut present in the real mode cannot appear in the model so that the estimate is very poor: almost 40% error in frequency. In models (b) and (c), internal dynamic degrees of freedom are added to the diagonal strut so that the strut resonance is represented and the error in frequency is about 1%. The differences between the behavior of these models and the highly refined model (d) are very small both in terms of frequency error and displacement and curvature shape error, so that a model of the truss with two finite elements per strut will be accurate even for the first internal resonance of the bay.

In conclusions the first mode of the bay is characterized by the resonance of the diagonal strut and an almost quasistatic behavior of the short struts. This characteristic

resonance is also found for the truss beam formed assembled bays and is the source of almost degenerated modes.

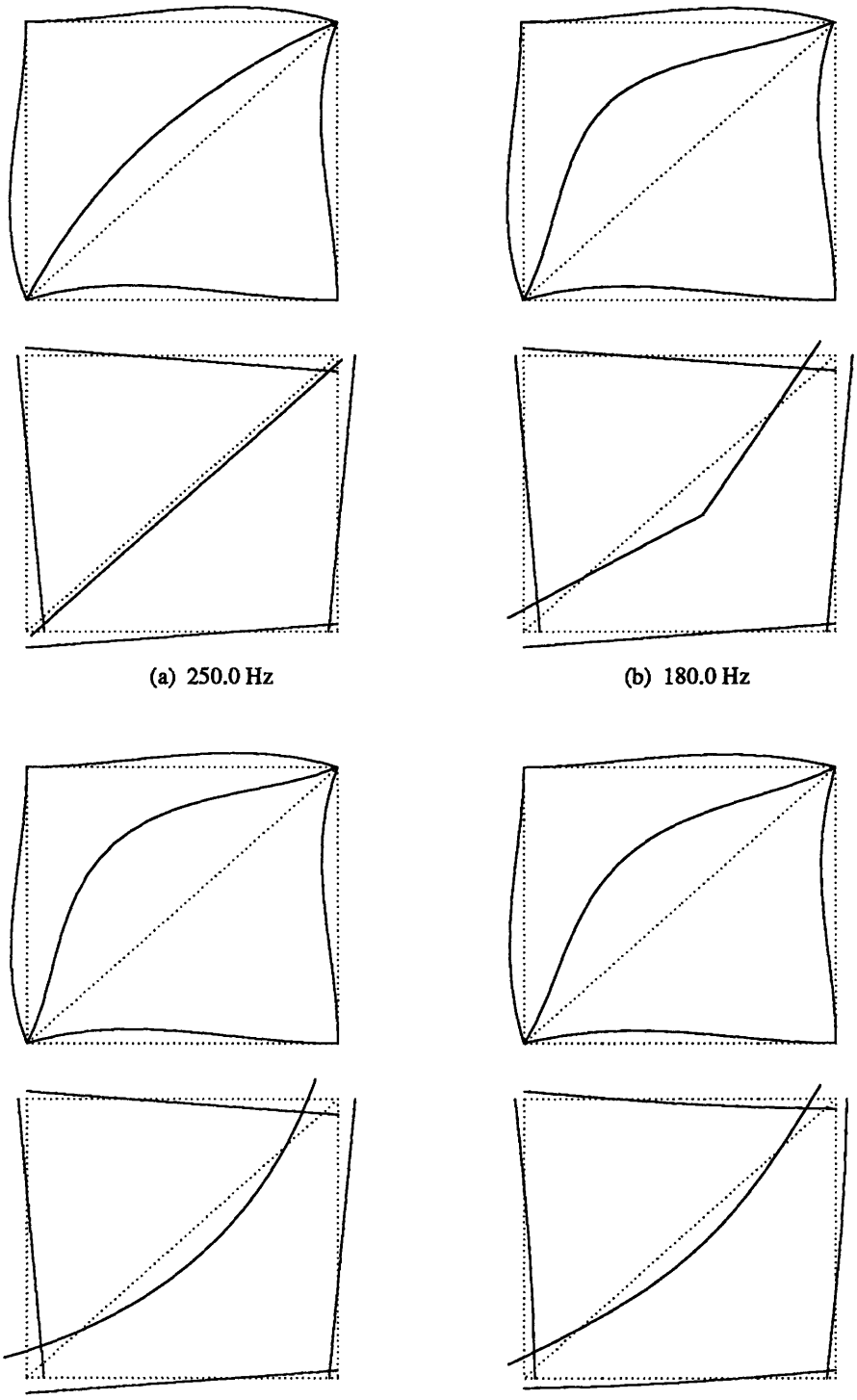

Figure 4.3. Modeshape and curvatures (plotted as a transverse displacement) of the first bay mode estimate for models: (a) all struts modelled as cubic elements, (b) the diagonal modelled as two cubic elements, (c) the diagonal modelled as a quintic element, (d) all the struts modelled as four quintic elements (almost exact)

Analysis of truss modal characteristics

Figure 4.4. shows different modes of the structure. Up to mode 5 the modes have global beamlike characteristics. In figure 4.4. mode 1 clearly has the shape of a first beam bending mode and mode 4 the shape of a first compression mode. The following modes show heavy local deformations that make the identification of a shape characteristic very difficult. However, as seen in the previous section, the diagonal struts begin to resonate around 180 Hz for a bay, so that one should expect heavy influences of this resonance in the truss around the same frequency, which corresponds here to the 6^{th} mode. To get a better idea of the relative influence of global truss bending and local diagonal strut resonance the horizontal displacement of the diagonal strut midspan point is plotted (figure 4.5.) for the first 14 modes. This figure clearly shows the global modeshapes of modes 1 to 5; and for modes 6 and 7, global modeshapes perturbed by local resonances of the diagonals near the tips of the truss-beam. The higher modes show the clear importance of diagonal resonance (with no visible global motions) and correspond to almost degenerated modes. As is usually done, these modes will be called *local modes*.

For a truss with pinned joints it is rather obvious that the bending resonance of struts is almost uncoupled from other motions so that it should appear as clumps of almost degenerated modes. In the case of clamped joints, it is interesting to note (as was already done in chapter II) that the resonance of diagonal struts is still the source of almost degenerated modes although the coupling is much stronger.

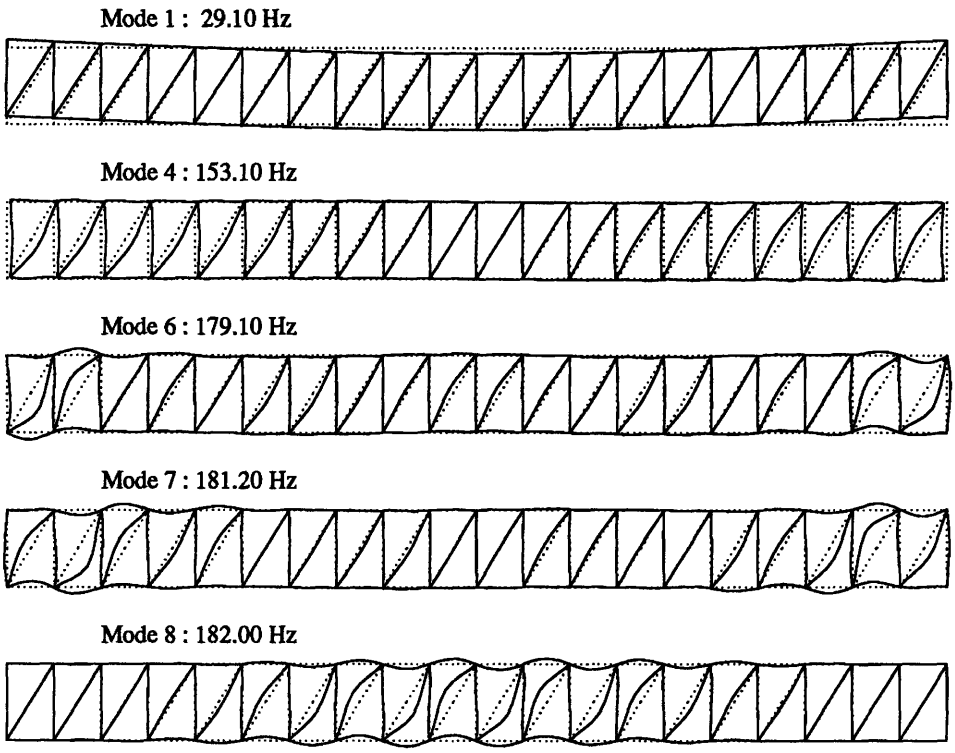

Figure 4.4. Modes 1, 5, 6, 7, 8 of the nominal structure.

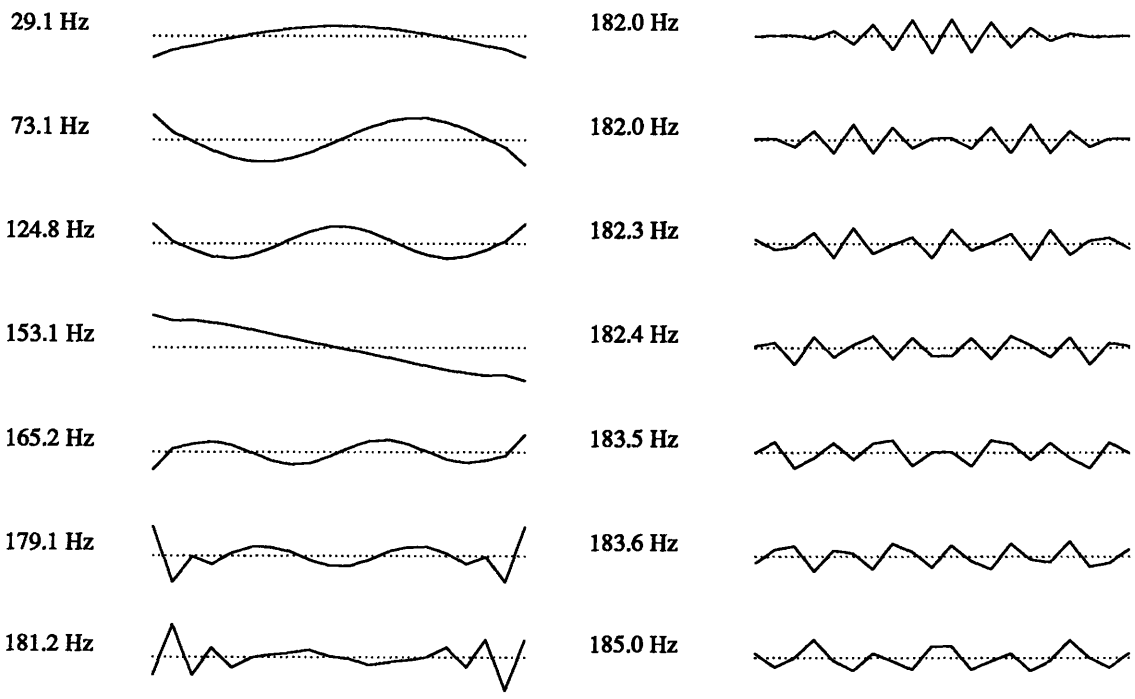

Figure 4.5. Horizontal displacement of diagonal strut midspan for modes 1 to 14.

4.3.3. Perturbations, localization, filtering properties

Based on the substructure vibration conjecture, it should be possible to localize modes 8 and 9 with a small perturbation. These modes are characterized by the resonance of the diagonal struts, so logically, a perturbation on the diagonal struts should localize these modes. Figure 4.6. shows the response of modes 7 to 9 for the nominal truss (n), a truss (2) perturbed by a 2g mass at the middle of the 8^{th} diagonal (1% of strut mass), and a truss (5) perturbed by a 5g mass at the same point. Figure 4.6. clearly shows how the perturbation localized the local modes to the left and the right side of the beam. In this case the perturbation could not be arbitrarily small since the modes are not exactly degenerated, but a 2 g added mass would be obtained for standard accelerometers, so that in any experimental setup these modes could not be considered separately but would have to be related by comparison of spanned vector-spaces.

The 5g perturbation shows an interesting phenomena: the perturbation is large enough for the frequency changes to be more than the modal frequency separation. So mode 8 (n) is now below the initial mode 7 (n), whose shape has not significantly changed (compare modes 8 (5) and 7 (n)). In general, such phenomena can be understood by the fact that the sensitivities of different modal characteristics to perturbations are greatly dependent on the perturbation. Here the added mass on the diagonal strut perturbs the resonance of that strut. Therefore the local modes (characterized by this resonance) but not the global modes (which barely depend on it) are heavily perturbed. At the point where the local and global modes have the same frequency, the conjecture would give the existence of a small perturbation that localizes the combination of local and global modes. But finding which seems rather difficult.

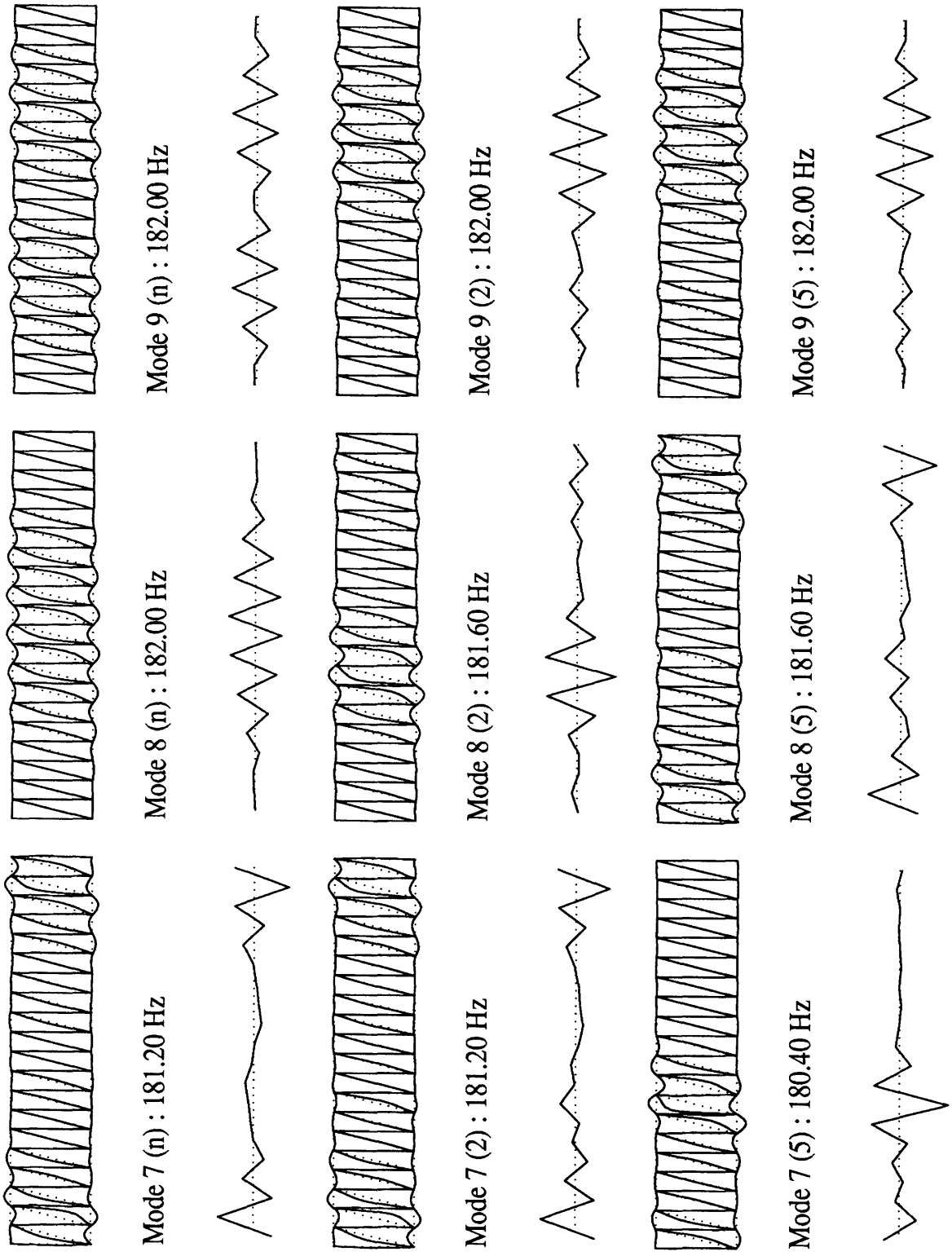

Figure 4.6. Modes 7 to 9 for: (n), nominal , (2), perturbed by a 2g mass (on the 8th diagonal strut midspan), and (5), perturbed by a 5g mass structures.

Distributed proof-mass damper conceptual model

The previous perturbation test showed how the local modes have decoupled substructures: left and right half of the truss-beam. Generalizing this idea, one could say that the resonance of each diagonal strut can be described as the resonance of a proof-mass oscillator coupled to beam motions, but not to the other oscillators. The resulting conceptual model (ref. [41] for example) is shown in figure 4.7. The oscillators are coupled by beam motions, but for a great number of bays the coupling is weak so that one has almost degenerated modes as in the truss-beam. If the proof-mass motions are damped, propagating waves at the resonant frequency of the proof-mass dampers will be attenuated very quickly, since much energy will be transfered to and dissipated by the proof-masses. Some interesting previous work exists on the damping of wave propagation by distributed proof mass dampers: see reference [40].

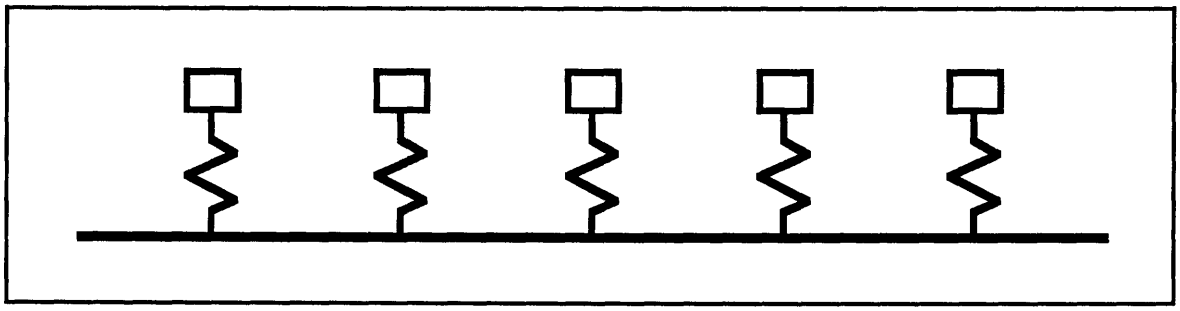

Figure 4.7. Diagonal strut vibration seen as distributed proof-mass effect

To verify the validity of this interpretation of the structure behavior, the transfer function from a vertical force at one end of the truss to a vertical displacement at the other end is plotted (figure 4.8.) for zero, .6%, 5% and 7% modal damping. The level of response in the frequency range of the local modes is low in general, and for 5% damping the local modes drastically enhance the effect of damping, reducing the response by more than 20 dB (see figure (4.8)). This is exactly the effects that one could expect from a beam

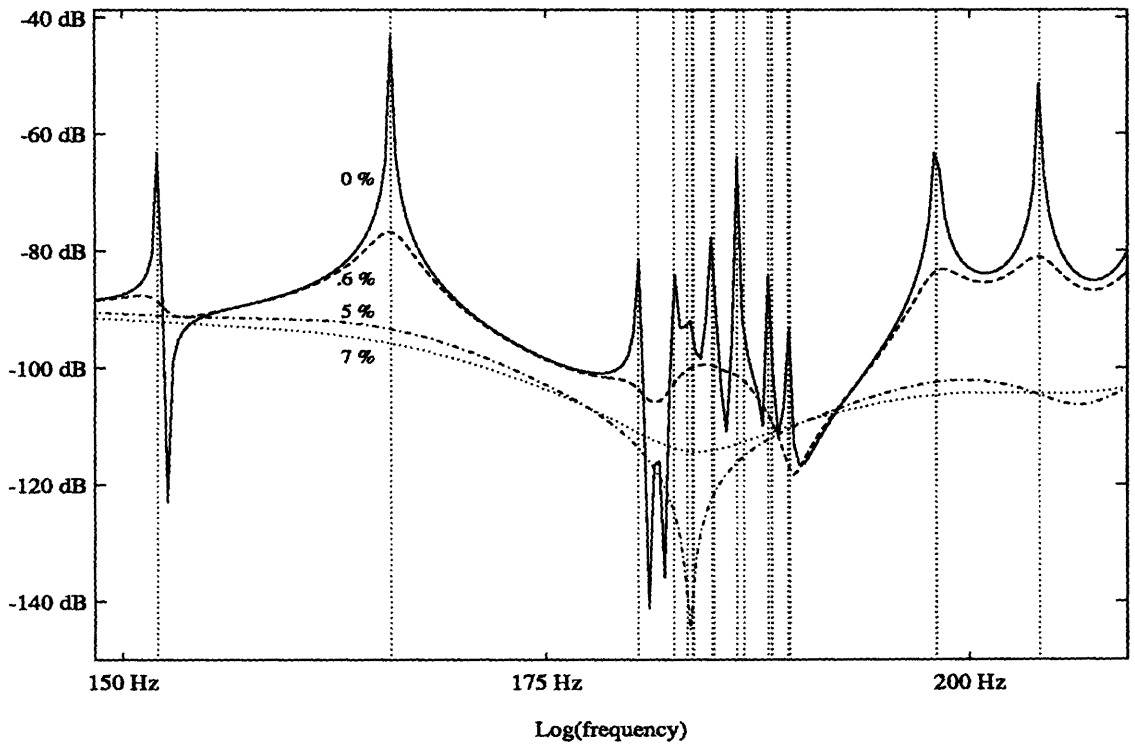

Figure 4.8. Transfer function from F_v, vertical force, at left-tip to v, vertical displacement, at right tip for zero, .6%, 5% and 7% proportional damping of all modes.

with distributed proof-mass dampers. For low levels of damping, much energy goes into the proof-mass dampers, but since it is not dissipated, it is eventually transmitted. For an optimal intermediate level of damping (5% here) a balance between energy input in the resonance of the proof-masses, and energy dissipated by them is obtained, so the global response of the group of local modes is that of a zero. For higher levels of damping, not enough energy can be transmitted to the diagonal struts, so that benefit from their resonance in terms of energy dissipation is lost.

To further validate the concept, the same transfer function was computed for the perturbed structure with localized modes. No measurable difference could be seen for the damped cases. The perturbation changed significantly the location and characteristics of the modes which are singularities of the problem (see chapter II), but the actual measurable

behavior for the damped structure was insensitive to the perturbation. For an experimental test one could not expect to be able to prove the localization of this sample problem.

This points out that the description of structural dynamics in terms of orthonormal real modes is, for structures with high modal density but a some damping, a description highly sensitive to perturbations that can give a distorted image of insensitive characteristics of the transfer functions.

CHAPTER V

MODELS FOR CONTROL

5.1. Introduction

While the previous analysis assessed the correspondence between modal estimates and actual modes, this chapter will discuss the construction of models for control purposes.

Models of structural dynamics for control must include an accurate representation of input-output behavior of the structure, in a given frequency range (which should include the expected cross-over region), with a finite (in fact small) set of dynamic states. The obvious dynamics to be retained are the modes of the structure found in the bandwidth but some of the effects of other modes are significant and should be included in the model (see previous work in ref. [44]). For a closed-loop system the truncated modes influence not only the output but also, through the feedback-loop, the dynamics of the system. Correcting for truncated modes in a closed-loop system, therefore implies many more corrections than for an open-loop system.

Section 5.2. discusses the creation of an open-loop model from a set of retained modes. The inclusion of the quasistatic displacement response of truncated modes is discussed for structures with and without rigid-body modes. The creation of state-space models is treated, for use in section 5.4., and the correction for modes below the bandwidth is discussed, for its importance in identification. Section 5.3. quickly reviews selection principles for retained dynamic states. Section 5.4. discusses the use of the static correction in the case of closed-loop systems, and considers the addition of filtered static

modes, called correction modes, as the practical way of using a correct model and a way of introducing a correction for the asymptotic low frequency velocity of the truncated modes.

5.2. Model truncation and static correction

5.2.1. Simple truncation

The response of a structure can be exactly represented by the infinite series of the dynamic modes. But all the modes will not be kept in the control model: some will be retained and the response of the others will be approximated. An exact measurement y would be expressed as the sum of the response of the retained modes and that of the modes which will be truncated:

$$y(x,t) = \sum_{i=1}^{N_r} \xi_i(t)\, c\phi_i(x) + \sum_{i=N_r+1}^{\infty} \xi_i(t)\, c\phi_i(x) \qquad (5.1)$$

with

$$\ddot{\xi}_i(t) + \omega_i^2\, \xi_i(t) = \frac{\Xi_i}{m_i}(t) \qquad (5.2)$$

and

$$\Xi_i(t) = \phi_i(x)^T Q(x,t) \qquad (5.3)$$

where $\phi_i(x)$ is the non-dimensional shape function of the mode, c the output operator (a matrix for a discretized model of the plant) which associates to a mode shape with unit amplitude the corresponding measurement y, $\xi_i(t)$ the modal coordinate, ω_i the frequency of mode i, Ξ_i the generalized modal force for the load profile Q(x,t), and m_i the modal mass of mode i. The normalization of equations (5.1)-(5.3) is done naturally by taking

$\phi_i(x)$ non-dimensional. In equation (5.2), the modal load can be normalized by the modal mass and a normalization of time can be introduced (so that $\omega_i = 1$).

ϕ_i verifies orthogonality conditions with respect to the mass distribution, from which the modal masses are derived, and orthogonality conditions with respect to the stiffness distribution:

$$\phi_i(x)^T m \phi_j(x) = m_i \delta_{ij} \quad \text{and} \quad \phi_i(x)^T k \phi_j(x) = m_i \omega_i^2 \delta_{ij} \tag{5.4}$$

Multiplying on the left by ϕ^{-T} and on the right by ϕ^{-1}, gives $m = \phi^{-T} m\delta \phi^{-1}$. Inverting this relation, a useful expression for m^{-1} is found. This expression and the corresponding one for k^{-1}, which will be called "inversion formulas", are:

$$m^{-1} = \sum_i \frac{\phi_i(x)\, \phi_i^T(x)}{m_i} \quad \text{and} \quad k^{-1} = \sum_i \frac{\phi_i(x)\, \phi_i^T(x)}{m_i \omega_i^2} \tag{5.5}$$

where m^{-1} is always defined as all degrees of freedom have inertias, but k^{-1} only exists if the structure has no rigid-body degrees of freedom. Cases with rigid-body motions can also be treated, using (5.5), but demand the use of special precautions which are the object of section 2.3. These formulas, although useful for the analysis, are useless in practice, as all the modes of a model are usually not known.

From (5.2) the modal response of an undamped system can be conveniently described in the frequency domain as a function of modal force and frequency:

$$\xi_i(\omega) = \frac{\Xi_i(\omega)}{m_i(\omega_i^2 - \omega^2)} \tag{5.6}$$

When a reduced order model is created, the simplest reduction process is to choose a certain number of modes, whose response is included completely in the modeled response, and to neglect completely the other modes. The selection of retained modes is an

important issue that will be briefly treated in section 5.3. Assuming the selection has been performed, the estimate of the structure behavior based on simple truncation is:

$$\hat{y}_s(x,t) = \sum_{i=1}^{N_r} \xi_i(t)\, c\phi_i(x) \tag{5.7}$$

or, using equation (5.6), in the frequency domain

$$\hat{y}_s(x,\omega) = \sum_{i=1}^{N_r} \frac{\Xi_i(\omega)}{m_i(\omega_i^2-\omega^2)}\, c\phi_i(x) \tag{5.8}$$

This approach, although simple, completely ignores truncated modes. But, even if the *dynamics* of truncated modes are negligible, their static influence is often significant, so that this estimate is not accurate.

5.2.2 Exact Static Correction

The response of each mode of the structure has the form shown on figure 5.1. At frequencies much below the resonance, the behavior of the mode is constant (1% error for ω/ω_i=.1, 4% for .2, 33% for .5, see the dashed line asymptote on the figure). This physically corresponds to the fact that time constants of the mode are, at low frequencies, much smaller than the time-steps of interest, so that the modal response can be considered as instantaneous or quasistatic. Thus, for modes well above the frequency range of interest, the response can be approximated by a constant feedthrough term corresponding to the modal static response. At high frequencies the mode behaves as a rigid-body: asymptote in $1/\omega^2$. For modes truncated below the bandwidth, the dynamics could be truncated and replaced by a single 40 dB/decade roll-off, but this is rarely useful and will only be outlined in section 5.2.5.

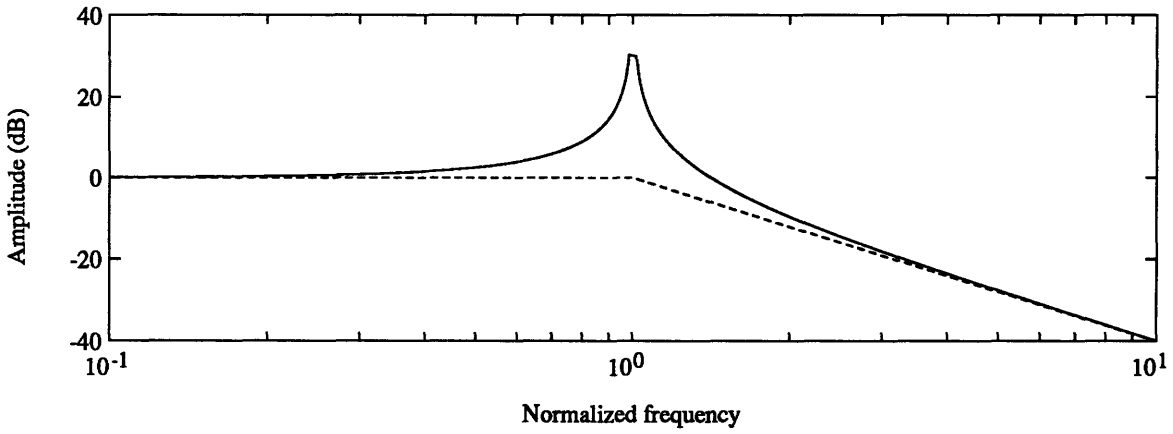

Figure 5.1. Response of a single mode.

The static correction of the simple modal truncation is achieved by including the low frequency asymptotic position behavior of the truncated modes (the velocity is assumed to be zero, which will be corrected in section 5.4.2.). By rearranging equation (5.2), the modal behavior can be expressed as the sum of a quasistatic response and a dynamic response corresponding to inertia effects. In the time and in the frequency domain, this gives:

$$\xi_i(t) = \frac{\Xi_i(t)}{m_i\omega_i^2} - \frac{\ddot{\xi}_i(t)}{\omega_i^2} \quad \text{and} \quad \xi_i(\omega) = \frac{\Xi_i(\omega)}{m_i\omega_i^2} + \frac{\omega^2\,\Xi_i(\omega)}{m_i\omega_i^2(\omega_i^2-\omega^2)} \tag{5.9}$$

The static contribution of each mode is $\frac{\Xi_i(t)}{m_i\omega_i^2}c\phi_i$. So the complete static response is given by:

$$\sum_{i=1}^{\infty}\frac{\Xi_i(t)}{m_i\omega_i^2}c\phi_i = \sum_{i=1}^{\infty}\frac{c\phi_i\phi_i^T Q}{m_i\omega_i^2} = ck^{-1}Q \tag{5.47}$$

where the passage to k^{-1} was done using the inversion formula (5.5). The modal dynamic contributions are $\frac{\ddot{\xi}_i(t)}{\omega_i^2}c\phi_i$. A statically correct model, that includes the complete static

response of the structure and the dynamic effects of the retained modes, has therefore the form:

$$\hat{y}_c(x,t) = ck^{-1}Q(x,t) - \sum_{i=1}^{N_r} \frac{\ddot{\xi}_i(t)}{\omega_i^2} c\phi_i(x) \qquad (5.10)$$

And in the frequency domain.

$$\hat{y}_c(x,\omega) = ck^{-1}Q(x,\omega) + \sum_{i=1}^{N_r} \frac{\omega^2 \Xi_i}{m_i\omega_i^2(\omega_i^2-\omega^2)} c\phi_i(x) \qquad (5.11)$$

In both cases the stiffness matrix (or operator for a continuous case) has to be inverted. When rigid body modes are present, assumptions can be made about the rigid body behavior of the structure, or special precautions, detailed in section 2.3., have to be taken in order to invert k and use the frequency domain form.

In practice the computation of this quasistatic response can be interpreted using different methods.

Mode Acceleration Method

This method has been mainly used in aeroelasticity (ref. [45]) to predict deflections, accelerations, and stresses, on wings and fuselages, due to disturbances. It is the direct application of the estimate form (5.10) or (5.11). The physical interpretation of it is relatively simple: the complete quasistatic response of the system is included and a dynamic correction for a few modes is added.

Residual Stiffness Method

This method (ref. [46]), which is completely equivalent to the mode acceleration method, has an interpretation which appears more like an addition of a correction to the simple truncation. The new estimate is the simple truncation estimate corrected by the

quasistatic effect of the residual load which has not yet been accounted for (in other words: the asymptotic effect of the truncated modes):

$$\hat{y}_c(x,t) = \sum_{i=1}^{N_r} \xi_i(t)\, c\phi_i(x) + ck^{-1}\,(Q(x,t) - \sum_{i=1}^{N_r} Q_i\,(x,t)) \qquad (5.12)$$

where the loads Q_i associated with the retained modes i are found using:

$$Q_i\,(x,t) = \frac{\phi_i\,(x)^T\, Q(x,t)}{m_i}\, m\phi_i\,(x) \qquad (5.13)$$

The actual load is the sum of all the modal loads $Q = \sum_{i=1}^{\infty} Q_i$. So that $Q - \sum_{i=1}^{N_r} Q_i$ is the residual load applied on all the truncated modes. The operator k^{-1}, in equation (5.12), is the compliance of the system, and operates here on the residual load $(Q - \sum_{i=1}^{N_r} Q_i)$, hence the name *residual stiffness method.*

Implementation

In all practical cases, mechanical structures are actuated by a finite number of actuators and disturbance sources, whose action can be expressed in a basis of N_s independent load patterns B_j (should be dimensional) applied with intensities u_j (should be non-dimensional): $Q = \sum_{j=1}^{N_s} B_j(x)\, u_j(t)$. For unit u_j these load patterns are typically a unit force, or moment, applied on one actuator, all the others being set to zero. *Attachment modes* are then defined to be the deformation shape $\overline{\gamma}_j$ associated with each of the load patterns B_j: $\overline{\gamma}_j = k^{-1}B_j$. The response estimate $\hat{y}_c$ can then be written easily, as in (5.10):

$$\hat{y}_c(x,t) = \sum_{j=1}^{N_s} c\,\overline{\gamma}_j(x)\, u_j(t) - \sum_{i=1}^{N_r} \frac{\ddot{\xi}_i\,(t)}{\omega_i^2}\, c\phi_i(x) \qquad (5.16)$$

or in the frequency domain

$$\hat{y}_c(x,\omega) = \sum_{j=1}^{N_s} c\overline{\gamma}_j(x)\, u_j(\omega) + \sum_{i=1}^{N_r} \frac{\omega^2\, \Xi_i\, \phi_i(x)}{m_i\omega_i^2(\omega_i^2-\omega^2)} \qquad (5.17)$$

In practice one wants to express $\hat{y}_c$ in terms of states so that $\ddot{\xi}$ (which is not a state) must be eliminated. This is done by grouping the static and dynamic contributions of the retained modes (the sum of the static and the dynamic modal contributions is $\xi_i\phi_i$, as seen in (5.9)), which leads to the final form that should be used. This form is given in the time domain by:

$$\hat{y}_c(x,t) = \sum_{j=1}^{N_s} c\gamma_j(x)\, u_j(t) + \sum_{i=1}^{N_r} \xi_i(t) c\phi_i(x) \qquad (5.18)$$

and in the frequency domain

$$\hat{y}_c(x,\omega) = \sum_{j=1}^{N_s} c\gamma_j(x)\, u_j(\omega) + \sum_{i=1}^{N_r} \frac{\Xi_i(\omega)\, c\phi_i(x)}{m_i(\omega_i^2-\omega^2)} \qquad (5.19)$$

As will be further detailed in section 5.2.4., in these equations the first sum corresponds to feedthrough terms correcting for the position contribution of truncated modes (this is the D matrix in the usual state-space form) and the second sum corresponds to the retained dynamics (A, B, and C matrices). The mode acceleration method computes the γ_j by orthogonalization of the $\overline{\gamma}_j$ to the retained modes :

$$\gamma_j(x) = \overline{\gamma}_j(x) - \sum_{i=1}^{N_r} \frac{\phi_i^T\, m\, \overline{\gamma}_j}{m_i}\, \phi_i(x) \qquad (5.20)$$

The fact, that the summed terms in equation (5.20) correspond to the static contributions of the retained modes ($\frac{\phi_i^T B_j}{m_i\omega_i^2}$ from (5.9)), can be easily found by replacing $\overline{\gamma}_j$ by $k^{-1}B_j$, using the inversion formula (5.5) to express k^{-1}, and applying the orthogonality condition for the mass matrix (5.4):

$$\frac{\phi_i^T m \overline{\gamma}_i}{m_i} = \frac{\phi_i^T m k^{-1} B_j}{m_i} = \sum_{k=1}^{N_r} \frac{\phi_i^T m \phi_k \phi_k^T B_j}{m_i m_k \omega_i^2} = \frac{\phi_i^T B_j}{m_i \omega_i^2} \qquad (5.14)$$

The residual stiffness method does the orthogonalization at the level of the loads by computing displacement due to the load that does not excite the retained modes:

$$\gamma_j(x) = k^{-1}\{B_j(x) - \sum_{i=1}^{N_r} B_{ji}(x)\} \qquad (5.15)$$

The two methods lead to the same final form (5.18) and (5.19), but do an orthogonalization at two different levels (load or displacement). In section 5.2.3. where rigid-body modes will be considered, two steps will be used, first an orthogonalization of the loads to the rigid-body modes, then an orthogonalization of the static flexible displacement to the retained flexible modes. The Mode Acceleration Method has the small advantage of being easier to implement for continuous structures: the orthogonalization in equation (5.20) is never a problem, and k^{-1} may be easier to compute for simple loads (as the B_j) than for the residual loads, which usually have non-zero components over the whole structure. Of course if the whole process is already programmed there is no difference between the two methods.

In some cases, the attachment modes are not a very convenient way to describe the system. For instance, if high impedance actuation (displacement actuation) is used, a unit force is not a good description of the system. Therefore *constraint modes* are defined as base displacement patterns $\overline{\gamma}_j(x)$ corresponding base actuation patterns. In this case, the state space description underlying the whole approach cannot be used, as it does not allow direct displacement actuation. So special corrections have to be made which are out of the scope of this presentation.

Finally it should be noted that although finite element methods give approximate results for the dynamics of a structure, they are usually constructed to give an exact static

response. So, if the continuous idealized model of the structure is exact (as seen in chapter III), for all purposes the static correction is exact and the dynamic correction for modes is approximate.

5.2.3 Cases with Rigid-Body Modes

When rigid-body modes are present the formalism linked to the static correction cannot be used as such, since the response to static loads is in many cases infinite. To get valid results one must consider separately the infinite rigid-body response (for static loads only the acceleration may be finite) and the finite flexible response. To get this separation the first step is to express the load as a sum of modal loads:

$$Q = \sum_{RB} Q_{RB} + \sum_{Flex} Q_{Flex} \tag{5.45}$$

where for each mode (rigid or flexible) the modal load is given by:

$$Q_i = \frac{\phi_i^T Q}{m_i} m\phi_i \tag{5.21}$$

with ϕ_i is the modeshape , m_i is the modal mass (found by $\phi_i^T m\phi_i = m_i$), and Q is the applied load. The rigid-body loads only excite rigid-body motions. The response of a rigid body mode is exactly described by equation (5.2) (with ω_{RB}=0) :

$$\ddot{\xi}_{RB}(t) = \frac{\phi_{RB}(x)^T Q(x,t)}{m_{RB}} \tag{5.46}$$

Each flexible modal load excites the corresponding flexible mode. If all the modes of a model could be known, the inversion formulas (5.5) used without the rigid-body modes would give the flexible response. But in practice, the number of modes is such that this cannot be done. Only the sum of the flexible modal loads is known ($Q_F = \sum_{Flex} Q_{Flex}$)

by subtraction of the rigid-body modal loads ($\sum_{RB} Q_{RB}$) from the total load (Q). The only thing that can be done is the computation of the flexible response of the structure to the flexible load Q_F. Although the solution is uniquely defined, finite element codes may have problems solving for the static response of a structure with rigid-body modes. This problem may be circumvented by computing the static flexible response of the structure with a point fully constrained ($\phi_{FCons}=k_{cons}^{-1}Q_F$), so that rigid-body motions are not present (the following might not be true if constraints were imposed at different points). The flexible response (ϕ_F) of the unconstrained structure can then be recovered by orthogonalizing the constrained response to the rigid body modes:

$$\phi_F = \phi_{FCons} - \sum_{RB} \frac{\phi_{RB}^T \, m \, \phi_{FCons}}{m_{RB}} \phi_{RB} \qquad (5.22)$$

The response can then be computed using the same steps as the previous sections.

In summary the procedure is the following. First a finite number of base loads B_j (corresponding to actuators or disturbance sources) is defined. Each base load is decomposed into different rigid-body modal loads and a flexible load (using equations (5.45) and (5.21)). The response of each rigid body mode is exactly described by equation (5.46). Using (5.22), the complete flexible response ($\overline{\gamma}_{jF}$) to each base load is found by solving for the static response to the flexible load (this involves the inversion of the stiffness matrix, which is routinely done by finite element codes). The dynamic response of the retained modes is then included, but, as previously, the static and dynamic response of the retained modes must be grouped to get a description in term of states (the modal acceleration is not a state). This is done by orthogonalizing the flexible response to the retained modes (as in equation (5.20)). The final form (corresponding to the state-space model described in section 5.2.4.) is then the sum of the rigid-body response (given by

(5.46)) and of the flexible response given by equations (5.18) or (5.19) (with "flexible" applying to all quantities). In the time domain this is:

$$\hat{y}_c(x,t) = \sum_{RB} \xi_{RB}\, c\phi_{RB} + \sum_{j=1}^{N_s} c\gamma_{jF}(x)\, u_j(t) + \sum_{i=1}^{N_r} \xi_i(t) c\phi_i(x) \qquad (5.23)$$

and in the frequency domain :

$$\hat{y}_c(x,\omega) = -\sum_{RB} \frac{\phi_{RB}^T Q}{m_{RB}\omega^2} c\phi_R + \sum_{j=1}^{N_s} c\gamma_{jF}\, u_j(\omega) + \sum_{i=1}^{N_r} \frac{\Xi_i(\omega)}{m_i(\omega_i^2-\omega^2)} c\phi_i \qquad (5.24)$$

5.2.4 State space description

Previously the response has been considered in the expanded residue form. Two other forms of description are generally useful. The polynomial transfer function form should not be used for structures having more than two or three modes since polynomial coefficients tend to be a numerically ill-conditioned way of conveying the information on roots. The state space form which is more commonly used has much better numerical properties and will be the only one considered here. The state space description of the structure, using *modal coordinates,* has the generic form (with no feedthrough term as all the modes of the system are considered):

$$\dot{X} = A\,X + B\,U \qquad (5.26)$$

$$Y = C\,X \qquad (5.27)$$

with

$$A = \begin{bmatrix} \begin{matrix} 0 & 1 \\ -\omega_1^2 & -2\zeta\omega_1 \end{matrix} & & \\ & \ddots & \\ & & \begin{matrix} 0 & 1 \\ -\omega_N^2 & -2\zeta\omega_N \end{matrix} \end{bmatrix} \qquad (5.28)$$

$$B = \begin{bmatrix} 0 & \cdots \\ \frac{\phi_1^T B_i}{m_1} & \\ \vdots & \end{bmatrix} \qquad C = \begin{bmatrix} C_q\phi_1 & C_{\dot{q}}\phi_1 & \cdots \end{bmatrix} \tag{5.29}$$

where each block in the matrix A corresponds to a mode, ω_i and ζ_i are the frequency and the damping ratio of the mode, the two states corresponding to the block are ξ_i and $\dot{\xi}_i$: the modal amplitude and the modal rate (as used in the preceding sections). In matrix B and C, ϕ_i is the non-dimensional modeshape, m_i the modal mass, B_j the dimensional load corresponding to a unit command on the j^{th} actuator, $C_q\phi_i$ and $C_{\dot{q}}\phi_i$ are column vectors (a row for each sensor) corresponding to the output that would be measured for, respectively, a unit modal amplitude and a unit modal velocity of mode i.

One should note the dissymmetry of sensing where position and rate can be sensed and actuation where only force can be input, and no direct change on the modal velocity can exist. In the limit of high gains the force is high enough for the time constant of modification of modal velocity or position to be small. This appears as rate or position actuation but corresponds to it only at low enough frequencies. Incidentally, this dissymmetry implies that damping has no influence on the static response of the structure so that the results on the static correction, given in the previous sections for an undamped structure, remain valid.

When modes are retained, the A, B, and C matrices are partitioned into a retained and truncated part (assuming that modal states are used):

$$\begin{bmatrix} \dot{X}_R \\ \dot{X}_N \\ Y \end{bmatrix} = \begin{bmatrix} A_R & 0 & B_R \\ 0 & A_N & B_N \\ C_R & C_N & 0 \end{bmatrix} \begin{bmatrix} X_R \\ X_N \\ Y \end{bmatrix} \tag{5.30}$$

The simple truncation approach drops the truncated part, but the static correction assumes that it behaves quasistatically ($\dot{X}_N = 0$) so that $X_N = - A_N^{-1} B_N U$ and the new model of the structure is:

$$\dot{X}_R = A_R X_R + B_R U \tag{5.31}$$

$$Y = C_R X_R + D U \quad \text{with} \quad D = - C_N A_N^{-1} B_N \tag{5.32}$$

The D term corresponds to the direct feedthrough term implied by neglecting the dynamics but not the static position response of truncated modes. The columns of the D matrix are the vectors $c\gamma_j$ found in the form of the previous sections. For computations from FEM code results, the following expression of D in terms of mode shapes can be used (this corresponds exactly to the mode acceleration method):

$$D = C_q k^{-1}(B) - \sum_{i=1}^{N_r} \frac{C_q \phi_i \phi_i^T B}{m_i \omega_i^2} \tag{5.33}$$

where C_q is the position observation matrix (note that velocity measurements will never influence this correction), k is the stiffness matrix, whose inverse is computed by finite element codes for static tests, and B is the control input shape matrix. Other forms using the inversion formulas (5.5) cannot be used, as in general all the modes of a model are not known.

The state space form is the standard form used for control design so that it will be used in section 5.3., which considers the closed loop response of the structure. In practice using a D term is not a good idea as it makes the computation of closed-loop dynamics rather difficult and does not allow a correction for the low-frequency velocity of truncated modes. This feedthrough term should be replaced by a correction mode rolling off above the bandwidth of interest. Further considerations on the use of correction modes will be given in section 5.4.2.

5.2.5 Correction at a non-zero frequency

As the exact static correction represented the exact response at DC, other approaches could correct at a non zero frequency ω_g. This is very useful to get accurate representations in the considered bandwidth if the DC behavior is not well known. For example if an identification is made using accelerometers the DC response is often unknown and there might be modes below the considered bandwidth. To explain the procedure the frequency response of the structure is used. The exact static approach estimated the response by:

$$\hat{y}_c(x,\omega) = \sum_{i=1}^{N_r} \frac{\Xi_i(\omega)}{m_i(\omega_i^2-\omega^2)} c\phi_i(x) + \sum_{i=N_r+1}^{\infty} \frac{\Xi_i(\omega)}{m_i\omega_i^2} c\phi_i(x) \qquad (5.34)$$

which of course does not correspond to the y we could find from the complete model. All the truncated modes well below the chosen frequency, ω_g, behave as $1/\omega^2$ so the inertia terms linked to these modes behave as $\frac{1}{\omega^2}\beta Q(x,t)$ (where β is a matrix to be determined) and introduce an error between y and $\hat{y}_c$. All the modes well above behave as constants near ω_g so the inertia terms linked to those modes induce a constant bias $\alpha Q(x,t)$ (where α is a matrix to be determined). So a better estimate of y would have the form:

$$\hat{y}_n(x,\omega) = \sum_{i=1}^{N_r} \frac{\Xi_i(\omega)}{m_i(\omega_i^2-\omega^2)} c\phi_i(x) + \alpha Q + \frac{1}{\omega^2}\beta Q \qquad (5.35)$$

The difficulty is to compute the matrices (or operators) α and β, but the exact response at ω_g is supposed to be known, and the operator $\alpha + \frac{1}{\omega_g^2}\beta$ is found using the following formula:

$$(\alpha+\frac{1}{\omega_g^2}\beta)\,Q = y(x,\omega_g) - \sum_{i=1}^{N_r} \frac{\Xi_i(\omega_g)}{m_i(\omega_i^2-\omega_g^2)} c\phi_i(x) \qquad (5.36)$$

If A and B are constant over the frequency range of interest, and this is the best assumption that can be done, the operator $\alpha+\frac{1}{\omega^2}\beta$ need only be known at two different frequencies. This approach is used extensively in identification softwares, such as STAR (ref. [48]).

In a state space description this correction would be done by adding two correction modes (4 states) per actuator or disturbance source. The first mode with a roll-off beginning below the bandwidth corresponding to the β matrix. The second mode with a roll-off after the bandwidth corresponding to the static correction and velocity correction (for cases with velocity measurement).

The exact static correction can in fact be considered as a special case of this method, where it is assumed that no mode is present below the bandwidth (B = 0) and the given frequency response is the static response.

5.3. Choosing retained dynamics

The purpose of this section is to review quickly the principles leading to the choice of retained dynamics. The simplest idea in truncating some of the structural dynamics of an open-loop system is that modes above the bandwidth only contribute with their static response and modes below the bandwidth only with their roll-off level (see section 5.2.5.). It is therefore unnecessary to represent their dynamics and the corrections introduced in section 5.2. account for these contributions with a fixed number of modes, depending only on the number of actuators. In many cases the number of modes obtained by doing this first simplification is still too important for the purpose of control design, and different

methodologies have been developed to evaluate the influence of different modes on the dynamics and be able to retain only the most important ones.

The *internal balancing* theory (ref. [49]) matches the controllability and observability grammians so that the Hankel singular values corresponding to each mode can be computed. In practice, internal balancing scales the different inputs, outputs, and states so that it becomes meaningful to compare the numerical amplitudes of states. The Hankel singular values give an estimate of the importance of each state in the response: if it is important the state will have a great influence and should be kept, if it is small it will be almost uncontrollable or unobservable so that neglecting its dynamics should not influence a later use of the model.

The *component cost analysis*, due to Skelton (refs. [50]-[52]), defines a cost for the open-loop model: response of a single performance metric to an expected form of input. Using a balanced realization, the cost of each state by itself (neglecting cross-products) is uniquely defined and one can retain the states with the highest cost. For modal systems, a modal cost is defined and the same approach can be used (*modal cost analysis*).

Other approaches, used essentially for compensators, consider different dynamics to get a reduced order realization of the model (ref. [53]). These approaches tend to use optimal solutions but, as often in optimal approaches, the reasons and implications of different results are not well understood, so that their exact value depends on the field of application and is not known in general.

Finally, in all these methods, the full problem is not addressed. The purpose of the open-loop model is in general to serve as a basis for the design of a controller, and it must therefore be able to represent accurately the closed-loop dynamics of the system. But the accuracy of the closed-loop response can only be computed once the controller is known, so that an iterative process between model reduction and control design is necessary.

The check of the accuracy of the closed-loop estimate is not often done, so section 5.4. will consider the way to compute accurately a reduced model of the closed-loop dynamics.

5.4. Models of closed loop systems

5.4.1 Static correction in presence of output feedback

For a closed-loop system the truncated dynamics not only influence the output but also the dynamics of the system through the feedback loop. The steps needed to account for the full static closed-loop influence of truncated modes will be described in this section. Assuming perfect sensors and actuators (with no dynamics and no noise) the response can be described in the standard form, with no feedthrough terms if all the modes of the model are included:

$$\begin{bmatrix} \dot{x} \\ z \\ y \end{bmatrix} = \left[\begin{array}{c|c|c} A & B_w & B_u \\ \hline C_z & 0 & 0 \\ \hline C_y & 0 & 0 \end{array}\right] \begin{bmatrix} x \\ w \\ u \end{bmatrix} \qquad (5.37)$$

where w corresponds to disturbance or command inputs, u is the control, y is the output used by the controller and z is the output used as performance metric. In this form z does not correspond to the cost that optimal control design theories use as a design parameter but rather to the ultimate engineering performance metric of interest in the experiment. For optimal designs another design-performance would have to be introduced.

The open-loop static correction introduced in section 5.2. becomes in the form of (5.37) :

$$\begin{bmatrix} \dot{x}_R \\ z \\ y \end{bmatrix} = \left[\begin{array}{c|c|c} A^{OL} & B_w^{OL} & B_u^{OL} \\ \hline C_z^{OL} & D_{zw}^{OL} & D_{zu}^{OL} \\ \hline C_y^{OL} & D_{yw}^{OL} & D_{yu}^{OL} \end{array}\right] \begin{bmatrix} x_R \\ w \\ u \end{bmatrix} \tag{5.38}$$

where $A^{OL} = A_R$, $B_i^{OL} = B_{iR}$, $C_i^{OL} = C_{iR}$, $D_{ij}^{OL} = -C_{iN} A_N^{-1} B_{jN}$. And the D_{ij}^{OL} can also be computed from FEM results using (5.33).

As mentioned earlier, even though all the dynamics described by the A matrix are not representative of the real dynamics, their quasistatic behavior is the most accurate estimate available. So $y = C x$ is the best available estimate of the output, with some of the dynamics truncated; either because they do not represent real phenomena, or because their influence is negligible in the frequency range of interest (modal cost considerations that have been described in 5.3.).

To compute the most accurate estimate of the closed-loop dynamics in the case of output feedback, the closed loop dynamics should be partitioned and some of the dynamics truncated, as was done in the open-loop case. In the subsequent development static output feedback is assumed but the results could easily be extended to dynamic feedback. Partitioning, as in section 2.4., the closed loop-dynamics into retained and truncated states gives:

$$\begin{bmatrix} \dot{x}_R \\ \dot{x}_N \end{bmatrix} = \begin{bmatrix} A_R - B_{uR}KC_{yR} & - B_{uR}KC_{yN} \\ - B_{uN}KC_{yR} & A_N - B_{uN}KC_{yN} \end{bmatrix} \begin{bmatrix} x_R \\ x_N \end{bmatrix} + \begin{bmatrix} B_{wR} \\ B_{wN} \end{bmatrix} d \tag{5.39}$$

To get an accurate response the dynamics but not the static response of the truncated states are omitted. Assuming a quasistatic response ($\dot{x}_N = 0$), the value of the truncated states is given at all times (or frequencies of interest) by:

$$x_N = (A_N - B_{uN}KC_{yN})^{-1} (B_{uN}KC_{yR}\ x_R - B_{wN}\ d) \tag{5.40}$$

This is the best possible low-frequency estimate of the state position if one measures truncated modal dynamics. The best estimate of modal velocity is this times jω, but this estimate is not recovered when doing a static condensation of the truncated modes. The introduction of correction modes in section 4.2. will permit the use of the velocity correction, which can have quite an importance for compensators based on rate feedback.

Using this expression the new closed loop system model can be found from equation (5.39):

$$\begin{bmatrix} \dot{x}_R \\ z \\ y \end{bmatrix} = \left[\begin{array}{c|c} A^{CL} & B_w^{CL} \\ \hline C_z^{CL} & D_{zw}^{CL} \\ \hline C_y^{CL} & D_{yw}^{CL} \end{array}\right] \begin{bmatrix} x \\ w \end{bmatrix} \tag{5.41}$$

$$A^{CL} = A_R - B_{uR}\, K\, (I + C_{yN}(A_N - B_{uN}KC_{yN})^{-1}\, B_{uN}K)\, C_{yR}$$

$$B_w^{CL} = B_{wR} + B_{uR}KC_{yN}\,(A_N - B_{uN}KC_{yN})^{-1}\, B_{wN}$$

$$C_z^{CL} = C_{zR} + C_{zN}\,(A_N - B_{uN}KC_{yN})^{-1}\, B_{uN}KC_{yR}$$

$$C_y^{CL} = C_{yR} + C_{yN}\,(A_N - B_{uN}KC_{yN})^{-1}\, B_{uN}KC_{yR}$$

$$D_{zw}^{CL} = -\, C_{zN}\,(A_N - B_{uN}KC_{yN})^{-1}\, B_{wN}$$

$$D_{yw}^{CL} = -\, C_{yN}\,(A_N - B_{uN}KC_{yN})^{-1}\, B_{wN}$$

If K is of rank the number of controls (otherwise the number of controls is arbitrarily expanded), one can simplify these expressions and make them computable using FEM results. First the inversion of the truncated dynamics can be reformulated as:

$$(A_N - B_{uN}KC_{yN})^{-1} = A_N^{-1} + A_N^{-1}B_{uN}\,(I - KD_{yu}^{OL})^{-1}\, KC_{yN}A_N^{-1} \tag{5.42}$$

Then using this expression to simplify those of (5.41) one finds a new statically correct model of the closed loop dynamics of this system with static output feedback:

$$\begin{bmatrix} \dot{x}_R \\ z \\ y \end{bmatrix} = \left[\begin{array}{c|c} A_R - B_{uR}(I-KD_{yu}^{OL})^{-1} K C_{2R} & B_{wR} - B_{uR}(I-KD_{yu}^{OL})^{-1} K D_{yw}^{OL} \\ \hline C_{zR} - D_{zu}^{OL}(I-KD_{yu}^{OL})^{-1} K C_{yR} & D_{zw}^{OL} - D_{zu}^{OL}(I-KD_{yu}^{OL})^{-1} K D_{yw}^{OL} \\ \hline C_{yR} - D_{yu}^{OL}(I-KD_{yu}^{OL})^{-1} K C_{yR} & D_{yw}^{OL} - D_{yu}^{OL}(I-KD_{yu}^{OL})^{-1} K D_{yw}^{OL} \end{array}\right] \begin{bmatrix} x \\ w \end{bmatrix} \quad (5.43)$$

In this form of the statically correct closed loop dynamics, all the terms can be computed from the open-loop form (5.38), which can be computed for a finite element model.

These results show that the compensator enters directly in the computation of statically correct sensor and actuator matrices (C_i^{CL},B_i^{CL}), adds a direct feedthrough term from the commands to the performance metric z (D_i^{CL}), as was the case for the open-loop system, but also modifies the closed-loop dynamics in a non-linear manner.

These corrections are based on a knowledge of the actual behavior of the plant and would not appear had the plant been taken to be its truncated model. It would certainly be useful to use these corrections in the controller evaluation stage where the most accurate model is looked for. But the use of feedthrough terms is usually cumbersome and not considered in control design methodologies, so that an alternative solution is proposed in the next section.

5.4.2. Correction modes: a basis for easier control designs

The use of the formulas given in 5.4.1. in the process of control design would not fit the usual working assumptions of control theories, especially since the compensator enters non-linearly in the definition of the closed-loop dynamics. As often the problem can be circumvented by adding dynamics to the retained modal states. The idea is to use

relatively high bandwidth filters to feedthrough the truncated mode static response up to a certain frequency. The use of modes instead of direct feedthroughs also introduces a correction for the truncated modes velocity, which was not possible using a static condensation of the truncated mode dynamics; but corresponds to the physical reality that the velocity contribution of modes, below their resonance, is an asymptote of slope 20 dB/dec and not zero as assumed in a static condensation.

For each actuator or disturbance source (each column of B_w and B_u in (5.37)) one defines a correction mode with dynamics of the following form:

$$\begin{bmatrix} \dot{x}_c \\ \ddot{x}_c \end{bmatrix} = \begin{bmatrix} 0 & 1 \\ -\omega^2 & -2\zeta\omega \end{bmatrix} \begin{bmatrix} x_c \\ \dot{x}_c \end{bmatrix} + \begin{bmatrix} 0 \\ \omega^2 \end{bmatrix} u_i \qquad (5.44)$$

The low frequency response of truncated modes is then approximated by the sensed output of these correction modes. For a truncated mode displacement response of the form $y_t = \sum_{trunc} C_q \phi \, \zeta$, the estimate of the truncated position response will be:

$$\hat{y}_t = - C_{qN} A_N^{-1} B_N x_c \qquad (5.48)$$

with $C_{qN} = [C_q\phi_1 \; 0 \; C_q\phi_2 \; 0 \; ...]$. For a truncated mode velocity response of the form $\dot{y}_t = \sum_{trunc} C_{\dot{q}} \phi \, \zeta$, the estimate of the truncated position response will be:

$$\hat{\dot{y}}_t = - C_{\dot{q}N} A_N^{-1} B_N \dot{x}_c \qquad (5.49)$$

with $C_{\dot{q}N} = [C_{\dot{q}}\phi_1 \; 0 \; C_{\dot{q}}\phi_2 \; 0 \; ...]$ (note the position of the $C_{\dot{q}}\phi$ in $C_{\dot{q}N}$). The computation of the correction terms $C_{\dot{q}N} A_N^{-1} B_N$ and $C_{qN} A_N^{-1} B_N$ is done exactly as the evaluation of the open-loop static correction (section 5.2.) and will therefore not be exposed again.

This corresponds to the classical feedthrough terms for position, but also corrects for the velocity asymptote of the truncated modes. The correction is only valid in the low frequency range of the correction mode whose dynamics are described by (5.44), but the

choice of ω and ζ is arbitrary. If they are such that the correction mode behaves statically in the bandwidth of interest and rolls off afterwards the correction is exact for all practical purposes. Typical numbers would be $\zeta = 1$ and ω about a decade above the frequency of the last retained mode. One might also think of having a pole near the roll-off of the controller and with a damping ratio such that the phase is correct.

This model of the feedthrough terms corresponds to a reduced order realization approach. One seeks to represent the behavior of all the truncated modes by one mode per actuator. The most important characteristic of the truncated modes in the bandwidth of interest is their asymptotic response, and this is exactly represented by the added modes for all the time derivatives: position, velocity, and also acceleration. Without much more complex considerations (reduced order realization, ref. [53]), one cannot choose adequate dynamics that would get the response of the added mode to match more closely the response of the truncated modes so a simple roll-off ($\zeta = 1$ and ω about a decade above the bandwidth of interest) is used.

The new augmented open-loop dynamic model includes an exact asymptotic response of the truncated modes in the bandwidth of interest (not only the asymptotic position response, as is the case for a model with feedthrough terms) and does not have the difficulty of direct feedthrough terms. The computation of closed-loop dynamics from the open-loop model is much simplified since one can just use $y=Cx$, where x is the augmented state vector (retained modes states + correction modes states) and C measures the contributions in position and velocity of both the retained and truncated modes. The intricate formula (5.43) becomes unnecessary since the truncated mode asymptotic response is present in the actuator modes. And, what may be the most important point, the correction for the truncated modes rolls off so that one has proper transfer functions.

For modes truncated below the bandwidth one could define similar correction modes rolling-off before the first frequency of interest (see section 2.5 which gave more

ideas on the subject). But rigid body modes should be included, and all the development can be applied, separating the rigid and the flexible response, as was done in section 5.2.3.

5.4.3. Example: three mode system

As an example, a three mode spring-mass system will be considered and different models will be used to compute the closed-loop response to collocated position and rate feedback.

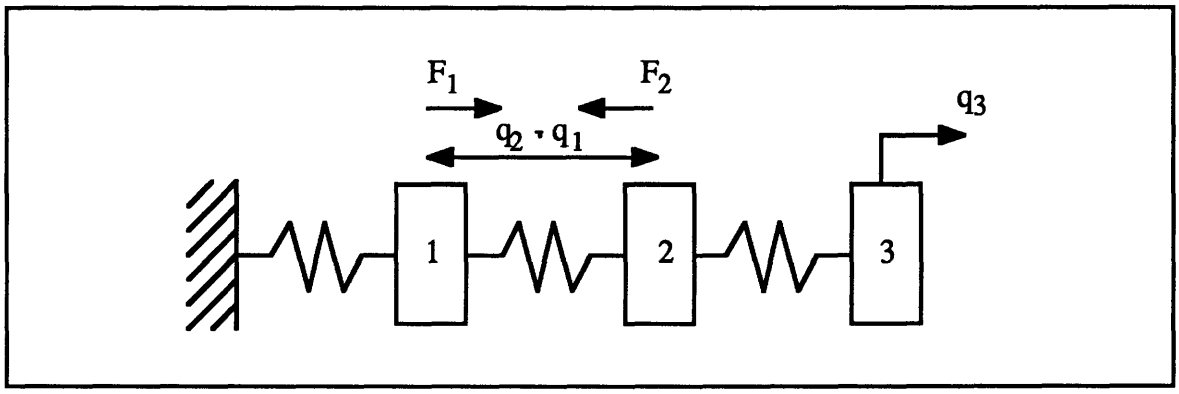

Figure 5.3. Three mode spring mass system

The numerical solution corresponds to m=1, k=1. As shown on the figure the output is displacement at node 3, and the feedback is a collocated force feedback of the displacement and displacement rate difference between node 2 and 3. Analytically this feedback loop is described by:

$$F_2 = -F_1 = -5\,(q_2-q_1) - 10\,(\dot{q}_2-\dot{q}_1)$$

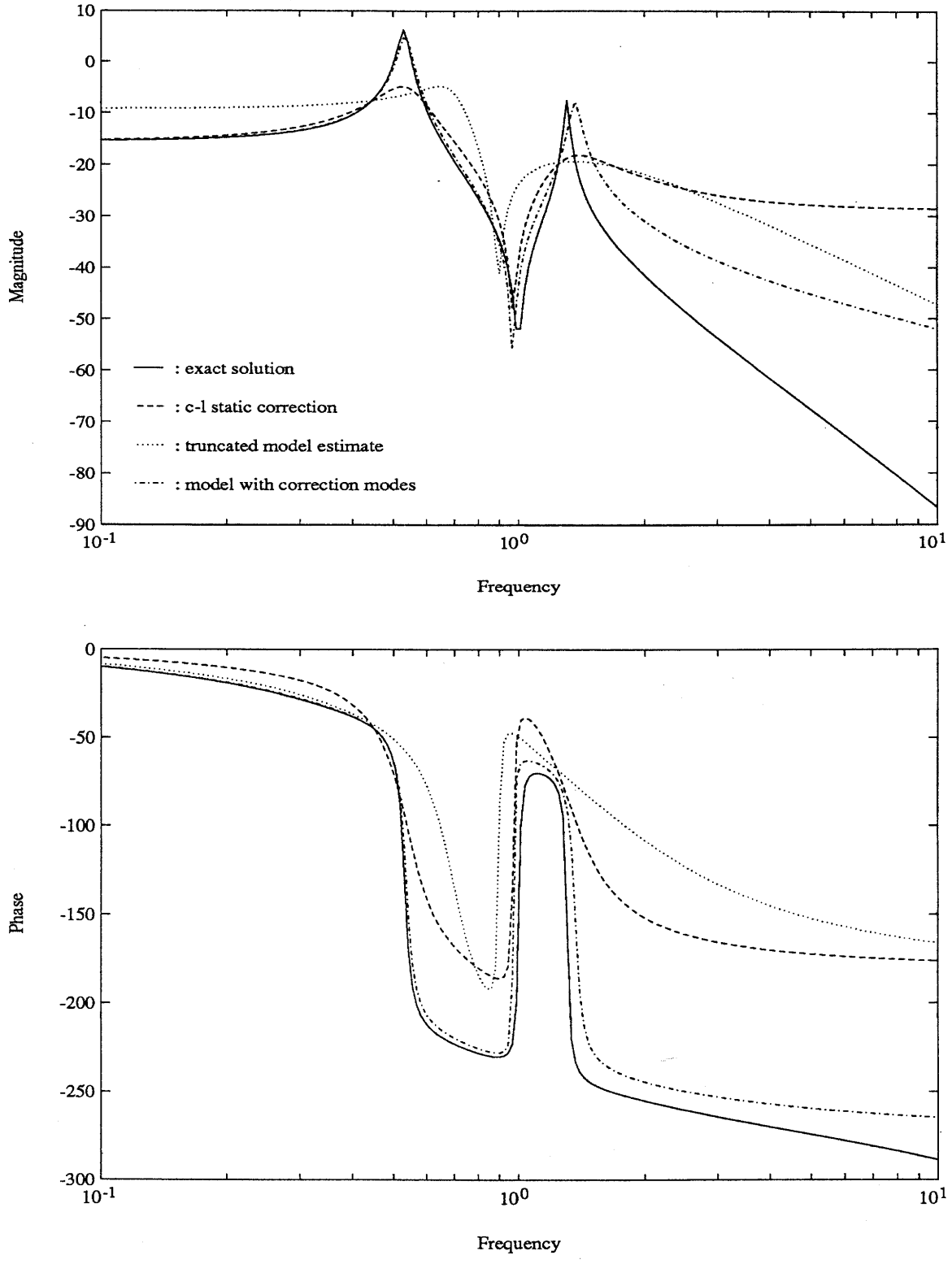

Figure 5.4. Models of the *closed-loop* response of the spring-mass system.

Figure 5.4. shows the estimated response for different models. The exact response is computed with the three modes of the system and the estimates have access only to the first two. The controller overdamps the third mode, which therefore does not appear in the plots of the exact closed-loop response. The simple truncation estimate gives a bad estimate of the closed-loop poles, misplaces the zero, and has not the right low frequency behavior. The exact closed-loop static correction gives an exact low frequency response (the correction has been made for this), places the poles and the zero much more accurately (as it models the position feedback accurately), but gives over-estimated damping levels (as the velocity contribution of the truncated mode is not accounted for). The model augmented with correction modes is very accurate up to the second closed-loop mode (as the effect of the truncated mode is well modelled at low frequencies) and differs afterwards (as the correction is not the exact third mode).

The main characteristics of the different models can be seen in this example:

- the static correction is necessary to get accurate models of open-loop and closed-loop responses.
- the introduction of feedthrough terms in the open or closed-loop model gives much better results and an exact low frequency response. The principal limitation of these models is the absence of correction for the velocity of truncated modes, so that velocity measurements and therefore rate feedback loops are inaccurately modelled.
- the model augmented with correction modes gives very good results and is probably the best estimate that can be used for both open and closed-loop systems.

CHAPTER VI

CONCLUDING REMARKS

Steps in creating state-space input-output models of the low frequency dynamics of continuous structures have been discussed throughout this report. First, a continuous idealized model of the structure was introduced. For structures composed of beams, exact closed-form solutions of the open and closed loop responses were introduced, although numerical conditioning became a limiting factor even for relatively simple problems. In practice approximate solutions are computed. Using the finite element method, the initial approximate solution is in many cases inaccurate. H- and p-refinements of the finite element model were introduced to get better approximations of the continuous idealized model solution. Compared to the h-refinement, the p-refinement tends to give more accurate approximations of the first modes, but usually has a smaller number of significant modes. For structures composed of beams, the two methods gave similar results, and could easily correct inaccuracies, leaving remaining errors that were smaller than expected discrepancies between the structure and the idealized model. For structures composed of beams, the h-refinement is easier to implement and should be used. For plates and other structural components, few exact solutions are known, the accuracy of the continuous idealized model depends on many refinements that have to be considered, and the accuracy of finite element solutions is limited by several factors such as the existence of line or surface boundaries. For such components, at least partial p-refinements should be considered, as they often have definite advantages over h-refinements.

In general, finite element models of structures composed of beams are constructed to have an exact DC response. Standard 2-node beam elements meet this requirement for

structures without rigid-body modes, and h-refined beam/rod elements can be used otherwise. Beam/rod finite elements were shown to be accurate up to a certain frequency. The simplest check of their accuracy is the comparison of their length with the wavelengths of harmonic motions present at the frequency of interest (a wavelength of two times the element length imply significant inaccuracies in the model). For usual structures, compression and torsion have resonances at very high frequencies, so that for practical purposes they are very accurately represented. The limit of accuracy for bending motions tends to be in the frequency range of interest, so that refinements are often needed. Modelling errors at the element level do not necessarily imply that the quantities of interest in the global modeshapes are inaccurate. Roughly, if the modal density is not too important, the relative error magnitude cannot be greater than the relative amount of energy present in inaccurately modelled elements.

For truss beams, the joint-plane model, which underlies equivalent continuum methods, must be refined if bending motions influence the behavior in the frequency range of interest. The influence of bending is usually important for frequencies corresponding to bending wavelengths shorter than two times the strut length. The midbay-plane model was shown to be an efficient way of doing the refinement, and to give the possibility of modelling joint behavior easily. After refinement, models often have too many degrees of freedom for practical uses. Degree-of-freedom condensations were performed, and smaller problems obtained without important losses of accuracy.

The second modelling step considered was the update of the continuous idealized model (and concurrently of the finite element model, as the idealized model solution is not actually computed) using measurements of component properties or global dynamics. The update using measured component properties although very useful, should be considered with care. It is often difficult to define which properties of the model correspond to measurable quantities, and the selective update of some properties may not lead to models that are more accurate for control purposes. When possible, the modifications should be

correlated with measured modal information to assess the validity of updates. For updates with structural dynamic measurements, one defines an assumed form for the error or uncertainty in the continuous idealized model and a measurement of the solution accuracy. These are then used to obtain a new model that matches the measured dynamic response better. As there is almost never a unique link between the idealized model definition and a finite set of measured properties of its solution (the measurable structural response), the update cannot be unique. The definition of the agreement, which leads to a particular update, is a relatively arbitrary choice whose consequences on the model validity are not well known. The form, condensed or expanded, of correlated modeshapes, the influence of different definitions of the agreement on stability guarantees for closed-loop systems, or the exact link between error for control design methods and for modal models are current research topics, which should lead to better model updates by enabling the specific reduction of uncertainty on parameters important for control design.

The assessment of the model validity required a study of sensitivities to different modelling errors. Human errors will always be the main limitation, but the effect of many usual modelling errors were evaluated, and if important they could be either corrected or kept as uncertainty in the model. Typical errors that were treated are global errors in component properties, and measurable local variation between the modelled and the actual structures. Future developments should lead to a better analysis of damping, non-linearities, prestress, and predeformation.

A fundamental limit to the accuracy structural dynamic models is the presence of high modal densities, which make both the prediction and measurement of modal characteristics inaccurate. The limiting case of high modal density is modal degeneration. Symmetry in a structure was shown to cause degeneration. Using the algebraic properties linked to the structural symmetry *a priori* cases of modal degeneration and corresponding modal geometric properties were determined. These properties gave essential information on the structure that were not experimentally identified. Local resonances, as those of struts

in truss structures, are another usual source of high modal density. For structures with such resonances, perturbations were shown to sometimes lead to modal localization, and generally induce important modifications of the modes, so that modelling errors and experimental modifications (such as the presence of sensors or actuators) might lead to inaccurate estimates of the modal characteristics. Damping, inducing modal overlap (this effect increases with modal density), was shown to have a desensitizing effect on the effective input/output characteristics. For low levels of damping, but high modal density, the transfer functions were known very accurately even if the uncertainty on modal characteristics was very high.

For further work on localization, the selective attenuation of wave modes due to disorder in the structure should be analyzed as a good point of view to study the effect of general, and not only mode-localizing, perturbations for mono-dimensional multi-coupled structures (see reference [38]). A study of the influence of substructure vibration could lead to interesting structural designs taking advantage of local vibration properties. But more important results should come from the study of high modal density in the presence of damping. The appearance of very uncertain modal systems with accurate transfer-function characteristics is a point of major interest for both system identification and control design. First a study of the influence of damping on the possibility of characterizing modes should be performed. Then, for identification, methods should be developed that enable, for structures with high modal density, the design of MIMO identification experiments, and give a methodology to correlate experimental results with finite element based models. For control, a multivariable treatment of closely spaced modes, as inseparable groups with known and relatively insensitive input-output properties, but high uncertainty on the individual modal characteristics, could be very useful for the definition of bounds on the achievable performance by controlled structure systems.

The last considered step in modelling structural dynamics for control was the construction of state-space input output models from modal characteristics. The creation of

such models implies the truncation of a certain number of modes. In a given frequency range, it is accurate to approximate the response of a certain number of modes by asymptotic responses. The usual approach of static corrections was extended to the case of closed-loop systems, but did not give accurate results for the estimation of velocities. The use of correction modes, that represent for each actuator the complete asymptotic response due to truncated modes, was introduced as an efficient approach that should be used both for control and identification. For future developments, a full understanding of the influence of errors in the representation of truncated modes, could lead to a better assessment of the guarantees offered by control design methodologies based on truncated modal models of continuous structures.

Bibliography

[1] Newsom, J.R., Layman, W.E., Waites, H.B., Hayduk, R.J., *The NASA Controls-Structures Interaction Technology Program*, 41st IAF Congress IAF-90-290

[2] Skelton, R.E., *A Tutorial On Model Error Concepts In Control Design*, To appear in Int. J. Control

[3] Enns, D., *Model Reduction for Control System Design*, Stanford PhD Thesis 1984

[4] Blackwood, G., Miller, D.W., Jacques, R., Hyde, T., *MIT Multipoint Alignement Testbed: Technology Development for Optical Interferometry*, SPIE conference on Active and Adaptative Optical Systems July 1991

[5] Irretier, H., *Refined Effects in Beam Theories and Their Influence on the Natural Frequencies of Beams*, Proceedings of the Euromech-Colloquium 219, Springer-Verlag

[6] Collins, S.A., Miller, D.W., von Flotow, A.H., *Piezopolymer Spatial Filters for Active Structural Control*, Conf. on Recent Advances in Active Control of Sound and Vibration 1991

[7] Miller, D.W., Collins, S.A., Peltzman, S.P., *Development of Spatially Convolving Sensors for Structural Control Applications*, SDM 1990

[8] Plunkett, R., Lee, C.T., *Length Optimisation for Constrained Viscoelastic Layer Damping*, Journal of the Acoustical Society of America 1970 **48**-1

[9] Hagood, N.W., von Flotow, A.H., *Damping of Structural Vibrations with Piezoelectric Materials and Passive Electrical Networks*, J.S.V. 1991 **146**-2

[10] von Flotow, A.H., *Disturbance Propagation in Structural Networks*, J.S.V. 1986 **106**-3

[11] Patnaik, Berke, Gallagher, *Compatibility Conditions of Structural Mechanics for Finite Element Analysis*, AIAA Journal 1991 **29**-5

[12] Pestel, E.C., Leckie, F.A., *Matrix Methods in Elastomechanics*, McGraw-Hill, N.Y. 1963

[13] Chen, W.J., Pierre, C., *Exact Linear Dynamics of Periodic and Disordered Truss Beams: Localisation of Normal Modes and Harmonic Waves*, SDM 1991

[14] Signorelli, J., von Flotow, A.H., *Wave Propagation, Power Flow and Resonance in a Truss Beam*, J. Sound and Vibration 1988 **126**-1 127-144

[15] Balmès, E., *Dynamic Models of Substructure Effects in a Truss Beam*, ONERA/OR internal

[16] Bennighof, J.K., Meirovitch, L., *Eigenvalue Convergence in the Finite Element Method*, Int J. Num. Meth. Eng. **23** 2153-2165

[17] Babuska, I., Szabo, B., *On the Rates of Convergence of the Finite Element Method*, Int.J. Num. Meth. Eng. 1982 **18** 323-341

[18] Noor, A.K., Mikulas, M.M., *Continuum Modelling of Large Lattice Structures*, NASA report TP-2767 1988

[19] Noor, A.K., Nemeth, M.P., *Analysis of Spatial Beamlike Lattices with Rigid Joints*, Comp. Meth. Appl. Mech. Eng. 1980 **24** 35-59

[20] Leissa, A.W., *Vibration of Plates*, NASA SP-160 1969

[21] White, C.W., *Dynamic Testing of a Two Dimensional Box Truss Beam*, NASA-CR-4039 (1987) Martin Marietta Denver Aerospace

[22] Peterson, L.D., Allen, J.J., et al., *An Experimental and Analytical Synthesis of Controlled Structure Design*, SDM 89-1170-CP

[23] Chen, J.C., Fanson, J.L., *System Identification Test Using Active Members*, SDM 89-1290 CP

[24] Ewins, D.J., *Modal Testing: Theory and Practice*, John Wiley and Sons, Inc., New York, NY, 1984

[25] Ljung, L., *System Identification: Theory for the User*, Prentice-Hall 1987

[26] Allen, J.J., Martinez, D.R., *Automating the Identification of Structural Model Parameters*, SDM 89-1242-CP

[27] He, J., Ewins, D.J., *Compatibility of Measured and Predicted Vibration Modes in Model Improvement Studies*, AIAA Journal 1991 **29**-5

[28] Lin, C.S., *Location of Modelling Errors Using Modal Test Data*, AIAA Journal 1990 28-**9**

[29] Flanigan, C.C., *Test/Analysis correlation of the STS Centaur Using Design Sensitivity and Optimization Methods*, 5th IMAC London 1987

[30] Berman, A., *System Identification of Structural Dynamic Models - Theoretical and Practical Bounds*, AIAA-Paper 84-0929

[31] Webster, M.S., *Modelling Beam-Like Space Trusses with Nonlinear Joints with Application to Control*, MIT PhD Thesis 1991

[32] Rey, D., *Modelling Gravity and Suspension Effects on Controlled Space Structures*, MIT MS Thesis 1991 (in preparation)

[33] Zlokovic, G.M., *Group Theory and G-Vector Spaces in Structural Analysis*, Ellis Horwood Series in Civil Engineering 1989

[34] Hodges, C.H., *Confinment of vibration by Structural Irregularity*, J.S.V. 1982 **82**-3 411-424

[35] Pierre, C., Dowell, E.H., *Localisation Vibrations of Disordered Multispan Beams: Theory and Experiment*, AIAA Journal **25**-9 (1987)

[36] Cornwell P.J., Bendiksen O.O., *Localisation of Vibrations in Large Space Reflectors*, AIAA-Paper 87-0949

[37] Bendiksen, O.O., *Mode Localisation Phenemena in Large Space Structures*, AIAA-Paper 86-0903

[38] Chen, W.J., Pierre, C., *Exact Linear Dynamics of Periodic and Disordered Truss Beams: Localization of Normal modes and Harmonic Waves*, SDM 1991

[39] Signorelli, J., von Flotow, A.H., *Wave Propagation, Power Flow, and Resonance in a Truss Beam*, J.S.V. 1988 **126**-1

[40] Corrado, C., Zavistoski, R., Dyer, I., *Coupled Wave Complexity in Strucutral Acoustics*, MIT to be published

[41] Von Flotow, A.H., *Control Motivated Dynamic Tailoring of Spacecraft Truss-Work Strucutre,* AIAA GC conference 1986 **1** 622-628

[42] Wehrli, E., *Analyse Vibratoire d'un Treillis Bidimesionnel à Structure Répétitive*, ONERA 1989

[43] Mills, R.A., *Natural Vibrations of Beam-Like Trusses*, MIT MS thesis 1985

[44] Fleming, F.M., *The effect of Structure, Actuator, and Sensor on the Zeroes of Controlled Structures*, MIT MS Thesis 1991

[45] Bisplinghoff, R.L., Ashley, H., and Halfman, R.L., *Aeroelasticity*, Addison-Wesley Publishing Co., Reading, MA, 1955

[46] Bathe, K.J., *Finite Element Procedures in Engineering Analysis*, Prentice-Hall Inc., Englewood Cliffs, NJ, 1982.

[47] Craig, R.R.Jr., *A Review of Time-Domain and Frequency Domain Component Mode Synthesis Methods*, Int. J. Analytical and Experimental Modal Analysis, **2**-2 1987 p 59-72

[48] *STAR, Theory and Applications*, Structural Measurement Systems, Milpitas, CA, 95035

[49] Gregory, C.Z. Jr., *Reduction of Large Flexible Spacecraft Models Using Internal Balancing Theory*, J. Guidance 1984 **7**-6

[50] Skelton, R.E., Singh, R., Ramakrishnan, J., *Component Model Reduction by Component Cost Analysis*, Book

[51] Skelton, R.E., Hughes, P.C., Hablani, H.B., *Order Reduction for Models of Space Structures Using Modal Cost Analysis*, J. Guidance 1982 **5**-4

[52] Skelton, R.E., Hughes, P.C., *Modal Cost Analysis for Linear Matrix-Second-Order Systems*, J. of Dynamic Systems, Measurements, and Control 1980 **102**

[53] Bryson, A.E., Carrier, A., *Second-Order Algorithm for Optimal Order Reduction*, J. Guidance 1990 **13**-5